Università degli Studi di Padova

Dipartimento di Scienze Chirurgiche, Oncologiche e Gastroenterologiche

SCUOLA DI DOTTORATO DI RICERCA IN

ONCOLOGIA E ONCOLOGIA CHIRURGICA

XVII CICLO

Cancer stem cells from epithelial ovarian cancer patients privilege oxidative phosphorylation, and resist glucose deprivation

Direttore della Scuola: Ch.mo Prof. ssa Paola Zanovello

Supervisore: Ch.mo Prof. Alberto Amadori

Dottoranda: Chiara Bellio

Anno accademico 2013 - 2014

TABLE OF CONTENTS

3. RESULTS

3.1 $CD44^{+}CD117^{+}$ cells from ascitic effusions of epithelial ovarian cancer patients are characterized by a CSC phenotype

3.2 Ovarian CSC show a peculiar expression profile of glucose metabolism- and fatty acid β-oxidation associated enzymes

3.3 Ovarian CSC overexpress key enzymes controlling the fuelling of pyruvate into the tricarboxylic acid cycle

3.4 Ovarian CSC show higher mitochondrial activity and are more sensitive to inhibitors of the electron transport chain

3.5 Ovarian CSC resist *in vitro* and *in vivo* glucose deprivation, while maintaining their CSC properties

3.6 Glucose deprivation modulates the metabolic profile of ovarian CSC, while sparing their OXPHOS profile

3.7 Metformin and CPI-613, innovative drug targeting metabolism

4. DISCUSSION AND CONCLUSIONS

5. FUTURE PERSPECTIVES

5.1 CPI-613 an innovative drug

6. REFERENCES

SUMMARY

INTRODUZIONE:

Il cancro all'ovaio viene considerato un tumore resistente alla terapia e questa farmaco-resistenza si pensa sia correlata alla presenza delle cellule staminali tumorali (CSC). Le cellule staminali tumorali sono una rara e piccola popolazione cellulare responsabile dell'insorgenza del tumore, del mantenimento della sua crescita, dei casi di recidive e metastasi, in seguito alla loro proprietà di farmaco-resistenza. Considerando queste premesse, è indispensabile caratterizzare queste cellule in modo da trovare un possibile bersaglio terapeutico e migliorare i risultati delle terapie attuali.

Le cellule tumorali sono caratterizzate da un metabolismo altamente glicolitico anche in presenza di ossigeno, denominato "Effetto Warburg". Poco si conosce riguardo al metabolismo delle cellule staminali tumorali, e soprattutto non è noto se l'effetto Warburg è una condizione condivisa.

Questo progetto di ricerca si prefigge di:

- caratterizzare le CSC nel campioni primari di liquido ascitico di cancro all'ovaio;
- studiare il profilo metabolico delle CSC isolate, per identificare eventuali differenze con la controparte differenziata.

RISULTATI:

Inizialmente abbiamo identificato le CSC, secondo la co-espressione dei marcatori CD44 (il recettore dell'acido ialuronico), e CD117 [c-kit, recettore della citochina SCF (Stem Cell Factor)] in 40 campioni di liquido ascitico di cancro all'ovaio di pazienti in cura all'ospedale di Padova. Questa rara popolazione cellulare $CD44^{+}CD117^{+}$ è in grado di formare strutture sferoidali; è altamente tumorigenica in topi immunodeficienti; presenta farmaco-resistenza, dimostrata con trattamenti *in vitro* con farmaci solitamente utilizzati in clinica; ed è caratterizzata da un'alta espressione di geni codificanti: pathway di staminalità (Nanog, Oct4, Sox2), pompe o enzimi detossificanti, coinvolti nei fenomeni di farmaco-resistenza (ABCG2, MRP1, MRP2 e ALDH1A) e enzimi coinvolti nel fenomeno della transizione epitelio-mesenchimale, importante nei processi di metastasi (SNAIL1, SNAIL2, ZEB1, ZEB2, TWIST1). Complessivamente, questi risultati dimostrano che le cellule $CD44^{+}CD117^{+}$ rappresentano una popolazione con caratteristiche di staminalità.

A seguito di questa caratterizzazione fenotipica, abbiamo studiato il profilo metabolico delle cellule $CD44^{+}CD117^{+}$, confrontandolo con quello della controparte non-staminale ($CD44^{+}CD117^{-}$). In primo luogo, abbiamo esaminato l'espressione di geni coinvolti in diverse importanti vie metaboliche, tra cui: il metabolismo del glucosio, il ciclo dell'acido tricarbossilico (TCA), la catena di trasporto degli elettroni (ETC) nel processo della respirazione mitocondriale, la via dei pentoso fosfati (PPP), e la β-ossidazione degli acidi grassi.

Le cellule $CD44^+CD117^+$ mostrano alti livelli di espressione dei geni associati alla glicolisi, e sono caratterizzate da una forte dipendenza dalla via dei pentoso fosfati e della β-ossidazione degli acidi grassi, dimostrata da una significativa diminuzione della loro vitalità in seguito a trattamento *in vitro* con due inibitori specifici delle due vie metaboliche (DHEA e Etomoxir rispettivamente).

Inoltre le cellule $CD44^+CD117^+$ sono caratterizzate da un'alta espressione dei geni codificati enzimi coinvolti nel ciclo di Krebs e nella fosforilazione ossidativa (OXPHOS). Questo risultato ci ha permesso di analizzare l'espressione di un enzima chiave del ciclo di Krebs, la piruvato deidrogenasi (PDH), fondamentale nel trasporto del piruvato dalla glicolisi alla respirazione cellulare. Abbiamo verificato livelli di espressione comparabili dell'enzima PDH nelle due popolazioni cellulari $CD44^+CD117^+$ e $CD44^+CD117^-$, mentre l'enzima PDHK1, che inattiva la piruvato deidrogenasi tramite fosforilazione, risulta meno espressa nella popolazione $CD44^+CD117^+$. Questi dati suggeriscono che nelle cellule staminali tumorali venga privilegiato il trasporto del piruvato verso i mitocondri, per catalizzare il metabolismo della respirazione mitocondriale.

Alla luce di questi risultati, abbiamo studiato l'attività mitocondriale nella popolazione staminale e nella controparte non staminale. In particolare le cellule $CD44^+CD117^+$ sono caratterizzate da bassi livelli di ROS (specie reattive dell'ossigeno) totali, da alti livelli di ROS mitocondriali, da una iper-polarizzazione del potenziale di membrana mitocondriale in seguito a trattamento con oligomicina (inibitore dell'ATP-sintasi) e da una drammatica diminuzione della vitalità cellulare in seguito a trattamento con inibitori specifici della catena di trasporto degli elettroni (ETC) (oligomicina inibitore dell'ATP-sintasi; rotenone inibitore del complesso I e antimicina inibitore del complesso III).

Complessivamente, questi risultati ci hanno suggerito un modello sperimentale del profilo metabolico delle cellule staminali tumorali $CD44^+CD117^+$, le quali privilegiano la via della respirazione mitocondriale, a discapito della via glicolitica.

Inoltre, abbiamo dimostrato che un trattamento *in vitro* e *in vivo* (2DG) di deprivazione di glucosio o blocco della via glicolitica seleziona una popolazione di cellule con caratteristiche di staminalità: incremento dell'espressione dei marcatori CD44 e CD117, farmaco-resistenza, tumorigenicità *in vivo*, formazion dii sferoidi *in vitro* ed espressione di geni convolti in pathway tipici delle cellule staminali. Questa popolazione cellulare ha mostrato una down-regolazione della maggior parte delle vie metaboliche, entrando in uno stato di quiescenza pur mantenendo livelli di espressione significativi dei geni codificanti enzimi del metabolismo ossidativo e iper-polarizzazione del potenziale di membrana mitocondriale, nonché dell'attività dei mitocondri.

A conclusione del progetto e come ulteriore dimostrazione del profilo metabolico ossidativo delle cellule staminali tumorali, contrario all'effetto Warburg sfruttato dalle cellule tumorali, abbiamo eseguito degli esperimenti *in vitro* con due farmaci che colpiscono le vie metaboliche della respirazione cellulare: Metformina e CPI-613. Metformina inibisce il complesso I della catena di trasporto degli elettroni ed è attualmente in uso in studi clinici come farmaco antitumorale promettente; CPI-613 è un farmaco innovativo che inibisce due enzimi chiave del ciclo degli acidi tricarbossilici, PDH e α-KGH. Trattamenti *in vitro* con questi farmaci hanno dimostrato una significativa diminuzione della vitalità delle cellule $CD44^{+}CD117^{+}$, fondamentale verifica della loro dipendenza da questo profilo metabolico.

CONCLUSIONI:

In questo studio abbiamo investigato il profilo metabolico delle cellule staminali tumorali, isolate ex-vivo da campioni di liquidi ascitici di pazienti con carcinoma ovarico, dimostrando che le CSC ovariche, a differenza delle cellule differenziate neoplastiche, sfuggono all'effetto Warburg, utilizzando preferibilmente una respirazione ossidativa.

Questa osservazione può indicare nuove strade e nuove strategie per approcci di terapie mirate nei confronti delle CSC, alla luce delle peculiari caratteristiche del loro metabolismo.

ABSTRACT

Ovarian cancer is the fourth leading cause of cancer-related death in women and the leading cause of gynecologic cancer death. Moreover, it is regarded as a therapy resistant tumor, because it shows the formation of more aggressive recurrence of the primary tumor as a result of chemotherapy. This chemo-resistance is thought to be related to the presence of the Cancer Stem Cells (CSC). Tumor cells are characterized by a high glycolytic metabolism even in the presence of oxygen, the so-called Warburg effect; however, it is unclear whether this condition is also shared by CSC.

We identified ovarian CSC, according to their co-expression of CD44 and CD117 markers, in 40 samples of ascitic effusions from ovarian cancer-bearing patients. We have analyzed phenotipic characteristics by investigating stemness marker expression by flow-cytometry, spheroid formation assay, tumorigenicity *in vivo* and gene expression in RT-PCR. For the analysis of metabolic characteristics, ovarian cancer cells were FACS-sorted in to $CD44^{+}CD117^{+}$ and $CD44^{+}CD117^{-}$ cell populations and analyzed through specific metabolic gene-cards. Results were confirmed also through Western Blot for specific metabolic enzymes and functional assay of mitochondrial activity.

We have demonstrated that $CD44^{+}CD117^{+}$ EOC cells presented high tumorigenicity and expressed stemness-associated markers and multidrug resistance pumps. Moreover, the $CD44^{+}CD117^{+}$ cell population overexpressed genes associated with glucose uptake, oxidative phosphorylation (OXPHOS), and fatty acid β-oxidation, indicating higher ability to direct pyruvate towards the Krebs cycle. Consistent with a metabolic profile dominated by OXPHOS, the $CD44^{+}CD117^{+}$ cells showed higher mitochondrial reactive oxygen species (ROS) production and elevated membrane potential, and underwent apoptosis upon inhibition of the mitochondrial respiratory chain. The CSC also had a high rate of pentose phosphate pathway (PPP) activity, which is not typical of cells privileging OXPHOS over glycolysis, and may rather reflect the PPP role in recharging scavenging enzymes. Furthermore, CSC resisted *in vitro* and *in vivo* glucose deprivation, while maintaining their CSC phenotype and OXPHOS profile.

In this study, we show that a subpopulation of $CD44^{+}CD117^{+}$ EOC cells fulfilling the canonical properties of CSC does not preferentially exploit a glycolytic metabolism, privileging instead the mitochondrial respiratory pathway. These observations could explain the CSC resistance to anti-angiogenic therapies, and indicate this peculiar metabolic profile as a possible target of novel treatment strategies.

1. INTRODUCTION

Cancer is a term used for diseases in which abnormal cells divide without control and are able to invade other tissues, through the blood and lymph systems. Cancer is the leading cause of death in economically developed countries, and the second cause of death in developing countries.

Cancer starts when cells in a part of the body start to grow out of control. Instead of dying, cancer cells continue to grow and form new, abnormal cells. Therefore, all cancers involve the malfunction of genes that control cell growth and division. Some cancers are strongly hereditary, but most cancers result from damage to genes occurring during a person's lifetime. Genetic damage may result from both intrinsic factors (inherited mutations, hormones, immune conditions and mutations that occur from metabolism) or extrinsic factors (such as tobacco smoke, infectious organisms, chemicals and radiations).

The traditional approaches designed to remove or kill rapidly-dividing cancer cells are surgery, radiation therapy and systemic treatments such as chemotherapy or hormonal therapy. It has been shown that all these methods have limitations in clinical use, because some types of cancer, like ovarian cancer, are characterized by high recurrence [1].

The idea is that this recurrence could be related to the presence of a rare cell population, characterized by stemness properties, called Cancer Stem Cells (CSC).

1.1 Anatomy of ovary and ovarian cancer

The ovaries, a pair of tiny glands in the female pelvic cavity, are the most important organs of the female reproductive system. Their importance relies on their role in producing both the female sex hormones that control reproduction and the female gametes that are fertilized to form embryos.

Each ovary is a small glandular organ of about the shape and size of an almond. The ovaries are located on opposite sides of the uterus in the pelvic cavity and are attached to the uterus by the ovarian ligament. Several paired ligaments support the ovaries. The ovarian ligament connects the uterus and ovary. The posterior portion of the broad ligament forms the mesovarium, which supports the ovary and houses its arterial and venous supply. The suspensory ligament of the ovary (infundibular pelvic ligament) attaches the ovary to the pelvic sidewall (Figure 1). This larger structure also contains the ovarian artery and vein, as well as nerve supply to the ovary.

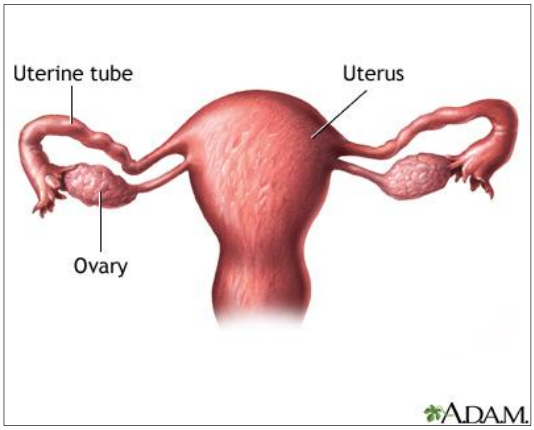

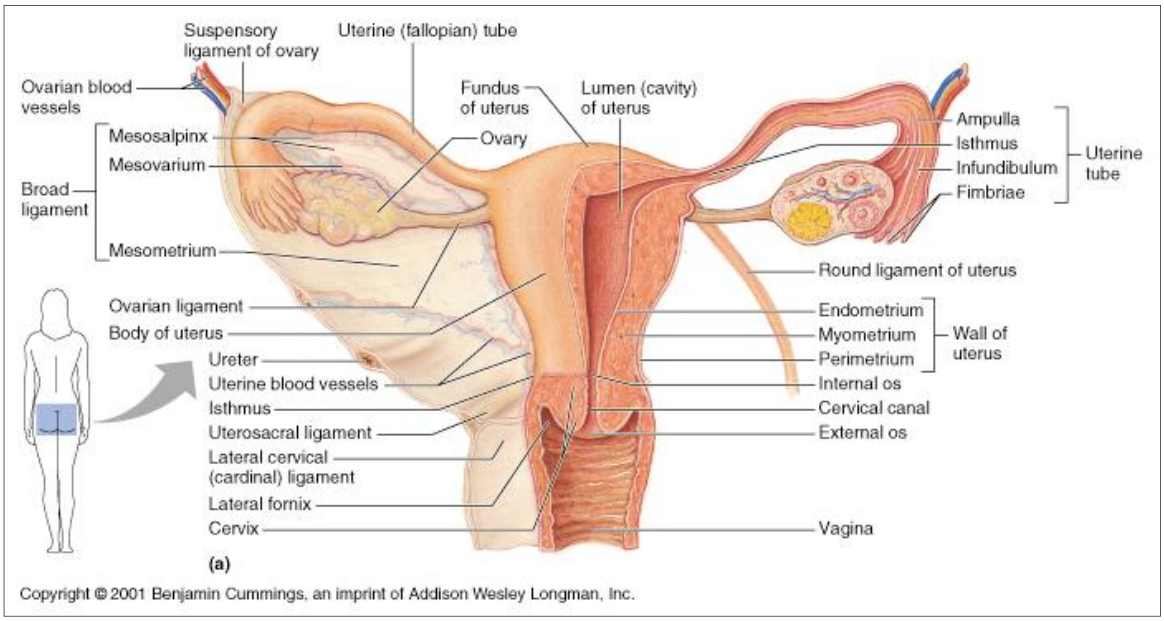

Figure 1: ***Anatomy of ovary.*** Animated Dissection of Anatomy for Medicine (A.D.A.M.) (www.adameducation.com) and Human anatomy and Physiology by Benjamin Cummings.

The tissues of the ovaries are arranged into several distinct layers:

- A most external layer of simple epithelium, known as the germinal epithelium, forms a soft, smooth covering of the ovary.
- The tunica albuginea is a thick band of tough fibrous connective tissue just below the germinal epithelium, which supports and protects the delicate underlying tissues.
- Deep to the tunica albuginea is the ovarian cortex, which contains follicles and their supporting connective tissues. The follicles contain oocytes that mature into ova throughout a woman's reproductive years.
- The innermost layer, the ovarian medulla, contains most of the vascular tissue that supports the other layers of the ovary.

The ovaries play two central roles in the female reproductive system by acting as both glands and gonads. Acting as glands, the ovaries produce several female sex hormones including

estrogens and progesterone. Estrogen controls the development of the mammary glands and uterus during puberty and stimulates the development of the uterine lining during the menstrual cycle. Progesterone acts on the uterus during pregnancy to allow the embryo to implant and develop in the womb.

The most important disorders of the ovaries are: ovarian cysts and ovarian cancer. Ovarian cysts are fluid-filled sacs that can form in the ovaries when either egg is not released or the follicle, a sac in which egg cells form, does not dissolve after the egg is released. Small ovarian cysts are common in healthy women, but some women have more follicles than usual (polycystic ovary syndrome), which inhibits the follicles to grow normally and this will cause cycle irregularities. Most cysts are not cancerous and will not become cancerous. In the past, surgery to remove cysts was the treatment of choice, but many studies showed that regular monitoring of the cyst, using ultrasound scan and blood tests, is possible for most women.

The protein CA125 (cancer antigen 125) is normally analyzed in the blood of women affected by ovarian cysts, and high levels are indicative of ovarian cancer. Other chemicals analyzed to diagnose ovarian cancer are: lactate dehydrogenase (LDH), alpha feta protein (AFP) and human chorionic gonadotropin (HCG).

Ovarian cancer is the seventh most common cancer in women (Figure 2) and the 18th most common cancer overall worldwide.

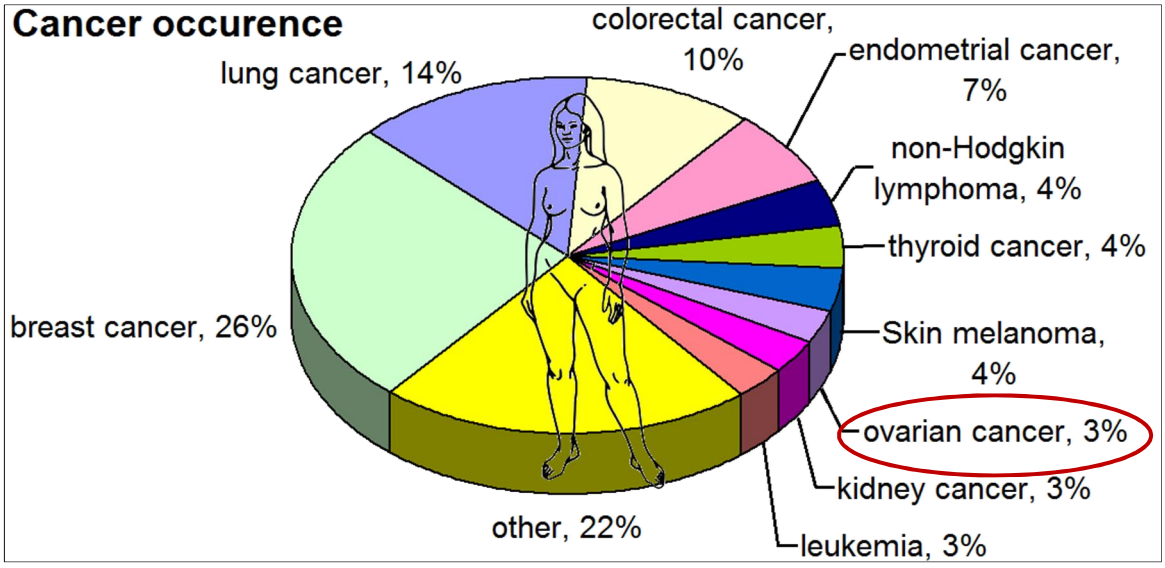

Figure 2: ***Cancer occurrence in women.*** Ovarian cancer is the seventh most common cancer in women. Jemal A, Siegel R, Ward E *et al.* (2008). "Cancer statistics, 2008". *CA Cancer J Clin* (2):71-96.

SEER (Surveillance, Epidemiology and End Results – Program of the National Cancer Institute, which works to provide informations on cancer statistics) estimates that in 2014, about 21.980 new cases of ovarian cancer are diagnosed and 14.270 women are died of ovarian cancer (Figure 3). A woman's lifetime risk of developing invasive ovarian cancer is 1 in 72 and of dying from it is 1 in 100.

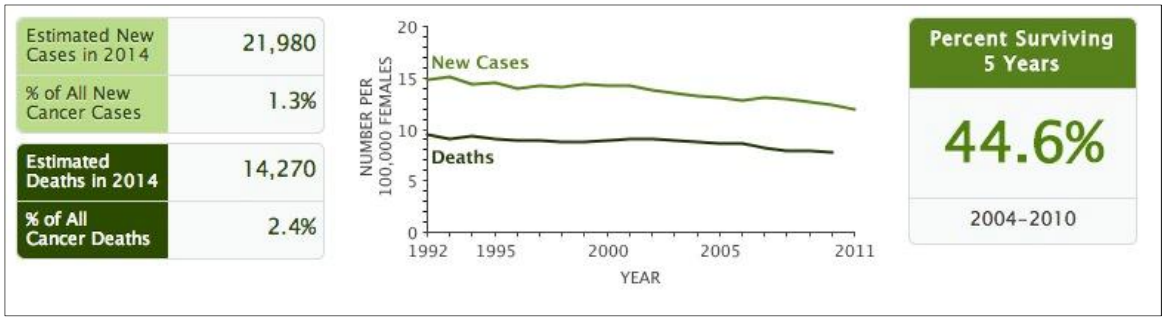

Figure 3: ***Statistics of ovarian cancer – SEER analysis.*** *National Cancer Institute (http://seer.cancer.gov/statfacts/html/ovary.html)*

Ovarian cancer rates are highest in women aged 55-64 years. Five-year survival rates are commonly used to compare different cancers and the relative survival rate for ovarian cancer is 44,6 percent. Survival rate varies greatly depending on the time of diagnosis, but approximately only 15 percent of ovarian cancer patients are diagnosed early with early stage disease. As a matter of fact, ovarian cancer is denominated "silent killer" [4, 5], because more than 80 percent of patients have symptoms, even when the disease is still limited to the ovaries. Moreover, the symptoms are shared with many more common gastrointestinal, genitourinary and gynecological diseases.
The diagnosis can be formulated through the following methods: transvaginal sonography (TVS), serum markers, and a combination of the two modalities .
Among the serum markers, the CA125 protein has received most attention, but greater specificity can be achieved by combining it and TVS. Data from a clinical trial, done in United Kingdom in 200.000 subjects, suggest that this strategy could increase the percentage of disease detection at early stages (48%) with adequate sensitivity (89,4%) and specificity (99,8%).

Ovarian cancer has a distinctive biology and behavior at the clinical, cellular and molecular levels.
Some factors and conditions may increase a woman's risk of developing this condition:

- A family history of ovarian cancer: Women who have two or more close relatives with the disease have an increased risk of developing ovarian cancer. Certain genes, such as the BRCA 1 and 2 genes, are inherited and result in a high risk for development of ovarian cancer.

- A family history of breast or colon cancer also confers an increased risk for the development of ovarian cancer.
- Childbearing and menstruation: nulliparous women have a greater risk of developing ovarian cancer compared to women who have had children. In fact, the number of childbirths correlates directly with a decrease in risk of developing ovarian cancer. The likely explanation for this risk factor seems to be related to the number of menstrual periods a women has had in her lifetime. Those who began menstruating early (before age 12), had no children, had their first child after age 30, and/or experienced menopause after age 50 have a greater chance of developing ovarian cancer than the general population.
- Medications: Some studies showed that women who have taken fertility drugs, or hormone therapy after menopause, may have a slightly increased risk of developing ovarian cancer. The use of oral contraceptives, on the other hand, seems to decrease the chance of manifesting the disease.

Most tumors of the ovary can be grouped into one of three major categories: epithelial-, sex cord-stromal-, and germ cell tumors, according to the anatomic structures from which the tumors presumably originate. Each category includes a number of subtypes.
Epithelial ovarian carcinoma is the most frequent form (95% of all the tumors); based on histopathology and molecular genetic alterations, it is divided into five main types: high-grade serous (70%), endometrioid (10%), clear-cell (10%), mucinous (3%), and low-grade serous carcinomas (<5%). These types are essentially distinct diseases, as indicated by differences in epidemiological and genetic risk factors, precursor lesions, patterns of spread, and molecular events during oncogenesis, response to chemotherapy, and prognosis (Table 1) [6]. For a successful specific treatment, reproducible histopathological diagnosis of the tumor cell type is critical. The five tumor types are morphologically diverse and resemble carcinomas of the uterus. Actually, recent investigations have demonstrated that a substantial number of cancers, traditionally thought to be primary ovarian tumors (particularly serous, endometrioid, and clear-cell carcinomas), originate in the Fallopian tubes and the endometrium and involve the ovary secondarily. Unfortunately the exactly origin of ovarian cancer is poorly understood and probably it is the cause of the failures of early detection and new therapeutic approaches to reduce mortality incidence [7].

	HGSC	LGSC	MC	EC	CCC
Risk factors	*BRCA1/2*	?	?	HNPCC[a]	?
Precursor lesions	Tubal intraepithelial carcinoma	Serous borderline tumor	Cystadenoma/borderline tumor?	Atypical endometriosis	Atypical endometriosis
Pattern of spread	Very early transcoelomic spread	Transcoelomic spread	Usually confined to ovary	Usually confined to pelvis	Usually confined to pelvis
Molecular abnormalities	*BRCA, p53*	*BRAF, KRAS*	*KRAS, HER2*	*PTEN, ARID1A*	HNF1, *ARID1A*
Chemosensitivity	High	Intermediate	Low	High	Low
Prognosis	Poor	Intermediate	Favorable	Favorable	Intermediate

Table 1: ***Epithelial ovarian carcinoma: clinical and molecular features of the five most common types.*** *HGSC, high-grade serous carcinoma; LGSC, low-grade serous carcinoma; MC, mucinous carcinoma; EC, endometrioid carcinoma; CCC, clear-cell carcinoma. [a]Hereditary nonpolyposis colorectal carcinoma.* Lalwani N., Prasad S.R., Vikram R., Shanbhogue A.K., Huettner P.C., Fasih N. Histologic, Molecular, and Cytogenetic Features of Ovarian Cancers: Implications for Diagnosis and Treatment. RadioGraphics 2011;31:3.

The International Federation of Gynecology and Obstetrics (FIGO) has classified ovarian carcinoma in four stages [8]:

- Stage 1: tumor is confined to ovaries and Fallopian tubes;
- Stage 2: tumor involves one or both ovaries or Fallopian tubes with pelvic extension or primary peritoneal cancer;
- Stage 3: tumor involves one or both ovaries or Fallopian tubes, or primary peritoneal cancer, with cytologically or histologically confirmed spread to the peritoneum outside the pelvis and/or metastasis to the retroperitoneal lymph nodes;

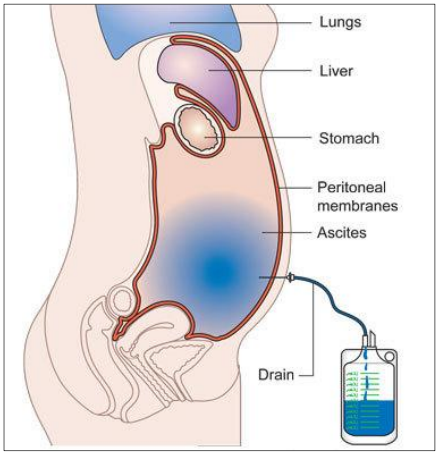

- Stage 4: distant metastasis excluding peritoneal metastases.

Furthermore, one third of ovarian cancer patients present with ascites, a generally voluminous exudative fluid with a cellular fraction consisting mainly of ovarian cancer cells, lymphocytes, and mesothelial cells (Figure 4). The neoplastic cells in the ascites are present either as single cells, as aggregates, or as spheroids, and may contribute to the spread of cancer to secondary sites [9].

Figure 4: ***Ovarian carcinoma ascitic fluid.*** *Cancer Research UK (www.cancerresearchuk.org).*

Treatment usually relies on surgery and chemotherapy, sometimes in combination with radiotherapy, and is obviously more efficient when the disease is confined to the ovary. Chemotherapy include paclitaxel, cisplatin, topotecan and gemcitabine. Due to the lack of

effective screening programs, ovarian cancer is diagnosed at an early stage only in about 20% of the cases. In most of these cases, surgery is able to cure the disease, and the five-year survival rate for early-stage (stage I or II) ovarian cancer is around 90%. Instead the standard treatment for patients with advanced ovarian cancer is maximal surgical cytoreduction followed by systemic platinum-based chemotherapy and, actually, is reasonable to expect a 5-year survival for 10-30% of women diagnosed with ovarian cancer at stage 3 or 4. Despite the activity of first-line chemotherapy, which gives response rates up to 80% in first line treatment, the majority of patients due to recurrencies. For this reason, ovarian carcinoma is considered a chemo-resistant cancer, and studying its biology to improve the therapies mandatory [10].

Many studies have demonstrated a correlation between the phenomenon of chemoresistance and the presence of a small and rare cellpopulation with characteristics of stemness, the Cancer Stem Cells [11].

1.2 Stem Cells and stemness

Stem cells are the precursor of all cells in the human body and what makes stem cells special is their extreme “flexibility”.

They are characterized by the following features:

- Self-renewal: it is the process by which stem cells divide to make more stem cells, perpetuating the stem cell pool throughout life in a non-differentiate state. This requires a tight cell cycle control and often maintenance of multipotency or pluripotency, depending on the stem cell. Self-renewal programs involve networks that balance proto-oncogenes (promoting self-renewal), gate-keeping tumor suppressors (limiting self-renewal), and care-taking tumor suppressors (maintaining genomic integrity). These cell-intrinsic mechanisms are regulated by cell-extrinsic signals from the “niche”, the microenvironment that maintains stem cells and regulates their function in tissues.

- Potency: it is the potential to differentiate into different cell types. Stem cells can be: totipotent, when they are able to form all cell types in a body; pluripotent, when they create all cell types except for extra-embryonic tissues; multipotent, when they can differentiate into specific cell types, closely related to the tissue where they are localized.

- Asymmetric division: it is the capacity to form, during cell division, two daughters cells, one identical to the original stem cell, and another differentiated.

- Ability to survive in stress condition: it includes the resistance to drugs and natural toxins through the expression of several ATP-binding cassette (ABC) transporters, the active DNA repair capacity, and the relative resistance to apoptosis.

- Unlimited proliferation: stem cells are usually maintained in a quiescent state, but they are able to exit and rapidly expand and differentiate in response to stress. This ability depends on intrinsic and extrinsic regulatory mechanisms. For example, p53 (a protein usually mutated in the tumor), plays a critical role in arresting cell cycle at the G1/S regulation point. The microenvironment or "niche" of stem cells is also important. A niche consists of signaling molecules, inter-cellular contact, and the interaction between stem cells and the neighboring extracellular matrix (ECM). This microenvironment is thought to control genes and properties that define "stemness", the self-renewal ability and development to committed cells. This is why stem cells implanted into a totally different niche can potentially differentiate into cell types of the new environment.

This last characteristic of the stem cells is much exploited in the clinic, in the treatment of various diseases. As a matter of fact, regenerative medicine is an emerging branch of medicine with the goal of restoring organ and tissue function for patients with serious injuries or chronic diseases (Figure 5). Stem cells have the power to join these damaged areas and regenerate new cells and tissues by triggering a repair and renewal process, thus restoring functionality.

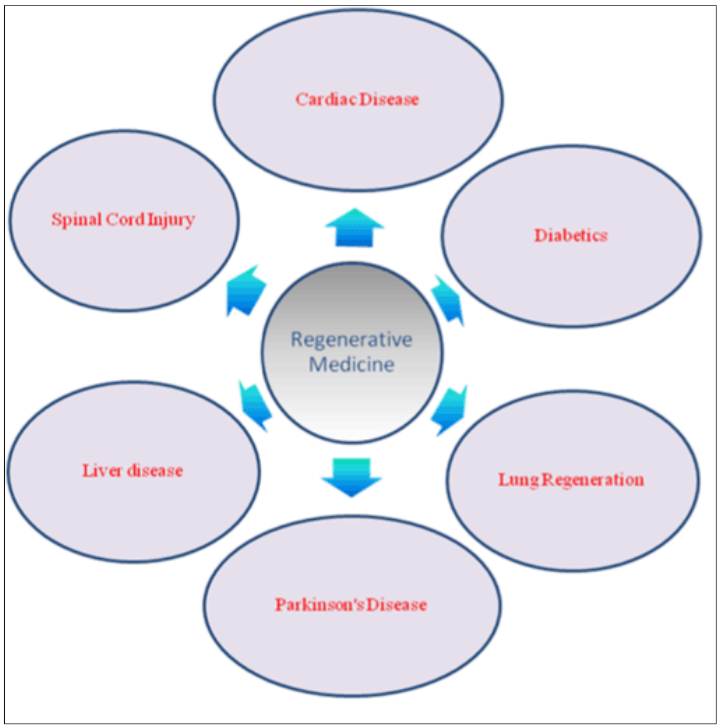

Figure 5: ***Application of stem cells in regenerative medicine.*** *Ramachandran R.P. and Yelledahalli L.U. Exploring the recent advances in stem cell research. J Stem Cell Res Ther 2011; 1:3.*

Bone marrow transplant is the most widely used stem cell therapy, suitable in the treatment of neurodegenerative disease and conditions such as diabetes, heart disease and other conditions. For example, embryonic stem cells and umbilical cord blood also shows promise in the field of cardiac regeneration, but there is a lot of ethical problems in this application. In fact the uses of adult stem cells are morally ethical, but it is unethical to use embryonic stem cells since it involves the destruction of the embryos. Excellent progress has been made with the discovery that organ regeneration is also possible through stem cells from one organ used to form cells of another organ. As a matter of fact, Mesenchimal Stem Cells (MSCs) have the capacity to differentiate into several cell types, and they can be isolated from adult tissues such as bone marrow and adipose tissue; for example, studies have demonstrated their ability to form neural cells both *in vitro* and *in vivo* [12].

Stem cells are also used as a cancer treatment. Stem cell transplants, from bone marrow or other sources, can be an effective treatment for people with certain forms of cancer, such as leukemia and lymphoma. While high doses of chemotherapy and radiation can effectively kill cancer cells, they have an unwanted side effects, as they can also destroy the bone marrow, where blood cells are made. The purpose of a stem cell transplant or a bone marrow transplant is to replenish the body with healthy cells and bone marrow when chemotherapy and radiation are completed. In some cases, the transplant can also have an additional benefit; the new blood cell may attack and destroy any cancer cells that survived the initial treatment [12].

Despite the above potential benefits of stem cells, these latter could also be regarded as a double-edge sword. In fact, it is now known their involvement in the onset of tumors, especially at later modifications, derived from the accumulation of gene mutations, in the pathways that control their self-renewal ability, such as Wnt, Hedgehog and Notch pathways.

1.3 Cancer Stem Cells (CSC)

CSC are the evil side of the stem cells, defined as “immortal tumor initiating cells that can self-renew and have pluripotent capacity” [13]. Hans Clevers adds that “the CSC concept postulates that, similar to the growth of normal proliferative tissues such as bone marrow, skin or intestinal epithelium, the growth of tumors is fueled by limited numbers of dedicated stem cells” [14].
Cancer cells with features of stem cells were discovered by Rudolf Virchow; in the mid – 19th century, he found that some cancer cells had histological characteristics and proliferation and differentiation capacities similar to embryonic cells. In the seventies, numerous studies showed that the tumorigenic ability of cancer cells was different in leukemia and in solid tumors. This idea underlined a new concept, that hematologic cancer is a new “stem-cell disease”, which is initiated from transformed stem cells and developes as a heterogeneous tissue, containing cancer stem cells and differentiated malignant subpopulations [15]. The

development of new technologies, such as flow cytometry, has permitted the characterization of these cells. The first evidence for CSC was published in 1997 by Bonnet and Dick [16], who isolated a rare cellular fraction of leukemia-initiating cells with stem cell-like features. In their reports, only the $CD34^{+}CD38^{-}$ cell population from acute myeloid leukemia (AML) patients could originate hematopoietic malignancy in NOD-SCID mice; indeed tumorigenicity *in vivo* is regarded as the most important CSC feature in the following studies of characterization. As a matter of fact, CSC have been consequently characterized in most solid tumors like breast, brain, colon, melanoma, pancreatic, prostate, ovarian, hepatic, lung and gastric tumors [17,18,19,20]. The first important evidence was the isolation of $CD44^{+}CD24^{-}$ breast cancer stem cells from breast cancer patients in 2003 by Al-Hajj et al. [17].

On the whole, these investigations have introduced the concept of a hierarchical model to explain the heterogeneity of the cancer. Some decades ago the most popular idea was represented by the so-called stochastic model, which assumed that every cell within a tumor has the same potential to maintain the growth of the tumor; in other words, there was a probability that a specific event in a tumor cell population could transform any tumor cell into a tumor-initiating cell [21, 22]. On the contrary, another model, the so-called hierarchical model, is now widely accepted; this model assumes that a pool of cancer stem cells represents a biologically distinct subset within the malignant cell population, which is responsible for the initiation and maintenance of the a heterogeneous tumor mass (Figure6).

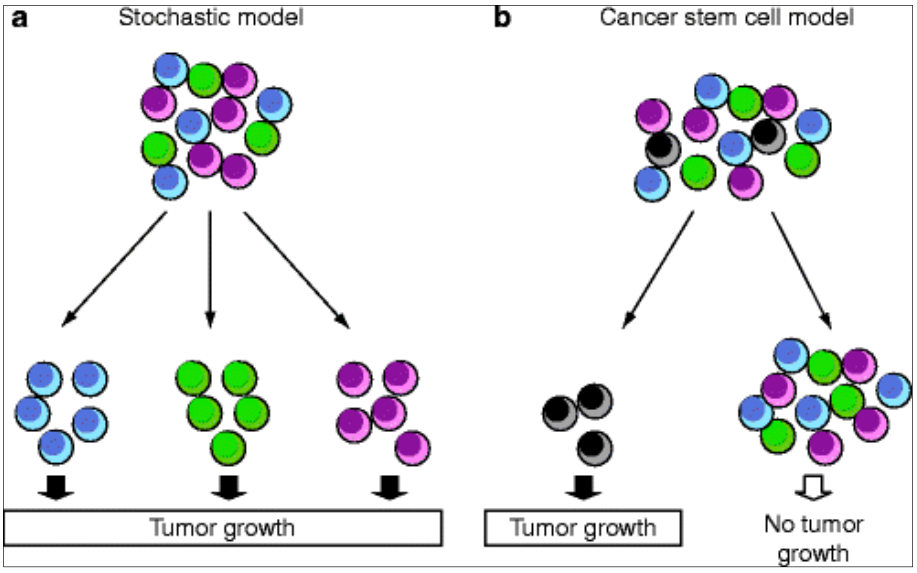

Figure 6: ***Two models to explain the cellular heterogeneity in cancer: the stochastic model and the hierarchy model.*** *In the stochastic model, every tumor cell can stochastically generate a tumor. In the hierarchy model, only the cancer stem cells (CSCs) will generate tumors.* Stem cells – Encyclopedia of Cancer 2012, pp 3517-3523.

There is not a firm evidence on the exact origin of the CSC , and different hypothesis have been proposed. It is possible that CSC arise by mutation of normal stem cells, and they maintain all the stemness features, like self-renewal, asymmetric division, property of unlimited proliferation and properties to differentiate into any cell type. However, some evidence also indicates that cancer stem cells could arise from mutated progenitor and differentiated cells (Figure 7) [23]. Such progenitor and differentiated cells can possess proliferation ability with different grade, but they do not have the self-renewal capacity, so to become a cancer stem cells they need to acquire specific mutations in genes controlling proliferation pathways.

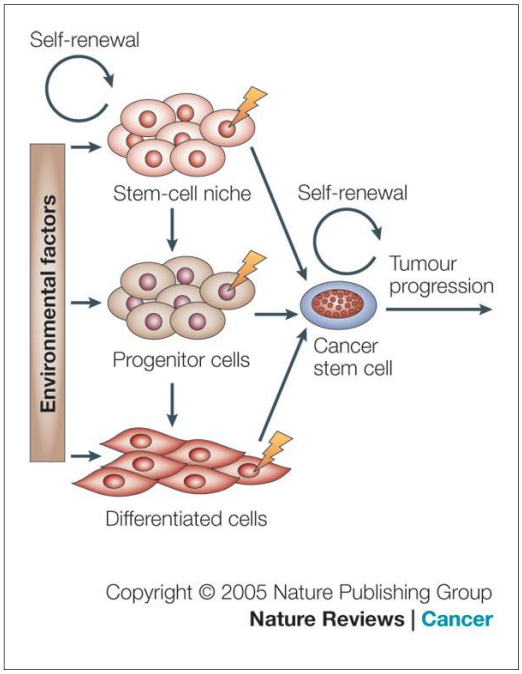

Figure 7: ***The origin of the cancer stem cells.*** *Cancer stem cells can arise from mutated normal stem cells, progenitor cells and differentiated cells, in response to a selective pressure given by environmental factors.* Bjerkvig R., Tysnes B.B., Aboody K.S., Najbauer J. and Terzis A. J. A. *The origin of the cancer stem cell: current controversies and new insights.* Nature Reviews 2005; 5: 899-904.

CSC are distinct populations of tumor cells, and a lot of work has demonstrated some of their peculiar properties:

- they are the responsible for the initiation and maintenance of the tumor growth, thanks to their self-renewal ability and to their state of quiescence, which permits them to survive in specific stress condition like nutrient or oxygen starvation;

- they are chemoresistant, thanks to some specific mechanisms including ABC transporter expression, aldehyde dehydrogenase (ALDH) activity, enhanced DNA damage response and activation of key signaling pathways [24];

- they are the responsible for cancer recurrence following chemo- or radiotherapeutic treatment, since they are able to maintain a state of dormancy [25]. Many of the biological mechanisms involved in controlling the dormant state of a tumor can also govern CSC behavior, including cell cycle modifications, alteration of angiogenic processes, and modulation of anti-tumor immune responses [14];

- they are responsible for metastasis, since many studies have demonstrated [26] the linkage between CSC and epithelial-to-mesenchymal transition (EMT), a key phenomenon in early steps of metastasis. Indeed, CSC express some pleiotropic transcriptional factors able to induce EMT through disruption of epithelial adhesion and junction, such as Snail, Slug, Zeb1 and Bmi-1 [27,28];

- they are characterized by the expression of specific surface markers, which in some cases allow their isolation a difficult task due to the fact that they are a rare population (<1% of the bulk tumor population). Unfortunately, a universal marker for characterizing the CSC in all types of tumors (Table 2) is not available yet.

Tumor type	Cell surface marker
Acute Myeloid Leukemia (AML)	$CD34^+/CD38^-$
Breast Cancer	$ESA^+/CD44^+/CD24^-/Lineage^-$
Ovarian Cancer	$CD133^+$ $CD44^+/CD117^+$
Glioblastoma	$CD133^+$ $CD15^+$
Medulloblastoma	$CD133^+$ $CD15^+$
small cell and non-small cell lung cancer	$CD133^+$
Hepatocellular carcinoma	$CD45^-/CD90^+$
Prostate cancer	$CD44^+/A2B1$ hi/$CD133^+$
Colon cancer	$CD133^+$ $CD44^+$
Melanoma	$CD20^+$ $ABCB5^+$
Pancreas adenocarcinoma	$CD44^+/CD24^+/EpCAM^+$
Renal carcinoma	CD133 enhances vascularization
Head and neck squamous cell carcinoma (HNSCC)	$CD44^+$

Table 2: ***Cancer stem cells markers in different tumors.*** *Miltenyi Biotec antibody for CSC markers.*

1.3.1 Cancer Stem Cells in ovarian cancer

Recent evidence suggests that ovarian tumors, like other solid tumors, contain distinct populations of cells that are responsible for tumor initiation, maintenance and growth. Moreover, there is some evidence about the contribution of stem cell dysfunction in adult mammalian ovaries to ovarian cancer and polycystic ovary syndrome [29].
In this context, Bapat and colleagues have reported the first study on the isolation and identification of stem-like cells in ovarian cancer [30]. Zhang and colleagues have defined two specific markers that recognize a specific cell population with stemness properties, such as CD44 and CD117 [31]. CD44 is the receptor for hyaluronic acid and CD117, also known as c-Kit, is a tyrosine kinase oncoprotein receptor of the Stem Cell Factor (SCF) cytokine. In particular, Zhang and colleagues have analyzed tumor spheroid generation from the ascites of 5 patients with serous ovarian cancer; after serial passages in a stem cell-based medium, they observed that the surviving spheroid cells were highly enriched in CD44 and CD117 co-expressing cells (Figure 8).

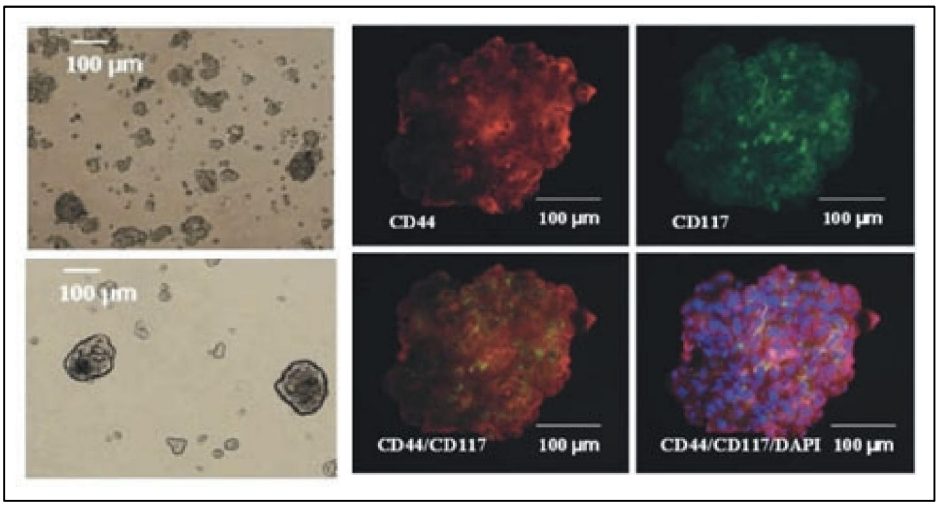

Figure 8: ***Spheroids of ovarian cancer stem cells.*** *(Left panel) Sphere forming in specific cell culture conditions, without serum and with the addition of specific growth factors; (Right panel) double staining for CD44 and CD117 in spheroids by immunofluorescence.* Zhang S., Balch C., Chan M.W., Lai H.C., Matei D., Schilder J.M., Yan P.S., Huang T. and Nephew K.P. Identification and characterization of ovarian cancer initiating cells from primary human tumors. Cancer Research 2008; 68(11): 4311-4320.

Moreover, these ovarian tumor spheroids cells were characterized by: overexpression of stem cell genes, like Bmi-1, SCF, Oct-4, Notch-1, Nanog, Nestin, ABCG2; resistance to conventional chemotherapies, such as cisplatin and paclitaxel. One of the most important feature, demonstrated in Zhang's work, was the high tumorigenicity of $CD44^+$ $CD117^+$ cells; in particular injection of 100 $CD44^+$ $CD117^+$ cells was tumorigenic in nude mice with tumor latencies of 73 to 102 days, whereas the injections of up to 10^6 bulk tumor cells failed to form tumors, tumorigenic with extended latencies [31].

Other reports demonstrate different ovarian CSC markers [32]. For example, one of the most widely described is CD133 or Prominin, that is a membrane glycoprotein encoded by the CD113/Prom-1 gene. CD133 was first detected as a marker of hematopoietic stem cells and then Baba and colleagues [33] have isolated $CD133^+$ cells in ovarian cancer cell lines and in primary ovarian tumors. In particular, they have demonstrated that $CD133^+$ cells have a significantly enhanced capacity to form tumors following injection in to immunocompromised mice, compared to the $CD133^-$ cell fraction. Moreover, tumors derived from $CD133^+$ cells comprise both $CD133^+$ and $CD133^-$ cells, suggesting that $CD133^+$ cells could regenerate two phenotypically distinct populations. Unfortunately, the specificity of this marker is uncertain, because other studies have shown that isolated $CD133^-$ cells are also able to generate tumors. There are two possible explanations about these results: the first is that the tumor-initiating capacity derived is due to a small percentage of CD133+ cells contaminating the largely purified CD133- population; the second is that another ovarian cancer stem cell population that is not characterized by CD133 expression could give rise to CD133 cells with tumor-initiating capacities [34] (Figure 9).

Another marker of ovarian cancer stem cells is ALDH (aldehyde dehydrogenase isoform 1), a detoxifying enzyme involved in the phenomenon of chemo resistance. As a matter of fact, cells with active ALDH ($ALDH^+$) isolated from ovarian cancer cell lines are chemo resistant and more tumorigenic than $ALDH^-$ cells [35]. This chemo resistance was also demonstrated by Landen and colleagues, who through experiments of ALDH gene silencing demonstrated that the down-regulation of ALDH1A sensitized resistant cells to chemotherapy both in culture and in an *in vivo* xenograft model [36].
In reference to the idea that the isolation of CSC is more effective through the overlapping expression of two or more CSC markers, Silva and colleagues reported the existence of a highly proliferative $ALDH^+CD133^+$ cell fraction in ovarian cancer cell lines. Moreover, ovarian tumor-derived $ALDH^+CD133^+$ cells had high tumor initiating capacity and formed tumors with shorter latency compared to the $ALDH^-CD133^+$, $ALDH^+CD133^-$ and $ALDH^-CD133^-$ cell populations (Table 3) [35].

Finally, ovarian CSC have also been identified as the so-called “Side Populations” (SP), in view of the property of CSC to efflux toxins like chemotherapeutic agents via members of the ATP-binding cassette transporter families, such as ABCG2. This property has allowed the identification of a side population fraction with enhanced ability to efflux lipophilic substrates like the dye Hoechst 33342. Many studies have demonstrated in SP cells the following characteristics: tumorigenicity, resistance to cytotoxic treatment and expression of stemness and multi-drug resistance genes [37].

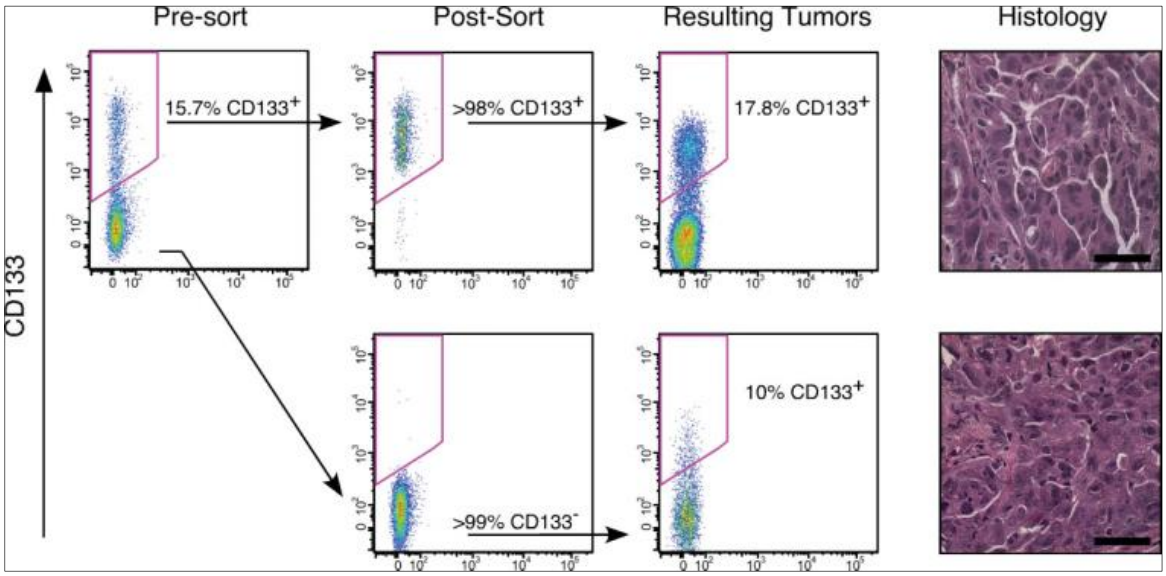

Figure 9: Sorted CD133$^+$ and CD133$^-$ cells generate histologically similar tumors that contain CD133$^+$ cell fraction. Curley M.D., Therrien V.A., Cummings C.L., Sergent P.A., Koulouris C.R., Friel A.M., Roberts D.J., Seiden M.V., Scadden D.T., Rueda B.R., Foster R. *CD133 expression defines a tumor initiating cell population in primary human ovarian cancer.* Stem Cells 2009; 27:2875-2883.

Cell type	ALDH$^-$CD133$^+$	ALDH$^+$CD133$^+$	ALDH$^+$CD133$^-$	ALDH$^-$CD133$^-$
No. of cells injected	Tumors formed	Tumors formed	Tumors formed	Tumors formed
10–500	0/9	**4/9**	0/9	ND
5,000	ND	ND	0/5	0/9
50,000	ND	ND	ND	0/9

Table 3: ***Tumor initiating capacity of limiting diluitions of ALDH$^{+/-}$CD133$^{+/-}$ cells from primary human ovarian tumors.*** Silva I.A., Bai S., McLean K., Griffith K., Thomas D., Ginestier C., Johnston C., Kueck A., Reynolds R.K., Wicha M.S., Buckanovich R.J. *Aldehyde dehydrogenase in combination with CD133 defines angiogenic ovarian cancer stem cells that portend poor patient survival.* Cancer Res 2011; 71:3991-4001.

Unfortunately, these studies show some discrepancies, such as in one work the SP fraction has been isolated in paclitaxel-resistant cell lines, but not in the cisplatinum-resistant fraction, and it is unclear whether SP is correlated with multidrug resistance [38]. Moreover, SP cells are more prominent in ascites, recurrent tumors and disseminated in the peritoneal cavity; however a correlation between SP and disease stage was not significantly demonstrated [39].

These premises suggest that CD117 is the marker that best allows the isolation of a cell population characterized by self-renewal, tumor-initiating capacity and chemo-resistance. Moreover, CD117+ cells with stemness phenotype have been isolated not only in cell lines but also in primary samples with different grade of tumor dissemination and metastasis.

CD117 (c-Kit) is a well-known tyrosine kinase and for this reason it is an attractive target for cancer therapy.

Ovarian CSC have been analyzed in the last years for many characteristics, which allow their survival and proliferation and consequently the maintenance of tumor growth. Several developmental pathways, including Notch, Wnt, Hedgehog and transforming growth factor-β (TGF-β) are crucial for the regulation of self-renewal. In particular, TGF-β plays a key role in the modulation of EMT (epithelial mesenchimal transition) and in the induction of CSC migratory properties [40].
Moreover, there are some genes involved in the regulation of ovarian tumor-initiating cells. For example p53, a tumor suppressor protein, is related to the pathogenesis of high-grade serous adenocarcinoma of the ovary; recent work has demonstrated that ovarian CSC can be generated by silencing of p53 expression in tumor cells [41], in support of the idea that p53 dysfunction can enhance the self-renewal ability of ovarian stem-like tumor cells. Recently, Chau and colleagues have shown the importance of c-kit in the regulation of survival of ovarian CSC as well as their chemo resistance, through some demonstrated pathways mediated by phosphoinositide 3-kinase (PI3K)/Akt and Wnt/β –catenin- ATP-binding cassette G2 (ABCG2). C-Kit is overexpressed in ovarian CSC and solid evidence has shown that knockdown of c-kit expression or inhibition of its activity by Imatinib decrease the tumorigenic capabilities and chemo resistance [42].
Lastly, also miRNA have recently emerged as an important regulator of CSC. The most important, characterized in ovarian CSC, are miR-214, miR-199a and miR-200. In particular miR-199a suppresses the tumorigenicity and chemo resistance of the $CD44^{+}CD117^{+}$ cell fraction, through the repression of CD44 expression, that in turn inhibits migration and invasion of these cells.

All the above features could be a potential target to improve ovarian cancer therapy, but a new idea is that capacity of self-renewal could also be maintained by the surrounding environment. In particular, the CSC niche in ovarian cancer includes immune cells, stromal cells, blood vessels and extracellular matrix components. All these cell types could be a target for therapy; indeed several biological processes, that occure in CSC niche, including inflammation, hypoxia and angiogenesis could be important to determine the fate of CSC. For these reason it is really fundamental to focus on tumor microenvironment to find the fundamental mechanisms of CSC survival and maintenance (Figure 10) [43].

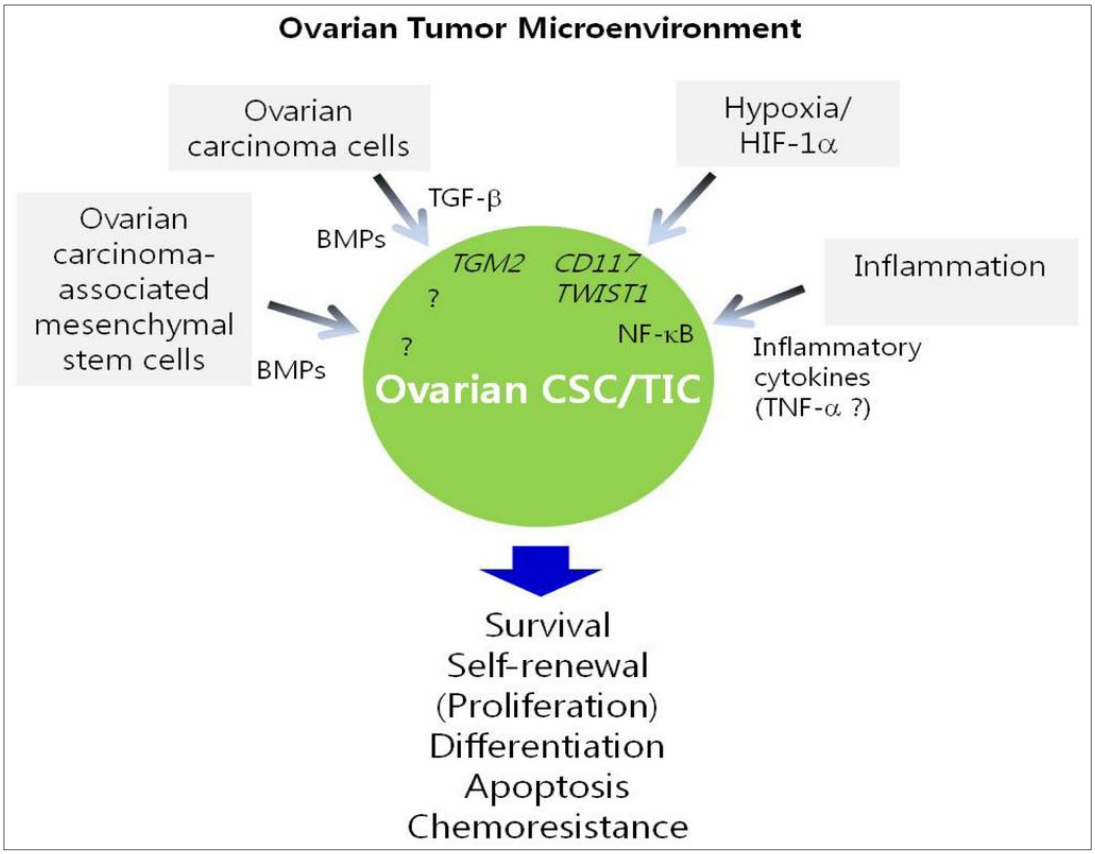

Figure 10: The tumor microenvironmet involved in the maintenance and regulation of ovarian cancer stem cells. Kwon M.J. and Shin Y.K. *Regulation of ovarian cancer stem cells or tumor-initiating cells.* Int. J. Mol. Sci. 2013; 14:6624-6648.

1.4 Role of cancer stem cells in chemoresistance and importance of targeting CSCs

One of the most important features of the CSC is their chemo resistance, in view of its fundamental implication in the clinics. As a matter of fact, all the current therapeutic strategies against cancer have severe limitations that frequently lead to treatment failure. The reason is that these strategies is not selective against CSC; thus, the incidence of recurrence and metastasis is high, because these therapies cannot eliminate CSCs. Several pathways could be involved in these mechanisms, including activation of anti-apoptotic factors, inactivation of pro-apoptotic effectors, and reinforcement of survival signals. These survival signals are: efficient DNA repair mechanisms, expression of drug pumps and altered cell-cycle. Moreover, CSC are mostly quiescent and therefore can escape chemotherapy-induced cytotoxicity which acts on dividing cells.

Based on these premises, it is essential to develop treatments that target CSC, but the challenges are formidable (Figure 11).

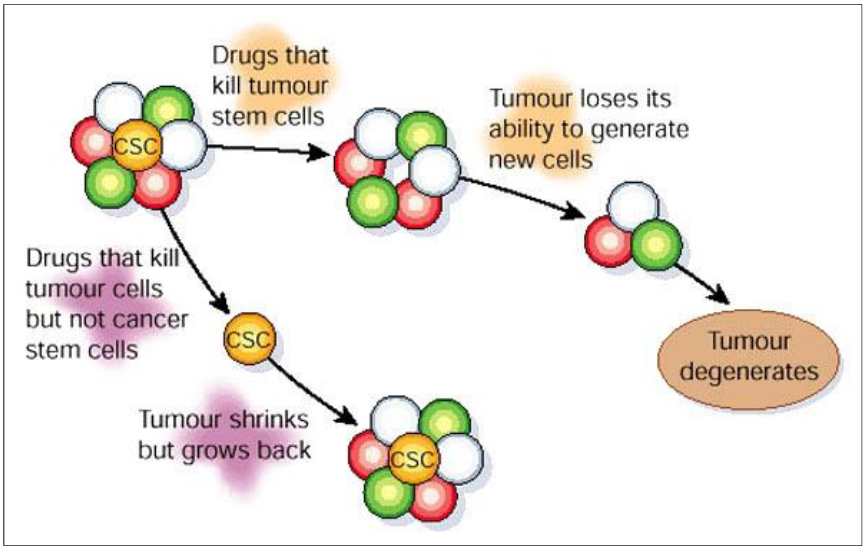

Figure11: ***"Stemline therapy", the new therapy must to target Cancer Stem Cells.*** Reya T., Morrison S.j., Clarke M.F. and Weissman I.L. *Stem cells, cancer, and cancer stem cells.* Nature 2001; 414:105-111.

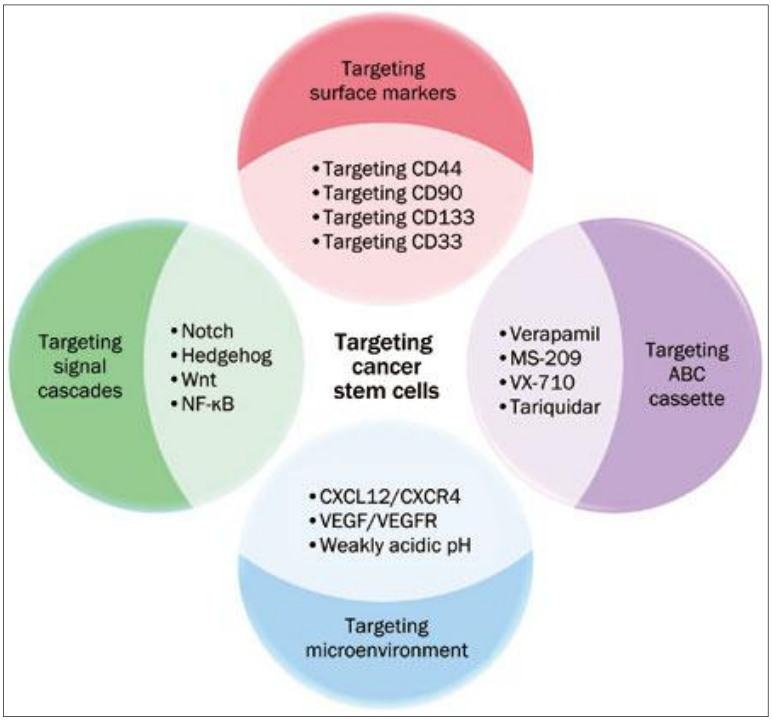

Figure 12: Therapies targeting cancer stem cells. Targeting surface markers of CSCs (*red area*), specific pathways involved in the self-renewal (*green area*), inhibiting ABC cassette (*purple area*), targeting microenvironment (*blue area*). Chen K., Huang Y. and Chen J. *Understanding and targeting cancer stem cells: therapeutic implications and challenges.* Acta Pharmacologica Sinica 2013; 34: 732-740.

Targeting CSC might be a strategy to improve outcome of cancer patients but the complexities that lie within this approach will provide many problems in clinical applications. Some of these hurdles include overcoming the immune heterogeneity in CSC population as well as the problem of epitopes shared with normal stem cells and the necessity to identify additional CSC antigens. Indeed, drug treatment for CSC may increase the risk of toxicity since CSC share common features with normal stem cells.

The current therapeutic strategies targeting CSC [44, 45] are discussed below (Figure 12). Important interest has been generated in the development of monoclonal antibodies to target CSC markers of CSCs. For example Imatinib, a potent CD117 (c-KIT) specific inhibitor, has been used in clinical trials for the treatment of many types of cancer, including epithelial ovarian cancer [45].

Researchers have also designed numerous pharmacological agents that can interact with ABC transporters, to inhibit multidrug resistance. In this regard, Verapamil was the first identified inhibitor, often used in side population analysis to block the exclusion of the dye Hoechst. Moreover, the combination of Tariquidar, another inhibitor, and Docetaxel is under investigation in ovarian cancer [46].

Another therapeutic strategy could be the induction of differentiation and loss of the self-renewal properties. Drugs such as retinoic acid or drugs that aim to generate epigenetic changes in the tumor can stimulate CSC differentiation. Whitworth and his colleagues reduced growth of ovarian CSC with carboplatin combined with three novel retinoid compounds [47]. Moreover, it is possible to find some specific inhibitors of the pathways that control self-renewal and cell fate decisions of stem cells and progenitor cells, such as Wnt, Hedgehog and Notch. Recently, McAuliffe and colleagues have demonstrated the importance of the Notch signaling pathway and Notch3 in particular in the regulation of CSC in ovarian cancer; interestingly they have shown that γ-secretase inhibitor (GSI), a Notch pathway inhibitor, depletes efficiently CSC [48].

Last but not least, tumor microenvironment has assumed a prominent importance in the last years, in term that it can create a niche to protect CSCs from drugs and specific nutrient or oxygen stress. The supporting role of the microenvironment in tumor growth and progression, including metastasis formation, clearly puts the CSC niche and, especially, the mediators of this interaction in the spotlight as future therapeutic targets [49].

Taking up the words of Weinberg in his seminal work “tumors have increasingly been recognized as organs and the biology of a tumor can only be understood by studying the individual specialized cell types within it as well as the tumor microenvironment that they construct during the course of multistep tumorigenesis” [50]. Tumor microenvironment include many cell types such as endothelial cells, immune inflammatory cells, cancer associated fibroblasts; all these cells could be a suitable therapeutic target. But tumor niche also means the conditions in term of oxygen, nutrients, metabolites in which the cells grow,

thus constraining or permitting cell survival. For this reason in the last decades targeting cellular metabolism acquired a high interest, to improve cancer therapeutics.

1.5 Metabolism of cancer – Warburg effect

Cancer cells, unlike normal cells, privilege conversion of pyruvate to lactic acid for ATP generation rather than mitochondrial oxidative phosphorylation even in the presence of oxygen: this peculiar metabolic profile is termed aerobic glycolysis or the "Warburg effect" (Figure 13).

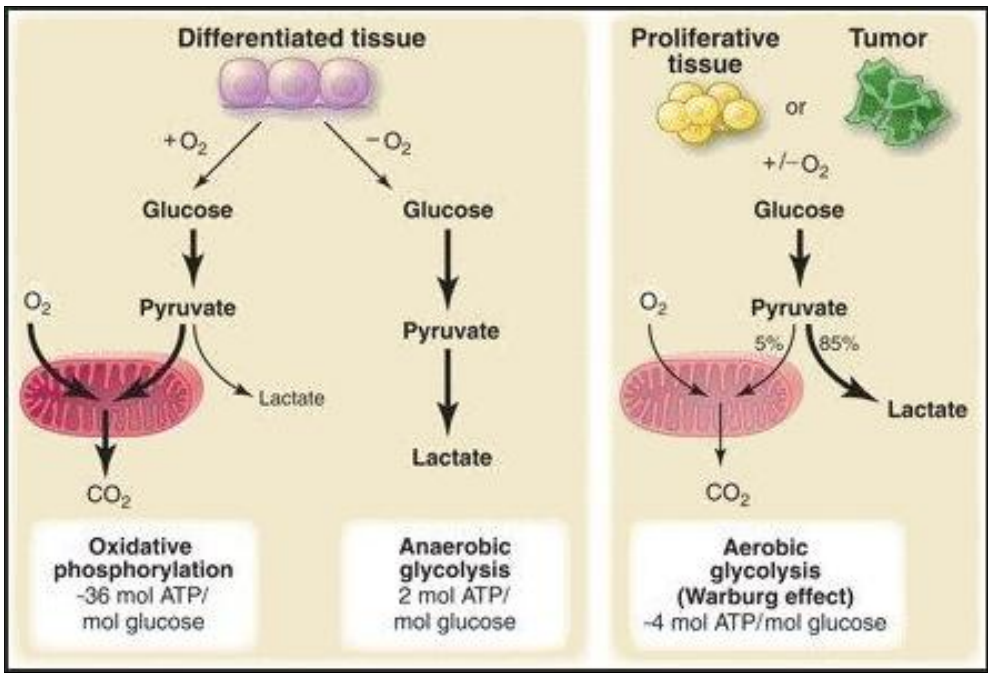

Figure 13: Warburg effect – aerobic glycolysis. Heiden MGV et al. *Understanding the Warburg Effect: The Metabolic Requirements of Cell Proliferation*. Science 2009; 324:1029.

Otto Warburg is a Nobel prize-awarded scientist (for the discovery of yellow enzymes (Flavins) and cytochrome oxidase). In 1930, Warburg observed an altered metabolism in cancer cells. In particular, by using a manometer, Warburg and his colleagues found that cancer cells did not consume more oxygen than normal tissue cells, even under normal oxygen circumstances [51]. Initially Warburg assumed that cancer cells had an impaired respiration due to the functional defects in mitochondria [52]. However, subsequent work showed that mitochondrial function is not impaired in most cancer cells, suggesting an alternative explanation for aerobic glycolysis in cancer cells. To explain the phenomenon observed, Warburg speculated some differences between normal cells and cancer cells.

Normal cells are characterized by a specific bioenergetics, essential to convert energy substrates (carbohydrates, proteins and lipids) in several metabolic intermediates that are used to synthesize nucleic acids, amino acids, glycogen and other biomolecules required for normal body functioning. In particular glucose, derived by the processing of carbohydrates, enters the cells through specific glucose transporters. In the cytosol, several enzymes catalyze glycolysis that ends with the production of pyruvate, which enters the mitochondria and it is converted to acetyl CoA by pyruvate dehydrogenase (PDH). Acetyl CoA condenses with oxaloacetate (OAA) to form citrate, which is completely oxidized in the Trichloeoacetic (TCA) cycle to generate reducing equivalents for the respiratory chain. The result of this metabolism called oxidative phosphorylation, in term of energy produced, is 2 ATP molecules from glycolysis and 34 ATP molecules from the respiratory chain. Therefore, normal cells in the presence of oxygen are able to produce 36 ATP molecules, which represent about the 90% of the energy requirements for the survival of a cell.
In some cases, the cells must survive in oxygen stress conditions, and they are able to switch their metabolism to anaerobic glycolysis. In particular, the cells can redirect the pyruvate generated by glycolysis away from mitochondrial oxidative phosphorylation by generating lactate, that allows glycolysis to continue by cycling NADH back to NAD^+, but results in minimal ATP production.

Cancer cells, according to the theory of Warburg, are characterized by an aerobic glycolysis, that means the ability to convert most glucose to lactate regardless of whether oxygen is present. It is conceivable that fast-growing cancer cells require more energy than normal cells and it is ironic to realize that, unlike normal cells, tumor cells use an inefficient reaction to generate considerable amounts of their energy. There are some specific reasons of this bioenergetics alteration and it is necessary to keep in mind that cancer cells must implement metabolic processes in very different and stressful environments, where nutrients supply may be low and where redox balance, pH and oxygen levels may not be maintained. First of all, the metabolism of cancer cells have to be adapted to facilitate the uptake and incorporation of nutrients into the biomass needed to produce a new cell: amino acids for protein synthesis, nucleic acids for DNA duplication and lipids for cell membrane synthesis. Moreover, glycolysis provides acidic environment, which is harmful to normal cells but has no effect onj tumor cells, underscoring the importance of glycolysis as a cellular defense mechanism for cancer cell growth. A third hypothesis is that glycolysis produces less reactive oxygen species (ROS), so that the genome of cancer cells might elude the damage incurred by high concentration of ROS. At the end, it is clear that glycolysis produce less ATP than oxidative phosphorylation, but it is reasonable to think that cancer cells need more metabolic intermediates than the simple ATP, which are essential to maintain their survival also in stress conditions.
Even though metabolism reprogramming in cancer cells is universally accepted as one of the hallmarks of cancer [3] and many questions about the efficiency of the Warburg effect remain largely unanswered, the Warburg's finding are exploited clinically by ^{18}F-

deoxyglucose positron emission tomography scanning, known as PET, for solid tumor detection. The ^{18}F-FDG is a glucose analogue which enters the cell in normal ways and it is phosphorylated like normal glucose to prevent its processing by glycolytic pathways before radioactive decay; thus, this parameters is a good reflection of glucose uptake in the body [53]. This ability to monitor glucose within tumors and the increase in glucose uptake by tumor cells confirm the Warburg's hypothesis and underline the importance of glucose in cancer metabolism and the contribution of this finding to clinical diagnosis.

Our major open question about cancer cell metabolic profile (Figure 14) is whether gene alterations could precede and cause metabolic derangements, or rather a special metabolic profile due to the energetic need of cancer cells could translate into genetic abnormalities.

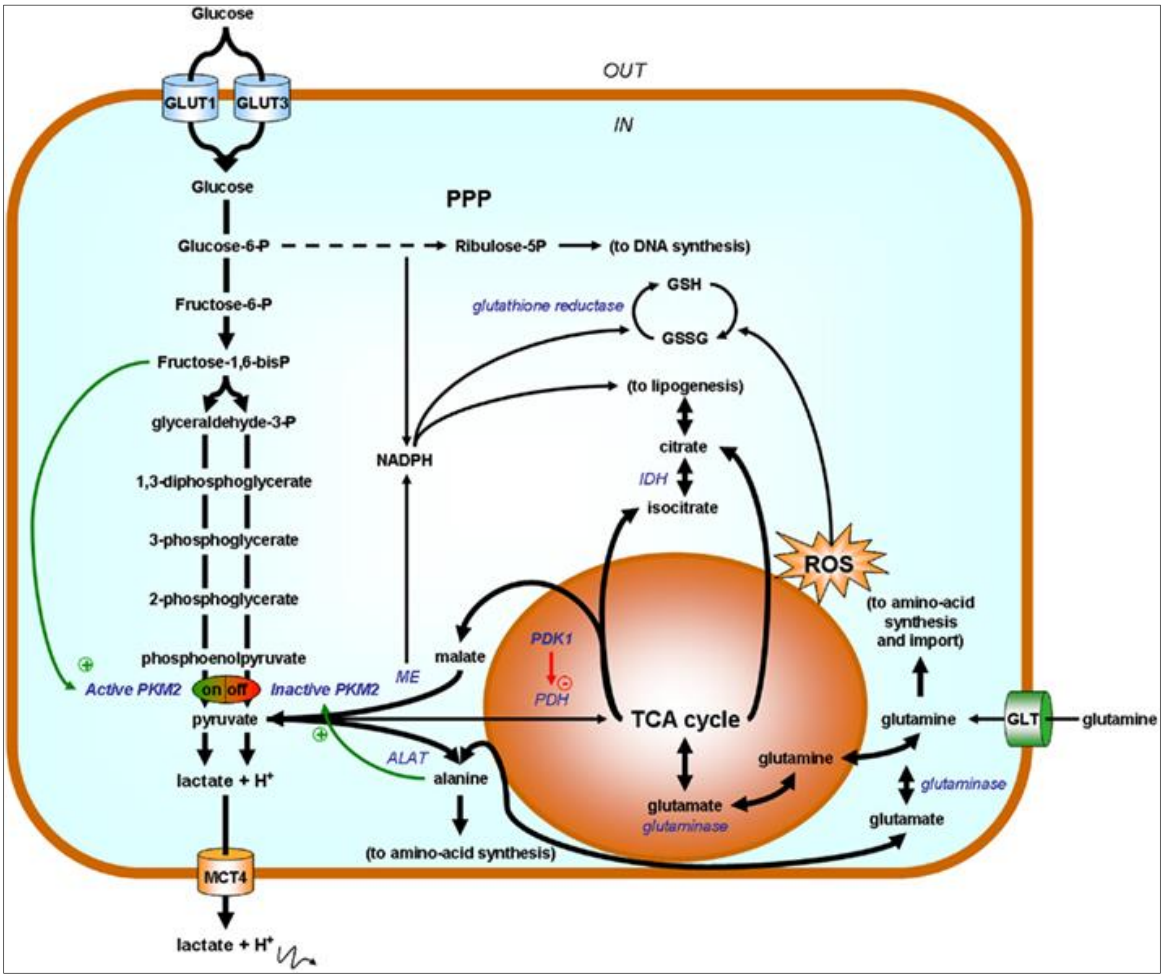

Figure 14: Cancer metabolism. Paolo E. Porporato, Suveera Dhup, Rajesh K. Dadhich, Tamara Copetti and Pierre Sonveaux. *Anticancer targets in the glycolytic metabolism of tumors: a comprehensive review.* Front. Pharmacol. 2011.

In fact, mutation of oncogenes or tumor suppressor genes is a well-known direct cause of cancer; on other hand, metabolic stresses, typical of tumor environment, may cause tumor-associated gene alterations and increment the probability of tumor growth. In this regard, mutations in metabolic genes also causes certain types of tumors and many of these genes encoding for mitochondrial enzymes, underlining the Warburg's hypothesis that cancer cells have primary defects in mitochondria.
The importance of some specific mutations in genes encoded metabolic enzymes is known: succinate dehydrogenase (SDH) [54], which catalyzes the conversion from succinate to fumarate in the TCA reactions, isocitrate dehydrogenase 1 (IDH1) [55], which converts isocitrate to α-ketoglutarate (α-KG), and pyruvate kinase form 2 (PKM2) [56], which is the key enzyme in the conversion of phosphoenol-pyruvate into pyruvate at the last second step in glycolysis.
At the end, one of the most important metabolic regulator is hypoxia-inducible factor (HIF), that is involved as a regulatory factor during hypoxia, a common phenomenon in tumors [57, 58]. HIF controls the expression of many target genes, such as genes encoding glucose transporters (GLUT), glycolysis enzymes like pyruvate dehydrogenase kinase (PDK) and lactate dehydrogenase A (LDH-A). Amplification of GLUT may allow cancer cells to compete with normal cells in the process of glucose uptake, while the up-regulation of PDK is able to inhibit the activity of pyruvate dehydrogenase (PDH), and the increased levels of LDH-A can accelerate the conversion of pyruvate to lactate. For these reasons, HIF target genes promote the Warburg effect.

All these premises show that there is still much to learn about how proliferating cell metabolism is regulated and many questions needed to be answered, such as if the metabolic properties of cancer cells are remarkably different from those of normal cells and if targeting metabolic enzymes could improve the efficacy of cancer therapy and overcome therapeutic resistance. In reference to Cancer Stem Cells, it is an exciting challenge to investigate of the CSC metabolism. In particular, little if anything is known about the metabolic profile of CSC and it is unclear whether CSC also present a prominent Warburg effect.

1.6 Therapies targeting the metabolic profile in cancer – possible targeting of CSC

The therapeutic window for targeting CSC includes two fundamental properties, possibly involved in the failure of current therapies: the chemo resistance and the dysregulation of metabolism. These two features are probably connected, but the molecular mechanisms by which targeting metabolism could impair chemo resistance is not fully understood and deserves further investigations. Given the explosion of interest and information on cancer metabolism, it is hoped that new therapies will emerge in the next decades; nonetheless there are already some drugs approved for clinical use in certain types of cancer and others under preclinical examination.

The dependence of cancer cells on aerobic glycolysis (Warburg effect) for ATP generation has been exploited as a target for anticancer therapies and many possibilities have been proposed [59] (Table 4).

a) The reduction of glucose entry into the cell, even though the toxicity associated to the glucose deprivation may be a major challenge for the use of this approach. Nonetheless, there are some drugs that reduce glucose uptake. For example: Imatinib (Glivec) is a tyrosine kinase inhibitor that leads to the internalization of cell surface GLUT1 (glucose transporter) and reduce glucose uptake [60]; 2-deoxyglucose (2-DG), a glucose analog, competes with glucose for transport across the cell membrane and, inside the cells, it is phosphorylated by the early enzymes of the glycolysis into 2-DG-6-phosphate, thus inhibiting glycolysis [61].
b) The inhibition of some fundamental enzymes of glycolysis, such as PKM2. TT-232 is an inhibitor of this enzyme [62].
c) The inhibition of pentose phosphate pathways (PPP), deemed as an important pathway for its role in the synthesis of nucleic acids, that are indispensable for rapid cell proliferation, and for production of NADPH, that reduces the oxidative stress. An analog of NADP (6-aminonicotinamide, 6-AN), inhibits glucose-6 phosphate dehydrogenase (G6PD, the first enzyme of the PPP pathway), thus increasing oxidative stress and reducing tumor growth [63]. However, different results have been obtained by Herter and colleagues, who demonstrated the neurotoxicity of high doses of 6-AN and the lack of anticancer activity of well-tolerated dose [64].
d) The inhibition of HIF-1, one of the most important regulators of glucose metabolism in cancer cells. Topotecan is an inhibitor of HIF-1 and promotes oxidative phosphorylation in tumor cells [65].
e) The promotion of oxidative phosphorylation in cancer cells, dependent on glycolytic metabolism. Different mechanisms have been proposed for the activation of mithocondrial respiration, such as the down-regulation of lactate dehydrogenase (LDH) by small interfering ribonucleic acid (siRNA) to prevent the conversion of

pyruvate in lactate [66] or the inhibition of pyruvate dehydrogenase kinase 1 (PDK1), which inhibits PDH the key enzymes of the TCA cycle, by antisense oligonucleotides [67].

Mechanism of action	Target gene	Inhibitor(s)	Reference(s)
Reduction of glucose entry into the cell	GLUT1	Imatinib	Barnes et al., 2005
		2-DG	Maher et al., 2005
		Phloretin	Cao et al., 2007
		Fasentin	Wood et al., 2008
Inhibition of phosphorylation of glucose	HK	LND	Floridi et al., 1981
		3-BrPA	Chen et al., 2007 and Zhang et al., 2012
		Mannoheptulose	Board et al., 1995, Scatena et al., 2008 and Pathania et al., 2009
		Methyl jasmonate	Madhok et al., 2011
Inhibition of fructose-6-PO_4 to fructose-1,6-bisphosphate	PFK1	3-PO	Clem et al., 2008
Inhibition of phosphoenolpyruvate to pyruvate	PKM2	TT-232	Szokoloczi et al., 2005
		Flourophosphates creatine phosphate oxalate, l-phospholactate	Madhok et al., 2011
Suppression of pentose phosphate pathway	TKTL1	Oxythiamine	Rais et al., 1999
	G6PD	6-AN	Kohler et al., 1970 and Varshney et al., 2005.
Promotion of pyruvate entry into mitochondria	PDK1	DCA	Michelakis et al., 2008
Reduction of HIF-1 activity	HIF-1α	Topotecan	Rapisarda et al., 2002 and Rapisarda et al., 2004
		Digoxin	Zhang et al., 2008
		YC-1	Semenza, 2003
		GA	Isaacs et al., 2002
		2ME2	Mabjeesh et al., 2003
		PX-478	Welsh et al., 2004
		Echinomycin	Cairns et al., 2007

Table 4: Anticancer therapies targeting aerobic glycolysis. Abbreviations: 2-DG, 2-deoxyglucose; LND, lonidamine; 3-BrPA, 3-bromopyruvate; 3-PO, 3-(3-pyridinyl)-l-(4-pyridinyl)-2-propen-l-one; 6-AN, 6-aminonicotinamide; DCA, dichloroacetate; GA, geldanamycin; 2ME2, 2-methoxyoestradiol; PX-478, S-2-amino-3-[4'-N,N,-bis(2-chloroethyl)amino]phenyl propionic acid N-oxide dihydrochloride. Upadhyay M[1], Samal J, Kandpal M, Singh OV, Vivekanandan P. *The Warburg effect: insights from the past decade.* Pharmacol Ther. 2013 Mar;137(3):318-30.

Moreover, recent studies suggest that targeting mitochondria is an attractive strategy for cancer therapy and the term “mitocans” has been used to classify mitochondria-targeted anticancer drugs [68]. The reason of this interest is that the Warburg’s hypothesis of the defects in mitochondria is not totally unfounded and cancer cells exhibit various degrees of mitochondrial dysfunction, such as changes in energy metabolism, increased transmembrane potential and ROS production. In particular, the increase in ROS production by cancer cells is associated with multiple changes in cellular functions, such as cell proliferation, migration, differentiation and apoptosis, all fundamental properties of cancer cells.

Finally, we need to mention the most innovative drugs used to target mitochondrial functions: Metformin and CPI-613.

Metformin (Figure 15), one of most widely prescribed oral hypoglycemic agents, has recently received increased attention because of its potential antitumorigenic effects that are thought to be independent of its hypoglycemic activity. This has been evaluated in multiple *in vitro* and *in vivo* studies, and it is now being tested in clinical trials as an adjuvant to classic chemotherapeutic regimens [69, 70]. Specifically, this compound exerts its pharmacological effects by inhibiting the mitochondrial ETC and by activating the AMPK pathway. Because, Metformin induces metabolic stress by reducing mitochondrial ATP production, it has been suggested that it could inhibit the growth of cancer cells by decreasing the cellular energy status.

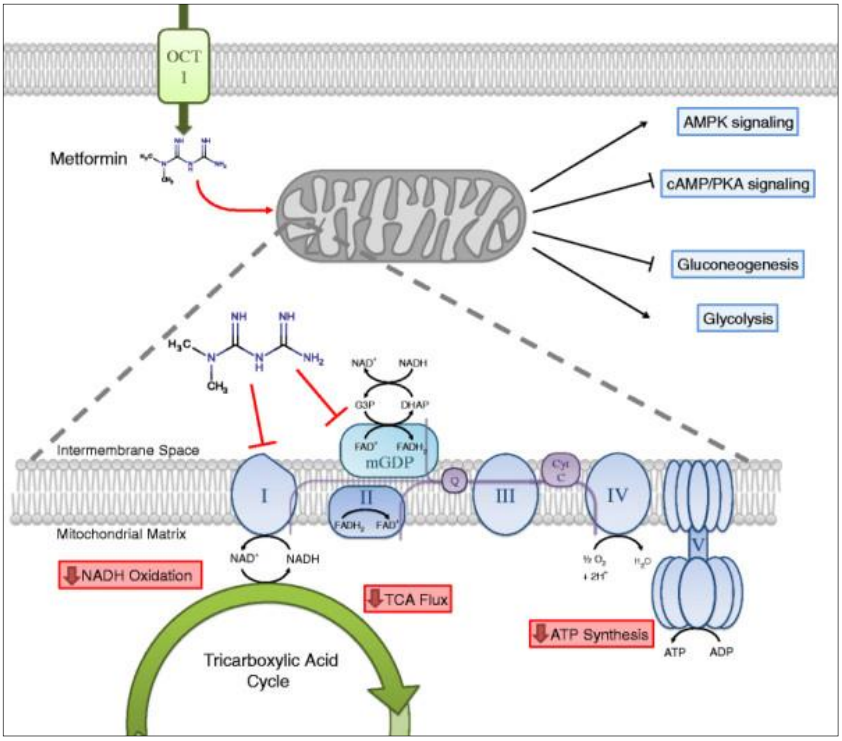

Figure 15: Metformin and cancer therapy. Luengo et al. BMC Biology 2014 12:82

CPI-613 is an analog of lipoic acid capable of disrupting mitochondrial metabolism and it seems to exhibit selective effects against cancer cells both *in vitro* and *in vivo* [71]. CPI-613 is an innovative drug, actually in clinical trial, targeting two key enzymes of the TCA cycle: pyruvate dehydrogenase kinase (PDK) and alpha-ketoglutarate dehydrogenase (α-KGDH) (Figure 16). In specificity, it stimulates PDK and consequently it induces the inactivation of PDH through phosphorylation, activating multiple tumor cell death pathways. Moreover, it induces of α-KGDH with an endogenous redox mechanism. So this single drug simultaneously and independently attacks two central, essential mitochondrial metabolic complexes.

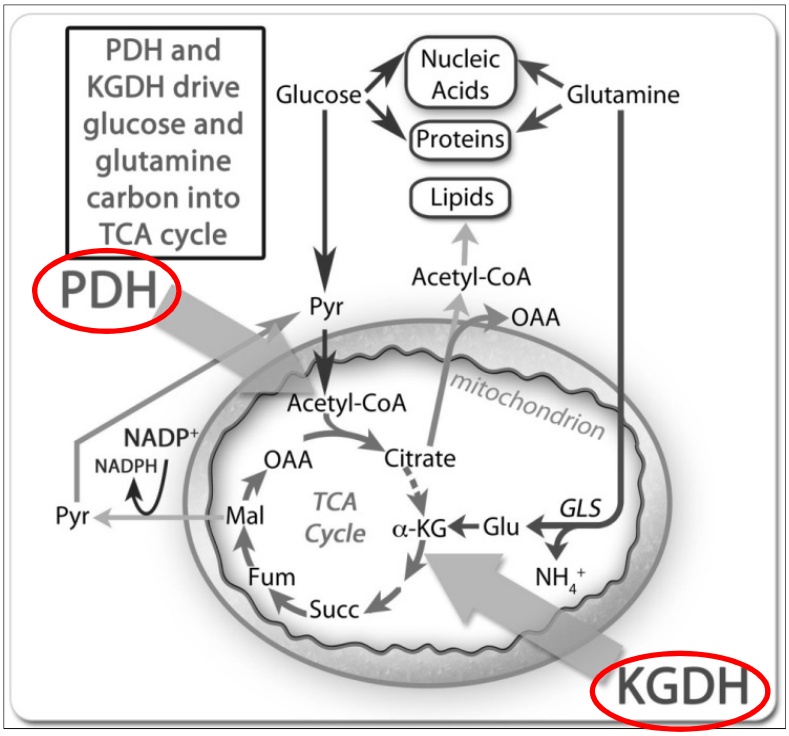

Figure 16: CPI-613 and target therapy in mitochondria. Paul M. Bingham and Zuzana Zachar *The Pyruvate Dehydrogenase Complex in Cancer: Implications for the Transformed State and Cancer Chemotherapy.*

The possibility that Metformin could efficiently target CSC [69, 70], suggests that this rare cell population is characterized by a different metabolism that the cancer cells, privileging a mitochondrial-dependent metabolism.

In view of the novelty of the drug, there is no significant evidence about the capacity of CPI-613 to induce the death of CSC. It has to keep into account that CSC could have different metabolic profiles depending on their tissue of origin and their degree of differentiation. For example, highly undifferentiated liver cancers tend to be more glycolytic than differentiated

cells [73], while a recent study using glioma stem cells show that these cells consume less glucose and produce less lactate, compared to their cancer cell counterpart [74].

In conclusion, the idea that CSC are characterized by a different metabolism than the cancer cells, could open new avenues to new target therapies.
The niche is the source of molecules that activate or inhibit signal transduction pathways and, while the stem cell microenvironment of a normal tissue is known to maintain a balance between self-renewal and differentiation, the tumor microenvironment predominantly displays proliferating signal to cancer cells and CSC. Accordingly, anti-metabolic reprograming strategies begin to provide a roadmap for the generation of novel "metabo-stemotoxic" therapies, counteracting therapeutic resistance, cancer aggressiveness and cancer recurrence.

1.7 Aims of the project

The aims of this project are:

a) The phenotypic characterization of CSC in ascitic effusions from ovarian cancer-bearing patients. The characterization will be carried out through the application of techniques such as: stemness marker expression, spheroid formation, chemo resistance assay and tumorigenicity *in vivo*.

b) The investigation of the metabolic profile of CSC isolated from patients with epithelial ovarian cancer, through specific metabolic assays to evaluate whether the CSC fraction is characterized by the known Warburg effect or by other particular metabolic pathways.

These studies have the ambition to define differences between CSC population and the non-stem counterpart, in order to discover specific therapeutic targets, because it is known that the niche protect CSC from drugs and specific nutrient or oxygen stress.

For this reason, we will also focus our attention on a key nutrient stress, glucose deprivation, to test the addiction of CSC to this nutrient and their ability to survive under starvation conditions. These experiments could in fact demonstrate *in vitro* the ability of CSC to persist in stress condition.

The final aim is to find a specific drug or drug combination that targets the relevant metabolic pathways.

2. MATERIALS AND METHODS

2.1 Primary samples and *in vitro* culture

Ascitic fluid and tumor samples of EOC patients were obtained following informed consent from 45 patients. Cells were maintained in RPMI-1640 medium supplemented with 10% fetal bovine serum (FBS; GIBCO Invitrogen, Monza, Italy), 1% sodium pyruvate (Lonza, Basel, Switzerland), and 1% L-glutamine (GIBCO). Cells were cultured at 37°C, 5% CO_2, and harvested at confluence using trypsin-EDTA (Invitrogen). In a set of experiments, the cells were cultured in the absence of glucose; at the end of the starvation period, glucose was added and marker expression evaluated 10 days later. In another set of experiments, the cells were cultured for 14 days in the absence of glucose, and then transferred to medium without glucose, without glucose and L-glutamine, or without glucose, L-glutamine and sodium pyruvate.

2.2 Cell lines

IGROV-1 cells were purchased from ATCC (Manassas, VA) and OC316 cells were kindly provided by S.Ferrini (IST, Genoa, Italy); the cell lines were used within six months from resuscitation. The cells were maintained in RPMI-1640 medium (GIBCO) supplemented with 10% FBS (GIBCO, Invitrogen), 1% sodium pyruvate (Lonza), 1% penicillin-streptomycin (Lonza) and 1 % L-glutamine (GIBCO). The cells were cultured at 37°C in a humidified atmosphere containing 5% CO_2 and harvested, when 80-90% confluent, using Trypsin-EDTA (Invitrogen).

2.3 Flow cytometry

The cells were stained with Live-Dead (Pacific Blue, 1:600; Invitrogen) to discriminate living cells. The following anti-human monoclonal antibodies were used: anti-CD44 (1:1,000; Abcam, Cambridge, U.K.), anti-CD117 (non-activating AC126 clone, 1:10; Miltenyi Biotec, Bergish Gladbach, Germany), anti-CD45 (1:10; Miltenyi Biotec), anti-CK7 (1:25; Abcam), anti-GLUT1 (1:1,000; Abcam). Intracellular staining was performed after fixation with 4% paraformaldeyde and permeabilization with 0.1% Triton X-100. After incubation with unconjugated antibodies, the cells were incubated for 30 min with the appropriate secondary antibody (Alexa 1:500; Invitrogen). All the cytofluorimetric analyses were performed using a FACS LSRII (BD Bioscience, Franklin Lakes, NJ); data were collected from at least 1 x 10^5 cells/sample and elaborated with FlowJo software (TreeStar, Ashland, OR). For FACS-sorting, antibody-labelled cells were separated with a MoFlo Astrios Cell Sorter (Beckman Coulter, Brea, CA); the purity of the sorted populations always exceeded 90%.
To evaluate glucose uptake, EOC effusion cells were labelled with anti-CD44 and anti-CD117 antibodies; 2-NBGD-FITC glucose (12.5 μM; Invitrogen) was then added and fluorescence intensity measured after 1 min. Cell viability was evaluated by incubating the cells for 15

min at 37°C with AnnexinV/PI staining kit (Roche, Basel, Switzerland); unless otherwise specified, results were expressed as the ratio between the percentage of Annexin V^{neg}/PI^{neg} cells at the experimental time points and the percentage at time 0.
To evaluate the effect of glucose starvation on cell proliferation, EOC effusion cells were stained with PKH26 (Sigma Aldrich, St. Louis, MO) as described elsewhere [31] and seeded at $2x10^5$ cells/well in RPMI medium or RPMI without glucose (Sigma Aldrich), both supplemented as above. Flow cytometry analysis was performed 14 days later.

2.4 Spheroid formation assay and *in vitro* cell differentiation

To promote *in vitro* spheroid formation, EOC ascitic effusion cells were seeded in poly-2-hydroxyethyl methacrylate (PhEMA)-coated plates (BD Bioscience, Franklin Lakes, NJ) in serum-free RPMI medium supplemented with bFGF (10 ng/ml) and EGF (20 ng/ml: both from Peprotech, Rocky Hill, NJ) at a density of 2×10^4 cells/well. Medium was replaced every 7 days.
To determine the frequency of spheroid-forming precursors, we performed an extreme limiting dilution analysis (ELDA) in unsorted EOC cells, and FACS-sorted $CD44^+CD117^+$ and $CD44^+CD117^-$ cells. Briefly, the cells were plated at different concentrations in 96-well flat-bottom ultra-low attachment PhEMA-coated plates (BD Bioscience) in a total volume of 0.1 ml of serum-free medium RPMI medium supplemented with EGF and bFGF. Thirty replicate wells were set up for each cell concentration. After 7 days of incubation, the wells were scored for spheroid formation; the frequency of spheroid-forming precursors in each population was calculated by ELDA web tool (http://bioinf.wehi.edu.au/software/elda). Data are expressed as the number of spheroid-forming cells/10^3 cells.
The ability to differentiate *in vitro* was evaluated by plating unfractionated EOC cells, previously cultured in serum-free conditions, in the presence of 10% FBS at a density of 2×10^4 cells/ml. The cells were maintained at 37°C in a 5% CO_2 humidified atmosphere, and the medium replaced every 7 days.

2.5 Chemotherapy sensitivity assays

To assess chemotherapy resistance, unfractionated EOC effusion cells were seeded at 2×10^5 cells/well in 6-well plates in complete RPMI medium in the presence or in the absence of Doxorubicin (1 µM; Ebewe Pharma, Wien, Austria); cytofluorimetric analysis was performed 48 h later.

2.6 *In vivo* xenograft propagation

Xenografts were generated by injecting intra-peritoneally (i.p.) 1×10^6 tumor cells, obtained from primary EOC effusion samples, into severe combined immunodeficient (SCID) mice as reported elsewhere [1] Mice were purchased from Charles River (Wilmington, MA); procedures involving animals and their care were performed according to institutional

guidelines that comply with national and international laws and policies (EEC Council Directive 86/609, OJ L358, 12 December 1987). About 2 months later, animals developed tumors, which contained a predominant ascitic component.

2.7 Tumorigenicity assay

To demonstrate the tumorigenic potential of the different EOC populations, different numbers of *ex vivo* FACS-sorted $CD44^+CD117^+$ and $CD44^+CD117^-$ cells were injected i.p. into seven-to nine-week-old Rag-2 $\gamma^{-/-}$ mice in a total volume of 300 µl. To evaluate the tumorigenic potential of glucose-starved cells, 5 x 10^3 cells, cultured for 14 days as above in the presence or in the absence of glucose, were injected i.p. into Rag-2 $\gamma^{-/-}$ mice. At tumor establishment, mice were sacrificed, tumors harvested and isolated cells analyzed by FACS.

2.8 RNA extraction, reverse transcription and gene card analysis

Total RNA was extracted by the TRIzol method according to manufacturer's instructions. cDNA was synthesized from 0.5-1 µg of total RNA with Superscript II reverse transcriptase (Invitrogen), and hybridized to TaqMan Custom Arrays specific for 62 genes (Applied Biosystems, Foster City, CA), with each sample run in triplicate. The PCR step was performed using an ABI PRISM® 7900HT Sequence Detection System (Applied Biosystems). Results were analyzed using the comparative ΔΔCt method; ΔΔCt values were utilized to calculate the $RQ=2^{-\Delta\Delta Ct}$. Data were expressed as the fold difference in gene expression (normalized to the housekeeping gene β_2-microglobulin) relative to a reference sample, as indicated in the individual figure legends. qRT-PCR efficiency ranged from 95% to 105%.

2.9 Western blotting (WB)

FACS-sorted $CD44^+CD117^+$ and $CD44^+CD117^-$ cells were lysed and subjected to SDS-PAGE and WB. Immunoreactivity was evaluated using the following rabbit antibodies: anti-actin (1:5,000; Sigma Aldrich), anti-PDHK1 (1:1,000; Cell Signaling, Boston, MD), anti-phospho-PDH (1:1,000; Abcam), anti-PDH (1:2,000; Abcam) and anti-G6PD (1:1,000; Cell Signaling). Mouse anti-IDH2 (1:10,000) and anti-MCT4 (1:1,000) were purchased from Cell Signaling; goat anti-HKII (1:1,000) from Santa Cruz (Dallas, TX). The blots were hybridized with a 1:5,000 dilution of HRP-conjugated anti-goat, anti-mouse or anti-rabbit antibody (Amersham-Pharmacia, Little Chalfont, U.K.), as appropriate. Finally, the signal was detected by chemiluminescence with SuperSignal kit (Pierce, Rockford, IL), and lane densitometry analyzed by standard procedures.

2.10 Total and mitochondrial ROS production, membrane potential analysis and *in vitro* inhibition of metabolic enzyme activity

Unfractionated EOC effusion cells were labelled with anti-CD44 and anti-CD117 antibodies. For total ROS evaluation, the DCFDA probe (1 µM; Invitrogen) was added for 30 min at

37°C; cells were then washed and mean fluorescence intensity (MFI) values were recorded. For mitochondrial ROS evaluation, H_2-MitoTracker Red probe (H_2-MTR, 20 nM; BD Bioscience) was added to the cells at 37°C for 15 min; to verify the specificity of the assay for ROS produced by the electron transport chain (ETC), we added pargyline, an inhibitor of mono-aminooxidases, which are an additional source of mitochondrial ROS [42]. H_2O_2 (100 μM) and Trolox (100 μM; both from Sigma Aldrich) were used as positive and negative controls. The kinetics of mitochondrial ROS production was calculated using the $\Delta F/F_0$ formula, where F_0 is the fluorescent signal measured at time 0, and ΔF is the difference in MFI measured at the indicated time points minus the F_0 value. Mitochondrial potential ($\Delta\psi_m$) was measured by incubating the cells with TMRM (20 nM; Invitrogen) in the presence of cyclosporin A (1.6 μM; Sigma Aldrich) for 20 min at 37°C. FCCP (100 nM; Sigma Aldrich) was used to induce depolarization; oligomycin (1 μM; Sigma Aldrich) and antimycin (1 μM; Sigma Aldrich) were added to perturb membrane potential.

To evaluate cell dependence on the ETC, fatty acid β-oxidation and the pentose phosphate pathway (PPP), 1 x 10^6 cells were plated in serum-free RPMI supplemented with oligomycin (1 μM), antimycin (1 μM), rotenone (1 μM), etomoxir (1 μM), DHEA (100 μM) or metformin (1 mM; all from Sigma Aldrich). Cell viability was evaluated with Annexin V/PI staining at different time points.

2.11 Mitochondrial mass analysis

To evaluate the mitochondrial mass, unfractionated EOC effusion cells were labelled with anti-CD44 and anti-CD117 antibodies, and incubated with the MitoTracker Green probe (0.1 μM; Invitrogen) for 15 min at 37°C. Results were expressed as MFI.

2.12 *In vitro* and *in vivo* 2-DG treatment

For *in vitro* experiments, unfractionated EOC effusion cells were seeded in 6-well plates at 2 x 10^5 cells/well, and treated with 6 g/L of 2-deoxiglucose (2-DG; Sigma Aldrich). At different time points (24, 48 and 72h), cytofluorimetric analysis was performed to evaluate CD44/CD117 co-expression and cell viability by AnnexinV/ PI staining.
For *in vivo* experiments, after red blood cell lysis and lymphocyte removal, 5 x 10^5 unfractionated EOC effusion cells were injected subcutaneously (s.c.) into seven-to-nine-week-old Rag-2 $\gamma^{-/-}$ mice in 200 μl of Matrigel (BD Bioscience) in both dorsolateral flanks. When tumors reached 100 mm^3 volume, mice were divided in two groups, one receiving i.p. three times/week 2 g/kg of 2-DG, the other a same volume of saline solution. Tumor growth was evaluated by caliper measurement; when tumors of the control group reached 600 mm^3 volume, the mice were sacrificed, tumors harvested by dissection, and isolated cells analyzed by FACS.

2.13 Oxygen consumption and Extracellular acidification rate

The oxygen consumption rate (OCR) and Extracellular acidification rate (ECAR) were determined using the SeaHorse XF Extracellular Flux Analyzer (Seahorse Biosciences, San Jose, CA) [3, 4]. Briefly, 24-well plates (XF24 V7, Seahorse Biosciences) were coated with 20 µl of Matrigel (Cultrex, Trevigen, Gaithersburg, MD) to allow cell adhesion to the bottom of the plates. Unfractioned EOC effusion cells and FACS-sorted populations were seeded at 3 x 10^4 cells/well in complete RPMI medium, and incubated for 4 h at 37°C, 5% CO_2. The XF assay was initiated by medium replacing with DME base supplemented with 10% FBS, 1% sodium pyruvate, 1% penicillin-streptomycin, 1% glucose (Sigma Aldrich) and 1% L-glutamine. The cartridge of the instrument was loaded to dispense four different metabolic inhibitors at 20 min intervals: oligomycin (1 µM), followed by FCCP (0.6 µM for primary samples, 0.3 µM for cell lines), antimycin (1 µM) and rotenone (1 µM; all from Sigma Aldrich) over 2 h. The assay was characterized by 3 sequential measurements of OCR and ECAR at time 0 and after each reagent addition thereafter.

2.14 Confocal and fluorescence microscopy analysis

For studying the kinetics of mitochondrial ROS production, FACS-sorted $CD44^+CD117^+$ and $CD44^+CD117^-$ cells were maintained at 37°C in DMEM medium (Sigma Aldrich) supplemented with 10% FBS, 1% sodium pyruvate, and 1% Hepes (Lonza). Cultures were pretreated with 2 mM pargyline, and then labeled with 20 nM H_2-MTR. ROS production was measured using an LSM510 confocal laser microscope (Zeiss, Jena, Germany) equipped with a 37°C, 5% CO_2 incubator using Helium Neon (543 nm) and Argon (488 nm) lasers. Laser intensity, pinhole aperture, and photomultiplier parameters were standardized to allow comparison of signals obtained in different samples; images were recorded at 1 min intervals for 60 min. The mean fluorescent signal of H_2-MTR in mitochondria of individual cells was quantitated with the Zeiss Histogram software tool, and expressed as $\Delta F/F_0$ as above. To evaluate MCT4 expression, FACS-sorted $CD44^+CD117^+$ and $CD44^+CD117^-$ cells were stained with anti-MCT4 antibody (1:100; Santa Cruz Biotechnology); nuclei were stained with TOPRO3 (1:10,000; Invitrogen), and images recorded by confocal microscopy.

2.15 CPI-613 treatment *in vitro*

For *in vitro* experiments unfractionated EOC effusion cells were seeded in 6-well plates at 2 x 10^5 cells/well, and treated with different concentrations (1, 5, 10, 25, 50, 100, 200 µM) of CPI-613 (Abcam). At different time points (24, 48, 72h), cytofluorimetric analysis was performed to evaluate CD44/CD117 co-expression and cell viability by AnnexinV/ PI staining. The analysis are compared to the control samples treated with DMSO, in which the drug is diluted, to check the toxicity of the reagent.

2.16 Statistical Analysis

Data from replicate experiments were shown as mean values ± Standard Deviation [43]. Comparisons between groups were done by the two-tail Student's *t*-test and Mann-Whitney test, as appropriate.

3. RESULTS

3.1 $CD44^+$ $CD117^+$ cells from ascitic effusions of epithelial ovarian cancer patients are characterized by a CSC phenotype

Previous studies identified the co-expression of CD44 and CD117 as a marker of ovarian CSC [37]. Before investigating the metabolic profile of this subset, we tested whether these same markers identified CSC cells in ascitic effusions from EOC patients. As shown in Figures 13A and 13B, $CD44^+CD117^+$ cells accounted for a small percentage of the neoplastic population (2.5 ± 1.4%; range 0.2-5.0%). A similar percentage was found in EOC masses (Figure 13B), thus indicating that ascitic effusions mirror the composition of solid tumors. This percentage of $CD44^+CD117^+$ cells was also maintained after xenotransplantation of ascitic effusion cells into immunodeficient mice (Figure 13B).
$CD44^+CD117^+$ cells displayed canonical hallmarks of CSC cells. EOC effusion cells formed spheroids when cultured in the absence of serum (Figure 13C), a phenomenon peculiar to CSC from different cancer histotypes. Spheroid formation was associated with a significant increase in the percentage of $CD44^+CD117^+$ cells and a reduction in the expression of the differentiation marker cytokeratin-7 (CK7) (Figure 13D), whereas culture in the presence of serum resulted in a significant increase in CK7 expression, and a decrease in the percentage of $CD44^+CD117^+$ cells (Figure 13D). Moreover, spheroid-forming cells, as judged by ELDA, were enriched in the double-positive population (Figure 13E). It is well-known that CSC present high tumor-initiating capacity. As shown in Table 4, 7 out of 12 RAG-$2\gamma^{-/-}$ mice injected intra-peritoneally (i.p.) with 5 x 10^3 purified $CD44^+CD117^+$ cells developed tumors, whereas no tumors were observed in 10 mice injected with the same amount of $CD44^+CD117^-$ cells. Tumors could only be obtained when the number of inoculated $CD44^+CD117^-$ cells was increased by 100-fold (Table 5).

	Cell number injected		
Cell type	**$5x10^3$**	**$5x10^4$**	**$5x10^5$**
$CD44^+CD117^+$	7/12	-	-
$CD44^+CD117^-$	0/10	0/1	5/5

Table 5: $CD44^+CD117^+$ cells from EOC effusions show a higher tumorigenic potential. FACS-sorted $CD44^+CD117^+$ cells from EOC effusions show a higher tumorigenic potential, compared to the $CD44^+CD117^-$ subset, when injected into RAG-$2\gamma^{-/-}$ mice.

When mice were injected subcutaneously (s.c.) with 1 x 10^5 cells, the tumors generated by $CD44^+CD117^+$ cells were far larger than those generated by the injection of $CD44^+CD117^-$ cells (Figure 17F).

We also compared the expression of several stemness-related genes and genes associated with epithelial-to-mesenchymal transition (EMT). In agreement with previous data, FACS-purified $CD44^+CD117^+$ cells displayed higher expression of all the stemness genes examined (Figure 17G), as well as of EMT-associated genes (Figure 17H). It is known that CSC are resistant to chemotherapy, in part due to the expression of drug-extruding pumps and detoxifying enzymes. Compared to single-positive cells, $CD44^+CD117^+$ cells displayed higher expression of *MRP1*, *MRP2* and *ABCG2* pumps, as well as of *ALDH1A* (Figure 17I), a detoxifying enzyme which is also considered as a canonical marker of CSC [30]. This observation was supported by the finding that the percentage of $CD44^+CD117^+$ cells increased dramatically following *in vitro* incubation of EOC effusion cells with Doxorubicin (Figure 17L). Altogether, these results indicate that the $CD44^+CD117^+$ cells represent a *bona fide* CSC population in EOC ascitic effusions.

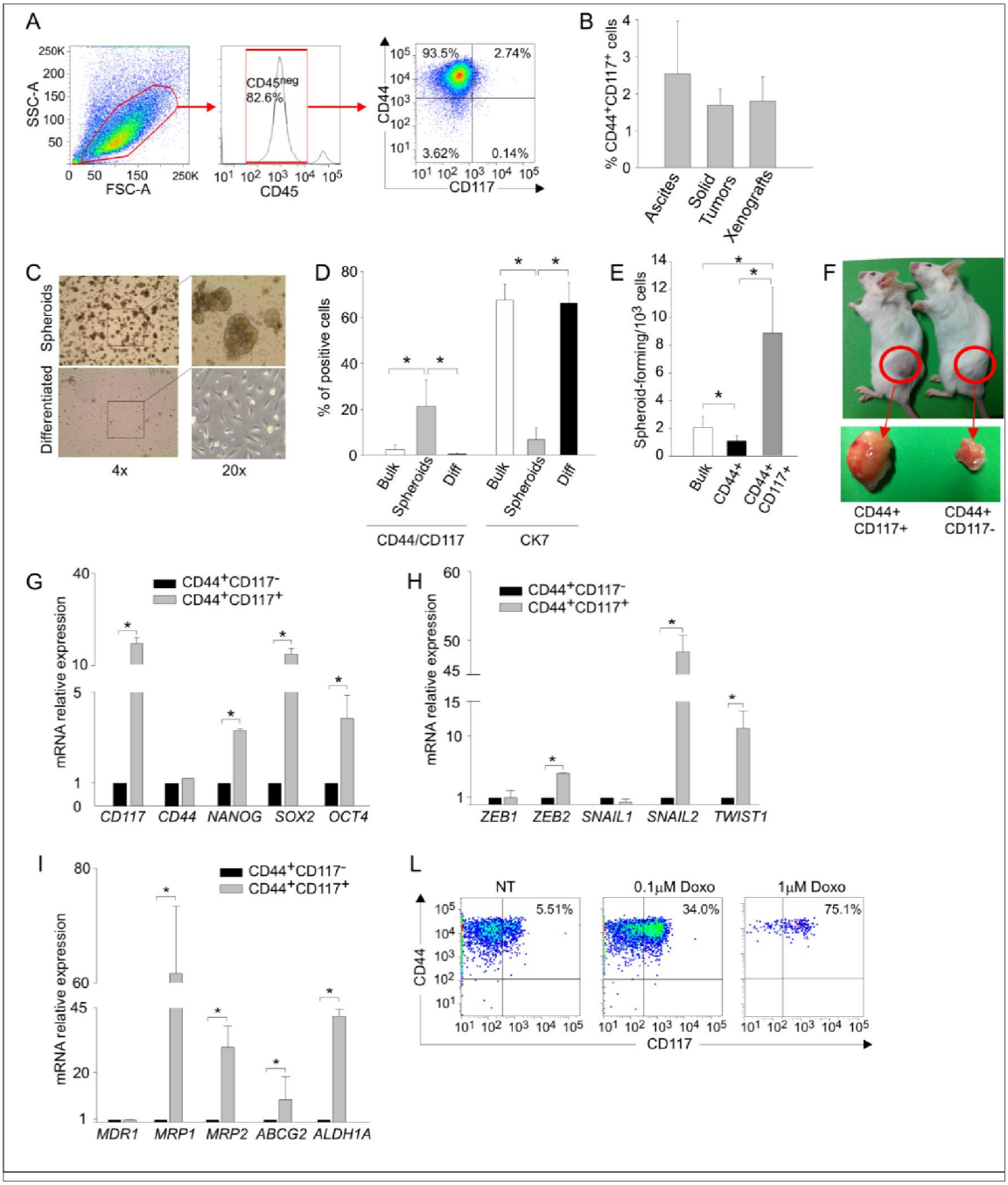
A
SSC-A
FSC-A
CD45neg
82.6%
CD45
CD44
CD117
93.5%
2.74%
3.62%
0.14%
B
% CD44+CD117+ cells
Ascites
Solid Tumors
Xenografts
C
Spheroids
Differentiated
4x
20x
D
% of positive cells
Bulk
Spheroids
Diff
CD44/CD117
CK7
E
Spheroid-forming/10^3 cells
Bulk
CD44+
CD44+ CD117+
F
CD44+ CD117+
CD44+ CD117-
G
CD44+CD117-
CD44+CD117+
mRNA relative expression
CD117
CD44
NANOG
SOX2
OCT4
H
CD44+CD117-
CD44+CD117+
mRNA relative expression
ZEB1
ZEB2
SNAIL1
SNAIL2
TWIST1
I
CD44+CD117-
CD44+CD117+
mRNA relative expression
MDR1
MRP1
MRP2
ABCG2
ALDH1A
L
NT
0.1μM Doxo
1μM Doxo
5.51%
34.0%
75.1%
CD44
CD117

Figure 17: $CD44^+CD117^+$ cells from ovarian cancer effusions show a phenotypic, molecular and functional profile compatible with a canonical CSC population. **A.** Cytofluorimetric analysis of a representative sample of ascitic effusion cells from an EOC–bearing patient. The expression of CD117 and CD44 was evaluated on $CD45^{neg}$ cells, thus excluding contaminating $CD45^+$ myeloid cells (middle panel). **B.** Percentage of $CD44^+CD117^+$ cells in EOC ascitic effusions (n=45), solid EOC tumors (n=6), and primary xenografts derived from injection of EOC effusion cells into immunodeficient mice (n=12). The graph shows mean percentages ± SD. **C.** Spheroid formation by EOC effusion cells cultured for 10 days in FBS-free RPMI enriched with EGF and bFGF (upper panels) followed by 10 days in complete RPMI to induce differentiation (lower panels). The results are representative of 5 experiments. **D.** FACS analysis of CD44/CD117 and CK7 expression in EOC effusion cells (Bulk), spheroids obtained after 10 days' culture in the absence of FBS (Spheroids), and after 10 days of culture in differentiating conditions (Diff). The graph shows mean percentages of positive cells ± SD measured in 10 experiments. *$p < 0.05$. **E.** Spheroid-forming cell frequency, calculated by extreme limiting dilution analysis (ELDA) and expressed as the number of spheroid-forming cells/10^3 cells. ELDA was performed on unsorted cells (bulk), and on FACS-sorted $CD44^+CD117^+$ and $CD44^+CD117^-$ cells. Shown are mean spheroid-forming cell frequencies ± SD calculated from 3 consecutive experiments. *$p < 0.05$. **F.** Tumor generation in RAG-$2\gamma^{-/-}$ mice injected s.c. with 1 x 10^5 FACS-purified $CD44^+CD117^+$ cells (left) or $CD44^+CD117^-$ cells (right) from EOC ascitic effusions. **G.** qRT-PCR analysis of stemness-associated genes in FACS-sorted $CD44^+CD117^+$ and $CD44^+CD117^-$ cells from EOC ascitic effusions. The relative expression of each mRNA in $CD44^+CD117^+$ cells compared to $CD44^+CD117^-$ cells was calculated as described in the *Supplemental Data*. Shown are mean values ± SD measured in ten samples. *$p < 0.05$. **H.** qRT-PCR analysis of genes coding for transcription factors involved in Epitelial-to-Mesenchymal Transition in FACS-sorted $CD44^+CD117^+$ and $CD44^+CD117^-$ cells from EOC effusion samples. Shown are mean relative expression values in $CD44^+CD117^+$ cells compared to $CD44^+CD117^-$ cells ± SD measured in ten samples. *$p < 0.05$. **I.** qRT-PCR analysis of the expression of multidrug resistance pumps and detoxifying enzymes in FACS-sorted $CD44^+CD117^+$ and $CD44^+CD117^-$ cells from EOC effusion samples. Shown are mean relative expression values in $CD44^+CD117^+$ cells compared to $CD44^+CD117^-$ cells ± SD measured in ten samples. *$p < 0.05$. **L.** Flow cytometry analysis of CD44/CD117 expression in EOC effusion cells incubated with different concentrations of Doxorubicin for 48 hr.

3.2 Ovarian CSC show a peculiar expression profile of glucose metabolism- and fatty acid β-oxidation associated enzymes

We next compared the *ex vivo* metabolic profiles of FACS-purified $CD44^+CD117^+$ and $CD44^+CD117^-$ cells by examining the expression of a panel of genes involved in key metabolic pathways, including glucose metabolism, the tricarboxylic acid (TCA) cycle, the electron transport chain (ETC), the pentose phosphate pathway (PPP), and fatty acid β-oxidation.

Results of qRT-PCR revealed that the expression of the *GLUT1* transporter was comparable in the two populations, whereas the levels of hexokinase II (*HKII*), phosphofructokinase (*PFK*) and total pyruvate kinase (*PKM*) were significantly higher in $CD44^+CD117^+$ cells (Figure 18A). Key TCA/ETC enzymes, such as citrate synthase (*CS*), isocitrate dehydrogenase (*IDH2*), and *ATP5B*, were also more highly expressed in the $CD44^+CD117^+$ subset (Figure 18A). To validate these findings, we investigated the protein levels of some of the above enzymes. It is known that GLUT1 exerts its glucose transporter function only when exposed on the outer cell membrane. Consistent with mRNA expression data, flow cytometry analysis of permeabilized cells indicated that the two subsets contained comparable total amounts of GLUT1 protein (Figure 18B, left panel). However, $CD44^+CD117^+$ cells expressed much higher levels of GLUT1 protein on the cell surface (Figure 18B, right panel). This finding was corroborated by analysis of fluorescent glucose uptake: $CD44^+CD117^+$ cells bound FITC-labelled glucose (2-NBDG) much more avidly, compared to $CD44^+CD117^-$ cells (Figure 18C). Results of Western blots analysis (WB) verified that HKII and the TCA enzyme IDH2 were much more abundant in the $CD44^+CD117^+$ subset (Figure 18D).

We also tested the expression of two enzymes involved in PPP, glucose-6-phosphate dehydrogenase (*G6PD*) and ribulose-5-phosphate isomerase (*Ru5PI*). The mRNAs coding for these enzymes were significantly more abundant in $CD44^+CD117^+$ cells (Figure 18E). This observation was confirmed at the protein level for G6PD (Figure 18F). Accordingly, incubation of ascitic effusion cells with dehydroepiandrosterone (DHEA), a known PPP inhibitor, resulted in a significant decrease in the viability of $CD44^+CD117^+$ cells, whereas no effect was observed in the $CD44^+CD117^-$ subset (Figure 18G).

An analysis of enzymes involved in the fatty acid β-oxidation pathway, i.e. carnitine O-acetyltransferase (*CPT2*), enoyl-CoA hydratase (*ECHS1*), acetyl-CoA acyl-transferase 1 (*ACAA1*), ketoacyl-CoA thiolase 2 (*ACAA2*) and glycerol kinase, showed that all were more more expressed at the mRNA level in $CD44^+CD117^+$ cells, compared to the single-positive counterpart (Figure 14H). The importance of this pathway in ovarian CSC was buttressed by an analysis of the effect of Etomoxir, an inhibitor of mitochondrial CPT1, which regulates the transport of long-chain fatty acids from the cytosol to mitochondria for β-oxidation. After 6 hr incubation with Etomoxir, $CD44^+CD117^+$ cells displayed a significant reduction in viability (Figure 18I), whereas $CD44^+CD117^-$ cells did not show any change, even after 24 hr of exposure to the drug.

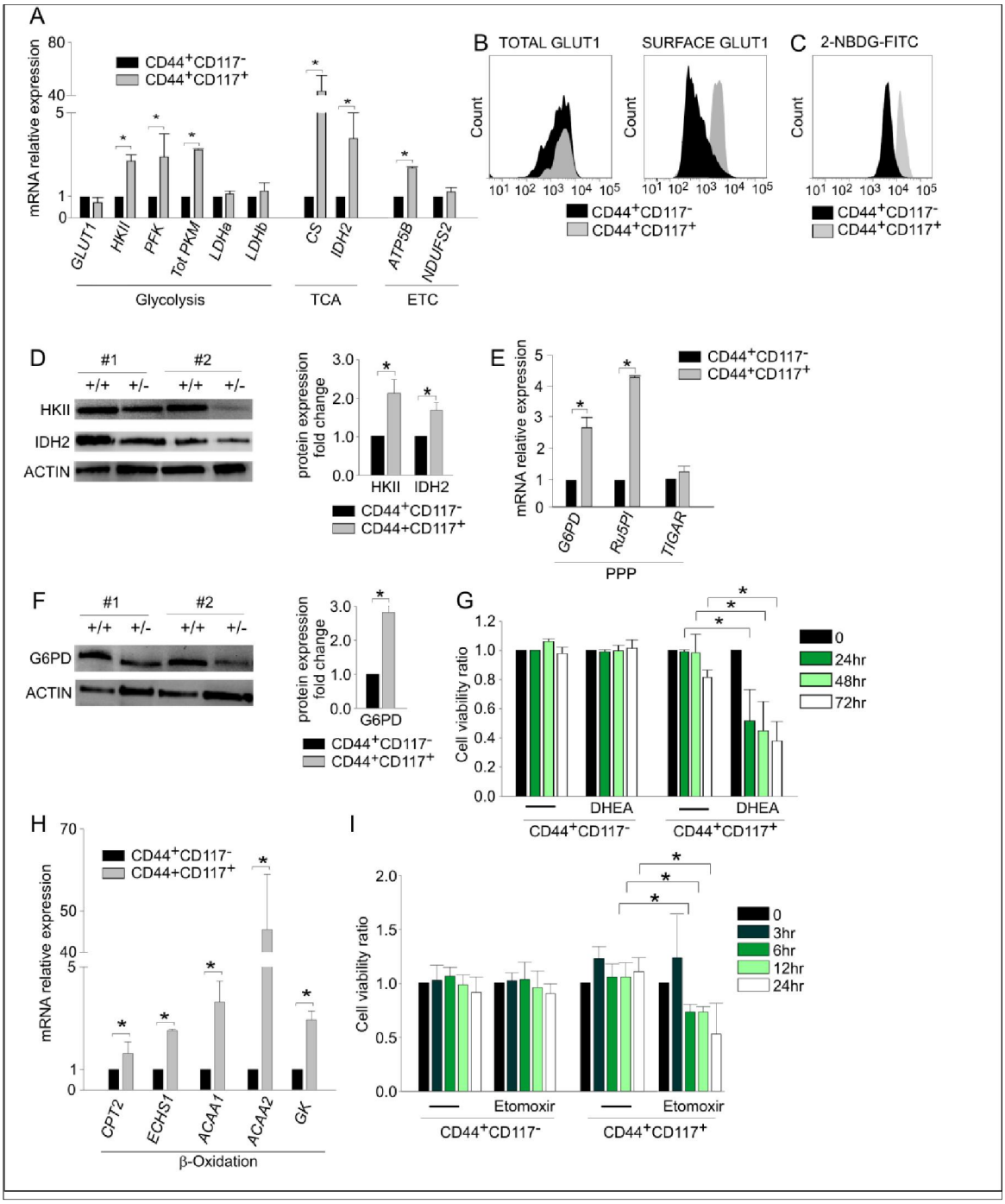
A
mRNA relative expression
CD44+CD117-
CD44+CD117+
GLUT1
HKII
PFK
Tot PKM
LDHa
LDHb
CS
IDH2
ATP5B
NDUFS2
Glycolysis
TCA
ETC
B
TOTAL GLUT1
SURFACE GLUT1
Count
C
2-NBDG-FITC
D
#1
#2
+/+
+/-
HKII
IDH2
ACTIN
protein expression fold change
E
mRNA relative expression
G6PD
Ru5PI
TIGAR
PPP
F
G6PD
ACTIN
G
Cell viability ratio
0
24hr
48hr
72hr
DHEA
H
mRNA relative expression
CPT2
ECHS1
ACAA1
ACAA2
GK
β-Oxidation
I
Cell viability ratio
0
3hr
6hr
12hr
24hr
Etomoxir

Figure 18: $CD44^+CD117^+$ ovarian cancer cells show a different profile of glucose metabolism- and fatty acid β-oxidation-associated enzymes. **A.** FACS-sorted $CD44^+CD117^+$ and $CD44^+CD117^-$ cells from EOC ascitic fluid samples were analysed by qRT-PCR for the expression of key enzymes of glucose metabolism, the tri-carboxylic acid (TCA) cycle and the electron transport chain (ETC). Shown are mean relative expression values in $CD44^+CD117^+$ cells compared to $CD44^+CD117^-$ cells ± SD measured in ten samples. *p < 0.05. **B.** Total and surface expression of the glucose transporter GLUT1 was evaluated by flow cytometry in permeabilized (left panel) and non-permeabilized (right panel) EOC effusion cells. One representative experiment out of five is shown. **C.** Flow cytometry analysis of fluorescent glucose uptake by $CD44^+CD117^+$ and $CD44^+CD117^-$ cells from EOC ascitic effusions. The cells were labelled with anti-CD44 and anti-CD117 antibodies, and 2-NBDG-FITC was added; fluorescence intensity was recorded after 1 min. One representative experiment out of eight is shown. **D.** WB analysis of HKII and IDH2 expression in FACS-sorted $CD44^+CD117^+$ and $CD44^+CD117^-$ cells from EOC effusions. Results in two representative samples are shown on the left; +/+ denotes $CD44^+CD117^+$ cells, and +/- indicates $CD44^+CD117^-$ cells. Signal intensities of the HKII and IDH2 bands were quantitated by scanning densitometry and normalized against the actin signal. Expression ratios were calculated by dividing normalized signal intensity values obtained for $CD44^+CD117^+$ cells by those obtained for $CD44^+CD117^-$ cells. The graph shows mean expression ratios ± SD from three experiments. * p < 0.05. **E.** FACS-sorted $CD44^+CD117^+$ and $CD44^+CD117^-$ cells from EOC ascitic fluid samples were analysed by qRT-PCR for the expression of some key enzymes of the Pentose Phosphate Pathway (PPP). Shown are mean relative expression values in $CD44^+CD117^+$ cells compared to $CD44^+CD117^-$ cells ± SD measured in ten samples. *p < 0.05. **F.** WB analysis of G6PD expression in FACS-sorted $CD44^+CD117^+$ and $CD44^+CD117^-$ cells from EOC ascitic effusions. Results obtained for two representative samples are shown on the left; +/+ and +/- denote CSC and non-CSC subsets, respectively. The ratio of G6PD expression in $CD44^+CD117^+$ cells vs. $CD44^+CD117^-$ cells was calculated as described in the legend to Fig. 2D. The graph shows the mean expression ratio ± SD calculated from three experiments. *p < 0.05. **G.** Unfractionated EOC effusion cells were incubated with the PPP inhibitor DHEA, and the viability of $CD44^+CD117^+$ and $CD44^+CD117^-$ cells was analysed at different times by Annexin V/PI staining. The graph shows mean cell viability ratios ± SD measured in three consecutive experiments (calculated as detailed in the *Supplemental Data*). *p < 0.05. **H.** FACS-sorted $CD44^+CD117^+$ and $CD44^+CD117^-$ cells from EOC effusion samples were analysed by qRT-PCR for the expression of some key enzymes of the fatty acid β-oxidation pathway. Shown are mean relative expression values in $CD44^+CD117^+$ cells compared to $CD44^+CD117^-$ cells ± SD measured in ten samples. *p < 0.05.
I. Unfractionated EOC effusion cells were incubated with the fatty acid β-oxidation pathway inhibitor Etomoxir, and the viability of $CD44^+CD117^+$ and $CD44^+CD117^-$ cells analysed at different times by Annexin V/PI staining. The graph shows mean cell viability ratios ± SD calculated from three consecutive experiments *p < 0.05.

3.3 Ovarian Cancer Stem Cells overexpress key enzymes controlling the fuelling of pyruvate into the tricarboxylic acid cycle

We next measured the expression levels of the key enzymes driving the commitment of pyruvate to the TCA cycle (Figure 19A). The ultimate destination of pyruvate to mitochondrial utilization is controlled by pyruvate dehydrogenase (PDH), whose activity is in turn regulated by PDH kinase (PDHK), which phosphorylates PDH, thus inactivating its function. Interestingly, while equal levels of total PDH were found by WB in the two subsets (Figure 19B), the levels of PDHK1 and of the inactive form of PDH (phospho-PDH) were significantly lower in $CD44^{+}CD117^{+}$ cells (Figure 19B).

We tried to measure Oxygen consumption rate (OCR) and extracellular acidification rate, as index of the metabolism of cells, although we could not directly prove higher oxygen consumption and lower lactate production in CSC, as FACS sorting-associated stress precludes determining these functional parameters (Figure 20). The finding that $CD44^{+}CD117^{+}$ and $CD44^{+}CD117^{-}$ cells express different amounts of PDHK1/phospho-PDH is a crucial clue indicating that ovarian CSC preferentially exploit the mitochondrial respiratory pathway compared to the non-CSC counterpart.

These data strongly suggest that pyruvate fuelling into the TCA cycle is privileged in $CD44^{+}CD117^{+}$ cells. Consistent with these findings, immunofluorescence analysis of *ex vivo* isolated EOC cells revealed significantly higher expression of the lactate transporter MCT4 in $CD44^{+}CD117^{-}$ cells, compared to the $CD44^{+}CD117^{+}$ population (Figure 19C). This observation was confirmed by WB, which showed significantly lower levels of MCT4 in the CSC (Figure 19D). Altogether, these data suggest that pyruvate is preferentially conveyed to the TCA cycle in $CD44^{+}CD117^{+}$ cells, while the higher MCT4 expression found in the $CD44^{+}CD117^{-}$ population is consistent with a more pronounced lactate flux and Warburg-like phenotype of this latter subset.

A role for routing pyruvate into the TCA cycle has also been advanced for PKM, which exists in several isoforms, and regulates conversion of phosphoenolpyruvate to pyruvate.

Results of qRT-PCR to compare the relative proportion of *PKM1* and *PKM2* between $CD44^{+}CD117^{+}$ and $CD44^{+}CD117^{-}$ cells showed that the *PKM2* isoform prevailed in both subsets, but we did not observe any difference in the expression of the two isoforms between CSC and the non-stem counterpart (Figure 21).

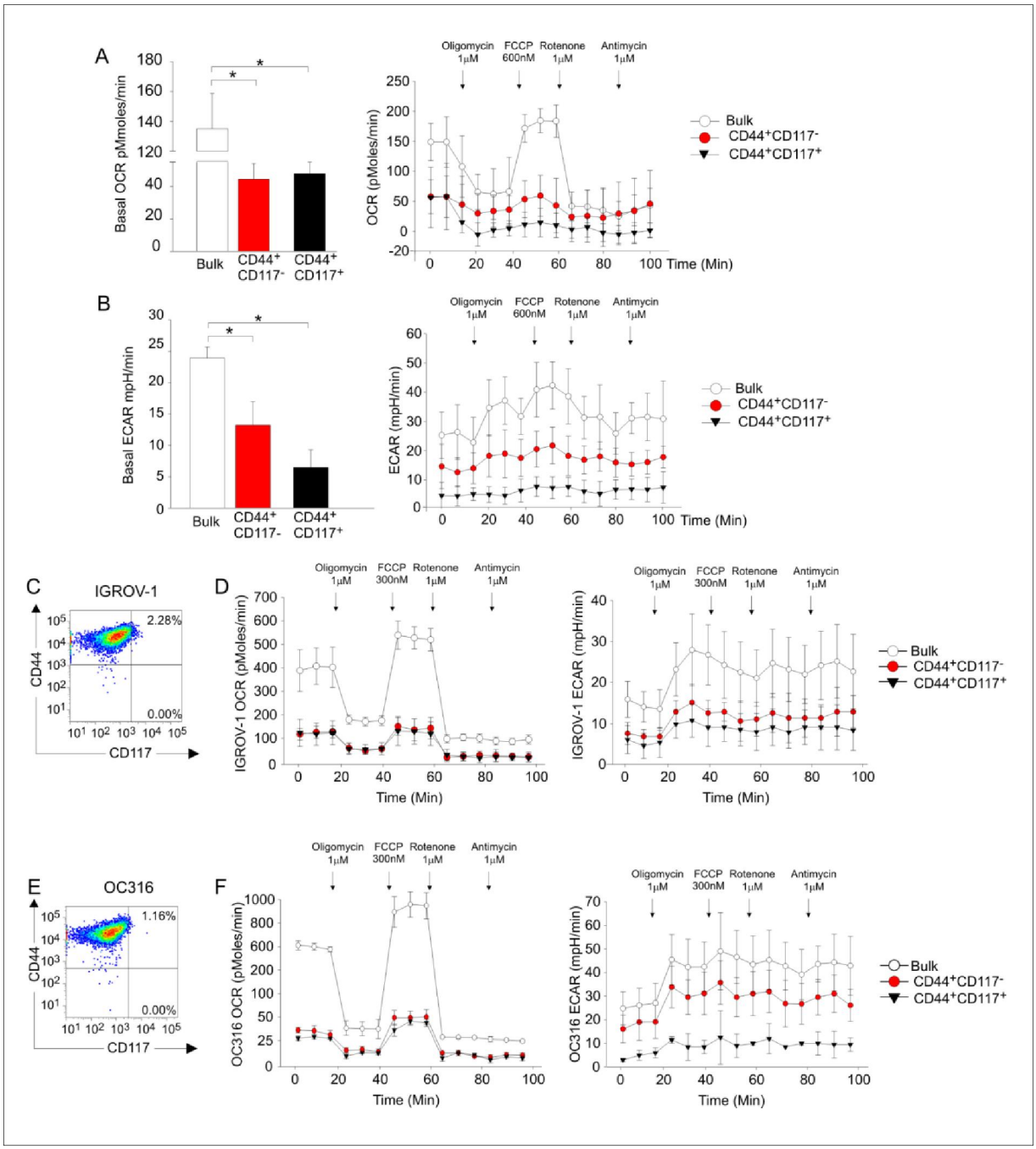
A
Basal OCR pMmoles/min
Bulk
CD44+ CD117-
CD44+ CD117+
Oligomycin 1μM
FCCP 600nM
Rotenone 1μM
Antimycin 1μM
OCR (pMoles/min)
Time (Min)
Bulk
CD44+CD117-
CD44+CD117+
B
Basal ECAR mpH/min
ECAR (mpH/min)
C
IGROV-1
2.28%
0.00%
CD44
CD117
D
Oligomycin 1μM
FCCP 300nM
Rotenone 1μM
Antimycin 1μM
IGROV-1 OCR (pMoles/min)
IGROV-1 ECAR (mpH/min)
E
OC316
1.16%
0.00%
F
OC316 OCR (pMoles/min)
OC316 ECAR (mpH/min)

Figure 20: SeaHorse analysis of Oxygen Consumption Rate (OCR) and Extra-Cellular Acidification Rate (ECAR) in CSC-like and non-CSC-like cell subsets is heavily affected by FACS sorting procedures. A. Basal OCR in unsorted (bulk) and FACS-sorted $CD44^+CD117^-$ and $CD44^+CD117^+$ populations from EOC effusion samples (left panel). Data are expressed as mean values ± SD of ten different experiments. The OCR curves of bulk and sorted populations in a representative sample are shown in the right panel. The first three points of the graph indicate the basal OCR ratio. At different time points the following mitochondrial inhibitors were added: oligomycin (1 μM), FCCP (0.6 μM), rotenone (1 μM) and antimycin (1μM). *p <0.05. **B.** Basal ECAR in unsorted (bulk) and FACS-sorted $CD44^+CD117^-$ and $CD44^+CD117^+$ populations from EOC effusion samples (left panel). Data are expressed as mean values ± SD of ten different experiments. The ECAR curves of bulk and sorted populations in a representative sample are shown in the right panel. The first three points of the graph indicate the basal ECAR ratio. At different time points the following mitochondrial inhibitors were added: oligomycin (1 μM), FCCP (0.6 μM), rotenone (1 μM) and antimycin (1μM). *p <0.05. **C.** Representative flow cytometry analysis of CD44/CD117 co-expression in the ovarian cancer cell line IGROV-1. **D.** OCR (left) and ECAR (right) curves of unsorted (bulk) and FACS-sorted $CD44^+CD117^-$ and $CD44^+CD117^+$ populations from the ovarian cancer cell line IGROV-1. The first three points of the graphs indicate the basal OCR and ECAR ratio. At different time points mitochondrial inhibitors were added as in **A** and **B**. One representative sample out of four is shown. **E.** Representative flow cytometry analysis of CD44/CD117 co-expression in the ovarian cancer cell line OC316. **F.** OCR (left) and ECAR (right) curves of unsorted (bulk) and FACS-sorted $CD44^+CD117^-$ and $CD44^+CD117^+$ populations from the ovarian cancer cell line OC316. The first three points of the graphs indicate the basal OCR and ECAR ratio. At different time points mitochondrial inhibitors were added as in **A** and **B**. One representative sample out of four is shown.

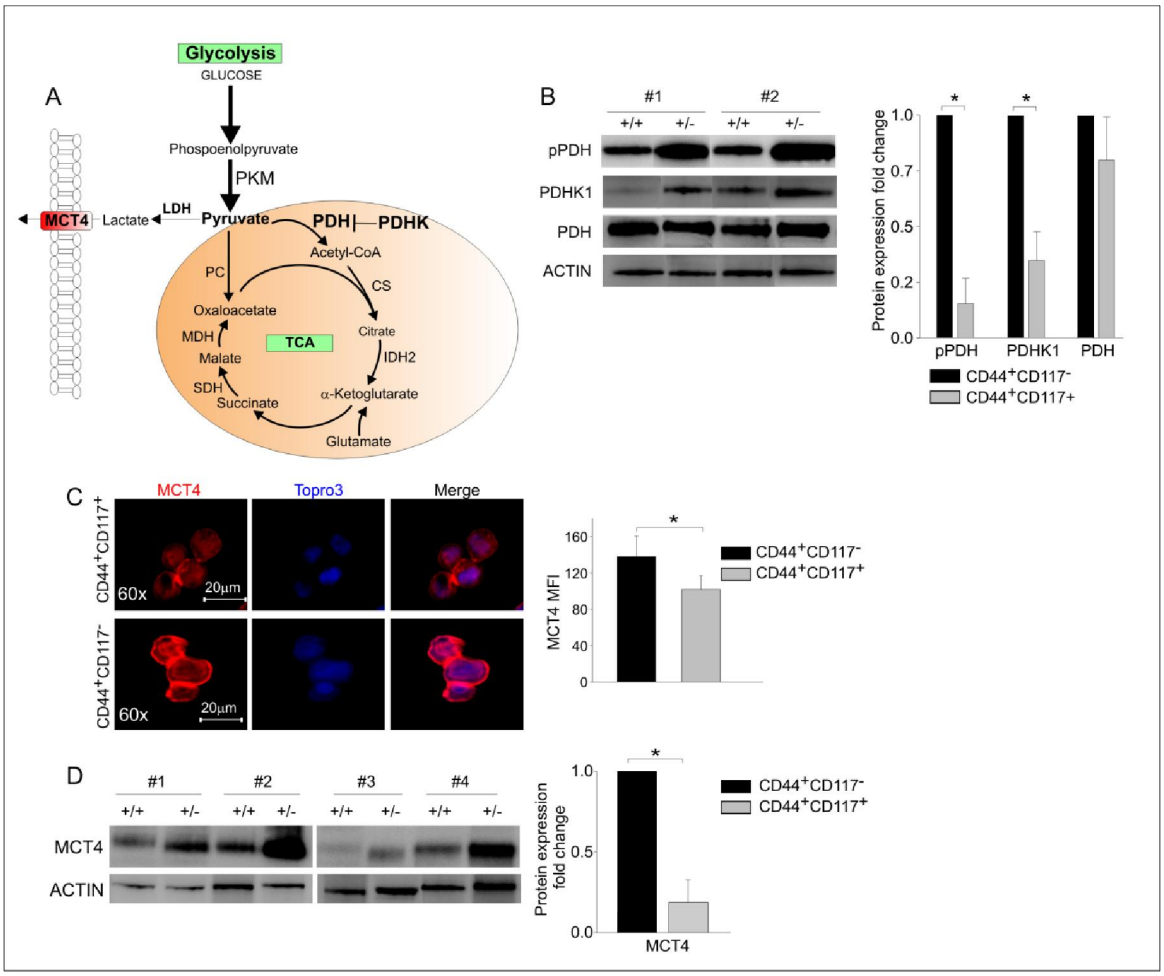

<u>Figure 19:</u> The key enzymes driving glucose commitment to the TCA cycle are highly expressed in CD44$^+$CD117$^+$ ovarian cancer cells. A. In this schematic representation of the major steps of glucose metabolism, the PKM enzyme catalyses the conversion of phosphoenolpyruvate to pyruvate, but the key enzyme that drives its ultimate destination to oxidative metabolism is pyruvate dehydrogenase (PDH). The action of PDH is in turn regulated by PDHK, which phosphorylates PDH, thus inhibiting its function. TCA, tricarboxylic acid. **B.** WB analysis of phospho-PDH (pPDH), PDHK1, and total PDH expression in FACS-sorted CD44$^+$CD117$^+$ (+/+) and CD44$^+$CD117$^-$ (+/-) cells from EOC effusions. Results in two representative samples are shown on the left. Ratios of protein expression in CD44$^+$CD117$^+$ cells *vs.* CD44$^+$CD117$^-$ cells were calculated as described in the legend to Fig. 2D. The graph shows mean expression ratios ± SD calculated from three experiments. *$p < 0.05$. **C.** FACS-sorted CD44$^+$CD117$^+$ and CD44$^+$CD117$^-$ cells from EOC ascitic fluid samples were analysed by confocal immunofluorescence for the expression of the MCT4 lactate transporter. Nuclei were stained with TOPRO3. One representative experiment is shown on the left, and the histogram on the right shows mean values ± SD of MCT4 mean fluorescence intensity (MFI) from 10 different fields. *$p < 0.05$. **D.** CD44$^+$CD117$^+$ (+/+) and CD44$^+$CD117$^-$ (+/-) cells from EOC ascitic fluid samples were FACS-sorted and MCT4 expression analysed by WB. Results from four representative samples are shown on the left. The ratio of MCT4 expression in CD44$^+$CD117$^+$ cells vs. CD44$^+$CD117$^-$ cells was calculated as described in the legend to Fig. 2D. The graph shows the mean expression ratio ± SD calculated from six experiments. *$p < 0.05$.

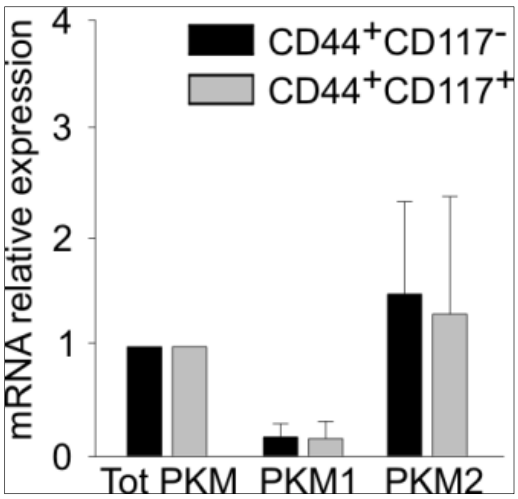

Figure 21: The expression of the PKM1 and PKM2 isoforms does not differ between CD44$^+$CD117$^+$ and CD44$^+$CD117$^-$ ovarian cancer populations. FACS-sorted CD44$^+$CD117$^+$ and CD44$^+$CD117$^-$ cells from EOC ascitic effusions were analyzed by qRT-PCR for the expression of total *PKM* and the *PKM1* and *PKM2* isoforms. The results were normalized to the housekeeping gene β_2-microglobulin (as described in *Supplemental Methods*). For each cell subset, mRNA expression of *PKM1* and *PKM2* was expressed related to total *PKM*, which was defined equal to 1. Data are expressed as mean value ± SD of ten different experiments.

3.4 Ovarian Cancer Stem Cells show higher mitochondrial activity and are more sensitive to inhibitors of the electron transport chain

We thus addressed the respiratory activity of the two populations, starting with a comparison of total and mitochondrial reactive oxygen species (ROS) production in living EOC effusion cells labelled with anti-CD44 and anti-CD117 antibodies. Total ROS levels, measured by flow cytometry of cells incubated with the H_2O_2-sensitive fluorescent probe DCFDA, were significantly higher in the non-CSC population than in the CD44$^+$CD117$^+$ subset (Figure 23A). Mitochondrial ROS levels were measured using MitoTracker Red (H_2-MTR), a mitochondria-specific probe that is converted to fluorescent MTR upon oxidation by H_2O_2. Changes in H_2-MTR fluorescence were measured using two approaches, (i) flow cytometry of unfractionated EOC cells following staining with anti-CD44/CD117 antibodies and (ii) *in situ* measurement by time-lapse laser scanning microscopy. Results showed that both the levels (Figure 23B) and rate of accumulation (Figure 23C) of mitochondrial ROS were significantly higher in the CD44$^+$CD117$^+$ than in the CD44$^+$CD117$^-$ cells.

To determine the metabolic *status* of the cells, independent of mitochondrial mass (Figure 22), we investigated the effects of oligomycin on mitochondrial membrane potential ($\Delta\psi_m$).

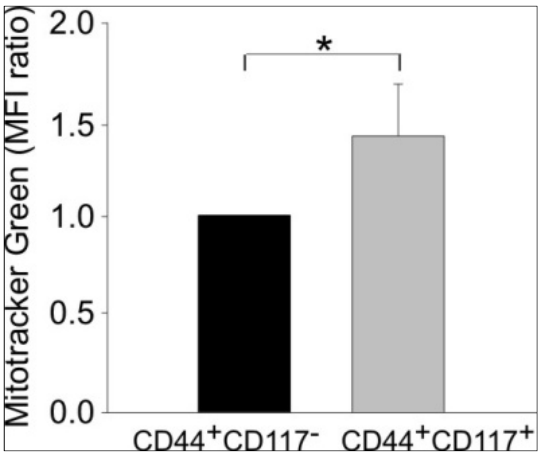

Figure 22: EOC CD44$^+$CD117$^+$ cells show higher mitochondrial mass. Mitochondrial mass in CD44$^+$CD117$^-$ and CD44$^+$CD117$^+$ populations from EOC effusion cells was assessed by flow cytometry with the mitochondrial probe MitoTracker Green. Data represent mean values ± SD of MFI ratios in five consecutive experiments. *p <0.05.

This mitochondrial F_1F_O-ATP synthase inhibitor can be employed to discriminate whether the synthase is used to dissipate $\Delta\psi_m$ in order to produce ATP (as expected in cells using OXPHOS), or rather functions in a "reverse mode" to maintain $\Delta\psi_m$ at the expenses of ATP hydrolysis (as expected in cells diverting pyruvate from TCA cycle). Changes in $\Delta\psi_m$ were monitored using tetramethylrhodamine methyl-ester (TMRM), a fluorescent probe that accumulates in mitochondria in a $\Delta\psi_m$-dependent manner. CD44$^+$CD117$^+$ cells showed a significant hyperpolarization in response to oligomycin, thus demonstrating that in these cells the F_1F_O-ATP synthase works in a $\Delta\psi_m$-dissipating "OXPHOS" mode (Figure 23D). In contrast, CD44$^+$CD117$^-$ cells showed a significant depolarization in response to oligomycin, thus indicating a "reverse" mode of function of the F_1F_O-ATP synthase, which is strongly suggestive of a glycolytic, Warburg-like profile (Figure 23E). Upon addition of antimycin (which inhibits the Complex III of ETC), CD44$^+$CD117$^+$ cells showed a significant depolarization (Figure 23D), thus implying that the ETC was the main $\Delta\psi_m$-generating pathway in these cells. On the contrary, antimycin did not alter $\Delta\psi_m$ in the CD44$^+$CD117$^-$ population (Figure 23E), consistent with poor ETC fuelling in these cells. Both cell subsets showed a comparable mitochondrial depolarization (Figure 23D-E) upon treatment with the control protonophore carbonylcyanide-*p*-trifluoromethoxyphenyl hydrazone (FCCP).

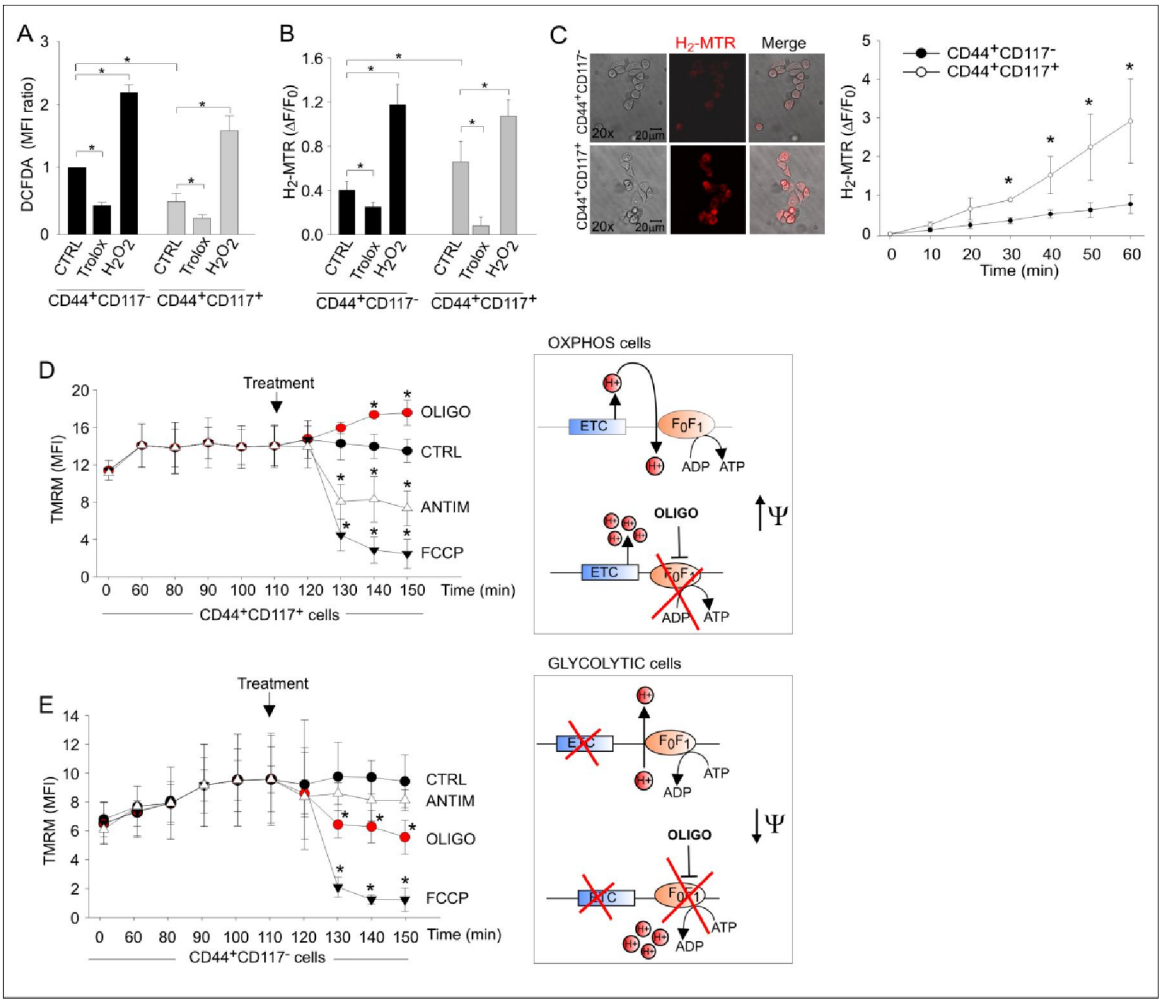

Figure 23: Ovarian cancer CD44$^+$CD117$^+$ cells exhibit higher mitochondrial ROS production and an OXPHOS metabolic profile compared to CD44$^+$CD117$^-$ cells. A. Total ROS levels in unfractionated EOC effusion cells were measured by flow cytometry with the DCFDA probe following staining with anti-CD44 and anti-CD117 antibodies. Exogenous H_2O_2 and the ROS scavenger Trolox were used as positive and negative control, respectively. Mean Fluorescence Intensity (MFI) ratios were calculated dividing the MFIs measured for CD44$^+$CD117$^+$ cells by those obtained for CD44$^+$CD117$^-$ cells. The graph shows mean MFI ratios ± SD from ten experimental repeats. *p < 0.05. **B.** Mitochondrial ROS levels in CD44- and CD117-labelled EOC effusion cells were measured using the H_2-MTR probe. Changes in H_2-MTR fluorescence were measured by flow cytometry after 20 minutes of incubation. H_2-MTR $\Delta F/F_0$ values were calculated as described in the *Methods*. Mean values ± SD from twelve experiments are shown. *p < 0.05. **C.** Time-lapse laser scanning microscopy of mitochondrial ROS production in FACS-sorted CD44$^+$CD117$^-$ and CD44$^+$CD117$^+$ populations. Images obtained at 60 min in a representative experiment are shown on the left; the graph shows mean values ± SD of H_2-MTR $\Delta F/F_0$ recorded in at least 60 cells per time point per sample in 3 independent experiments. *p < 0.05. **D, E.** Mitochondrial membrane potential ($\Delta\psi_m$) in CD44$^+$CD117$^+$ **(D)** and CD44$^+$CD117$^-$ **(E)** cells was measured by flow cytometry with tetramethylrhodamine methyl ester (TMRM). FCCP was used as a control for the specificity of the probe, whereas antimycin and oligomycin were added to test the $\Delta\psi_m$-generating mode of F_1F_O-ATP synthase. The graphs show mean values ± SD of TMRM MFI values in five experimental repeats. CD44$^+$CD117$^+$ cells showed a significant hyperpolarization in response to oligomycin, thus demonstrating the usage of the F_1F_O-ATP synthase in a $\Delta\psi_m$-dissipating "OXPHOS" mode (**D,** right panel). In contrast, CD44$^+$CD117$^-$ cells showed a significant depolarization in response to oligomycin, thus demonstrating a "reverse" $\Delta\psi_m$-generating mode of function of the F_1F_O-ATP synthase, which is strongly suggestive of a glycolytic metabolic profile (right panel in **E**). In both cell populations, mitochondria were rapidly and comparably depolarized in response to the control protonophore FCCP. *p < 0.05 compared to control (TMRM).

To corroborate these data, we compared the effects of the ETC inhibitors oligomycin, rotenone (an inhibitor of Complex I) and antimycin on the viability of the $CD44^+CD117^+$ and $CD44^+CD117^-$ cells. Inhibition of oxidative phosphorylation had a dramatic effect on the survival of $CD44^+CD117^+$ cells, with a >50% decrease in viability after 6 hr treatment (Figure 24A-C), whereas $CD44^+CD117^-$ cells did not show any change in viability when cultured for 24 hours in the presence of each inhibitor.

A tentative model of the metabolic profile of $CD44^+CD117^+$ *vs*. $CD44^+CD117^-$ EOC effusion cells that draws from these findings is proposed in Figure 24D.

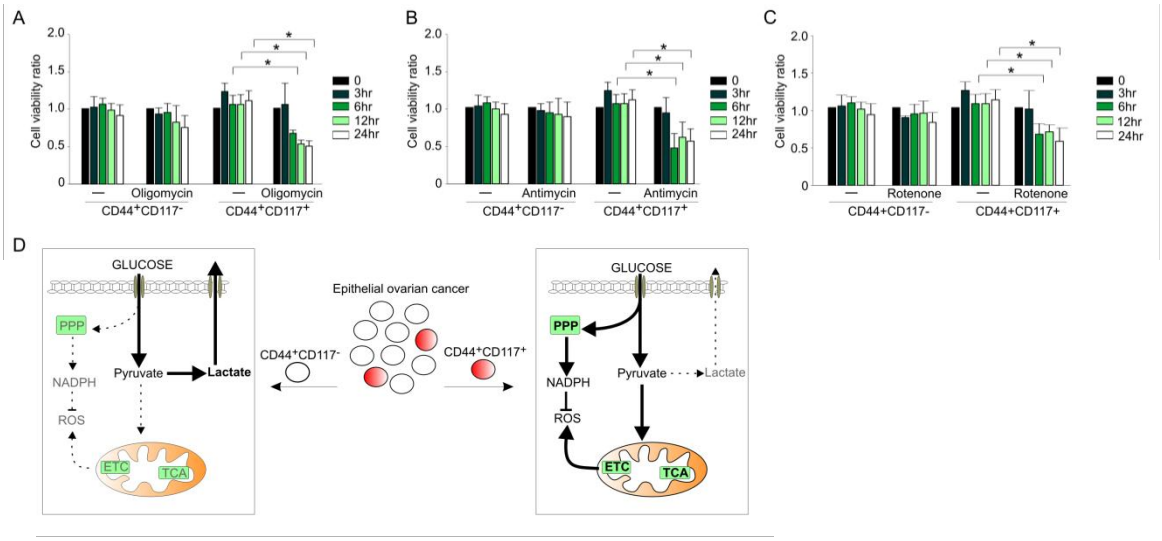

<u>Figure 24:</u> OXPHOS inhibitors significantly affect viability of $CD44^+CD117^+$ but not $CD44^+CD117^-$ ovarian cancer cells. A-C. Unfractionated EOC effusion cells were incubated in the absence or presence of oligomycin (**A**), antimycin (**B**) or rotenone (**C**), and the viability of $CD44^+CD117^+$ and $CD44^+CD117^-$ cells was analysed at different times by Annexin V/PI staining. Cell viability ratios were calculated as described in the *Supplemental Data*. Shown are mean values ± SD from three consecutive experiments. *$p < 0.05$. **D.** Schematic model of the metabolic profile of $CD44^+CD117^+$ (CSC) and $CD44^+CD117^-$ (non-CSC) cells from EOC ascitic effusions. Left panel: bulk tumor cells present a glycolytic metabolic profile, in which most of the glucose entering the cells is converted to pyruvate, and eventually extruded as lactate by the MCT4 transporter. Right panel: in the CSC subset, a large proportion of the glucose entering the cell is converted to pyruvate to fuel the TCA cycle and ETC, which in turn increases mitochondrial ROS production. In these cells, a significant glucose fraction is shunted to PPP to potentiate the redox power of the cells (through NADPH and ROS scavenger generation). The thick arrows denote more active pathways, and the dotted arrows indicate non-preferential pathways. ETC, electron transport chain; PPP, pentose phosphate pathway; ROS, reactive oxygen species; TCA, tricarboxylic acid.

3.5 Ovarian Cancer Stem Cells resist in vitro and in vivo glucose deprivation, while maintaining their Cancer Stem Cell properties

The finding of high glucose uptake and elevated PPP and OXPHOS activity in the CSC prompted us to investigate their response to glucose deprivation. This issue was particularly compelling in view of data indicating that anti-angiogenic therapy causes glucose starvation in experimental tumors and it is associated with enhanced survival of CSC in patients. We thus cultured ascitic effusion cells in the presence and absence of glucose, and evaluated their phenotypic and functional profiles. Glucose starvation of EOC effusion cells was associated with a dramatic decrease in viability (Figure 25A, left panel), due to the preferential death of $CD44^+CD117^-$ cells (not shown), and a significant enrichment in $CD44^+CD117^+$ cells (Figure 25A, right panel), conditions reverted by the re-addition of glucose (Figure S3).

Cultivation of EOC effusion cells in the presence of 2-DG, a glucose analogue which prevents glucose accumulation *via* HKII blockade, resulted in a dramatic decrease in cell viability, while the percentage of CD44/CD117 co-expressing cells increased in parallel (Figure 18B). Administration of 2-DG to mice injected with ovarian cancer xenografts caused a conceivable reduction in the tumor growth rate (Figure 25C, left panel). Intriguingly, however, a significant enrichment in $CD44^+CD117^+$ cells was also found in tumors from 2-DG-treated animals, compared to controls (Figure 25C, right panel).

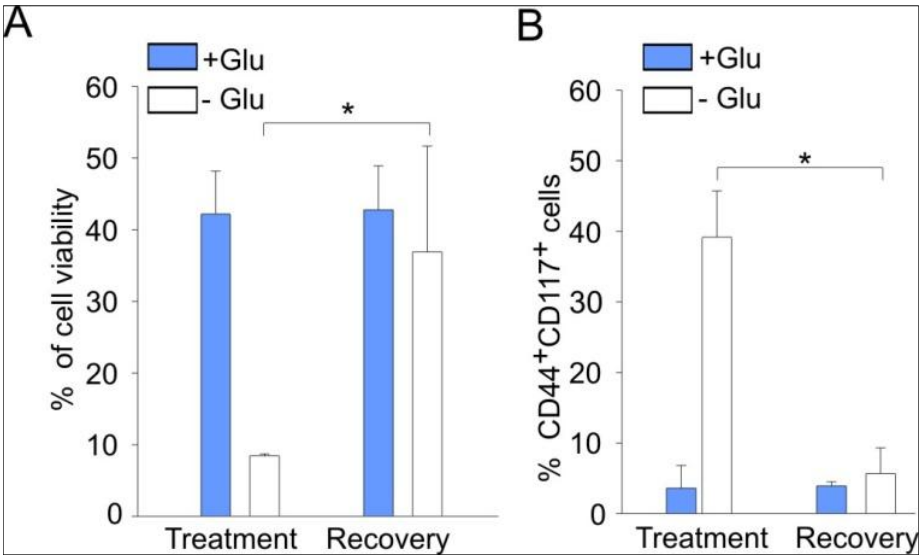

Figure 25: Glucose starved $CD44^+CD117^+$ cells reconstitute the entire cell population after glucose re-addition. A, B. Flow cytometry analysis of cell viability (A) and CD44/CD117 co-expression (B) of unfractionated EOC effusion cells cultured for 14 days in the presence (+Glu) or in the absence (-Glu) of glucose (Treatment) and after 10 days of glucose restoration (Recovery). Data are expressed as mean percent values ± SD of five different experiments. *$p < 0.05$.

Nevertheless, glucose-starved cells fully maintained their original CSC properties. In fact, as judged by ELDA, culture in the absence of glucose was associated with a significantly higher ability to form spheroids, compared to cells kept under standard conditions (Figure 26D). Furthermore, 4/4 RAG-2 $\gamma^{-/-}$ mice injected i.p. with 1 x 10^3 cells previously cultured in the absence of glucose developed tumors, whereas no tumor formation was observed in 6 animals injected with the same number of cells kept under normal culture conditions (not shown). In addition, tumors obtained by s.c. injection of 1 x 10^5 glucose-starved or non-starved cells were much larger when glucose-starved cells were injected (Figure 26E). Altogether, these data indicate that glucose-starved $CD44^+CD117^+$ cells maintain the fundamental properties of CSC, and that glucose deprivation resistance is a consistent feature of the $CD44^+CD117^+$ subset in different *in vitro* and *in vivo* conditions.

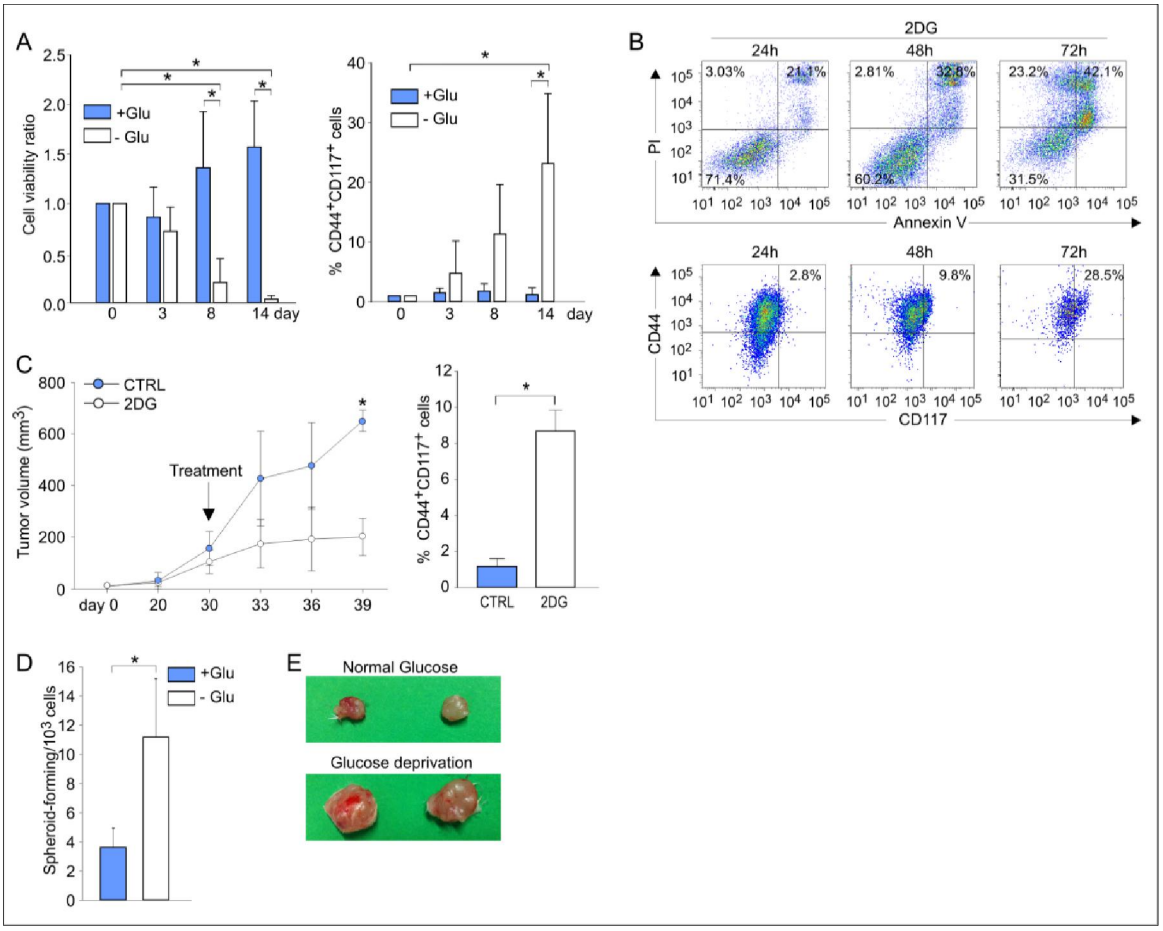

<u>Figure 26:</u> Ovarian cancer $CD44^+CD117^+$ cells resist *in vitro* and *in vivo* glucose deprivation, while maintaining their CSC properties. A. Unfractionated EOC ascitic effusion cells were cultured in the presence (+Glu) or absence (-Glu) of glucose for 14 days; cell viability (left panel) and the percentage of $CD44^+CD117^+$ cells (right panel) were evaluated at different time points. Shown are mean values ± SD from ten consecutive experiments. *p < 0.05. **B.** Flow cytometry analysis of cell viability (upper panel) and CD44/CD117 co-expression (lower panel) of unfractionated EOC effusion cells cultured in the presence of the glucose analogue 2-DG. One representative experiment out of three is shown. **C.** Six RAG-2 $\gamma^{-/-}$ mice were injected with 5 x 10^5 cells/flank from EOC effusion xenografts; when the tumors reached a volume of 100 mm^3, 3 animals were treated with 2-DG, and 3 received saline as a control (CTRL). The left panel shows the kinetics of tumor growth, and the right panel reports the percentage of $CD44^+CD117^+$ cells in the resulting tumor masses. Data are mean values ± SD for six tumors/group. *p < 0.05 **D.** unfractionated EOC effusion cells were

cultured in the presence (+Glu) or absence (-Glu) of glucose. After 14 days the ability to generate spheroids was evaluated by ELDA. Shown are the mean values of spheroid-forming precursors/10^3 cells ± SD in five consecutive experiments. *p < 0.05. **E.** RAG-2 $\gamma^{-/-}$ mice were injected with 1 x 10^5 cells/flank from EOC effusion xenografts. Before inoculation, the cells were cultured for two weeks in standard medium (upper panel) or in medium without glucose (lower panel).

3.6 Glucose deprivation modulates the metabolic profile of ovarian Cancer Stem Cells, while sparing their oxidative phosphorylation profile

The relative increase in $CD44^+CD117^+$ cells in the absence of glucose was not due to their *in vitro* expansion or *de novo* co-expression of these receptors. In fact, the absolute number of input $CD44^+CD117^+$ cells did not significantly change over the glucose starvation period (Table 5).

	$CD44^+CD117^+$ cell number in culture		
Sample no.	**day0**	**day14 (+ GLU)**	**day14 (– GLU)**
PDOVCA #11	1950	2192	2346
PDOVCA #12	2260	2199	2002
PDOVCA #13	2000	2400	1472
PDOVCA #14	2000	2788	2736
PDOVCA #15	2400	2520	2560
PDOVCA #17	2200	1740	1980
PDOVCA #27	2346	2223	2488
PDOVCA #29	1093	2270	1840
PDOVCA #32	1375	1960	1364
PDOVCA #39	2900	1219	1938
mean	2052.4±514.8	2151.1±434.7	2072.6±456.2

P=0.88 ANOVA test

Table 5: The absolute number of $CD44^+CD117^+$ cells is not affected by glucose starvation. The number of CD44/CD117 co-expressing cells in EOC effusions cultured for 14 days in the presence (+Glu) or absence (-Glu) of glucose was calculated from the percentage of $CD44^+CD117^+$ cells obtained by flow cytometry analysis of 2x10^5 cells/culture condition.

Moreover, when ascitic effusion cells were labelled with PKH26, a fluorescent dye used to monitor cell division, mostly PKH^{high} cells were found after glucose deprivation, whereas in normal culture conditions several peaks of PKH intensity were observed, reflecting serial dilution of the dye due to cell replication (Figure 27A). These findings indicated that $CD44^+CD117^+$ cells did not undergo proliferation, but remained quiescent when cultured in the absence of glucose. This observation was corroborated by qRT-PCR analysis of *cyclin D*, *E*, and *B* expression, which was strongly down-modulated in glucose-starved cells (Figure 27B). Interestingly, expression of the pro-apoptotic genes *BAX* and *BAD* was also significantly reduced in glucose-starved $CD44^+CD117^+$ cells, whereas no change in expression of the anti-apoptotic genes *BCL-2* and *BCL-X* was observed (Figure 27B).

Glucose-starved $CD44^+CD117^+$ cells showed an overall down-regulation in expression of glucose metabolism-related genes, as well as in genes involved in fatty acid β-oxidation, compared to cells cultured in the presence of glucose (Figure 27C). However, *GLUT1* was expectedly up-regulated by glucose deprivation (Figure 27C); interestingly, the TCA/ETC genes *CS*, *IDH2* and *ATP5B* did not change significantly following culture in the absence of glucose (Figure 27C). Accordingly, the response of mitochondrial $\Delta\psi_m$ to oligomycin showed a comparable OXPHOS profile in freshly isolated (see Figure 23D) and glucose-starved $CD44^+CD117^+$ cells (Figure 27D). Thus, it is reasonable to conclude that ovarian CSC resist glucose starvation by entering a quiescent state, while maintaining their preferential OXPHOS profile. It is possible that ovarian CSC could resist glucose deprivation thanks to the exploitation of anaplerotic pathways such as glutaminolysis to support ATP production. To test this hypothesis, we cultured unfractionated EOC cells under glucose deprivation for 14 days, followed by an additional L-glutamine and/or sodium pyruvate starvation for 72 hr. As shown in Figure 7E, L-glutamine deprivation of glucose-starved $CD44^+CD117^+$ cells caused a >50% decrease in cell viability, while withdrawal of both L-glutamine and sodium pyruvate caused death of virtually all the cells (Figure 27E).

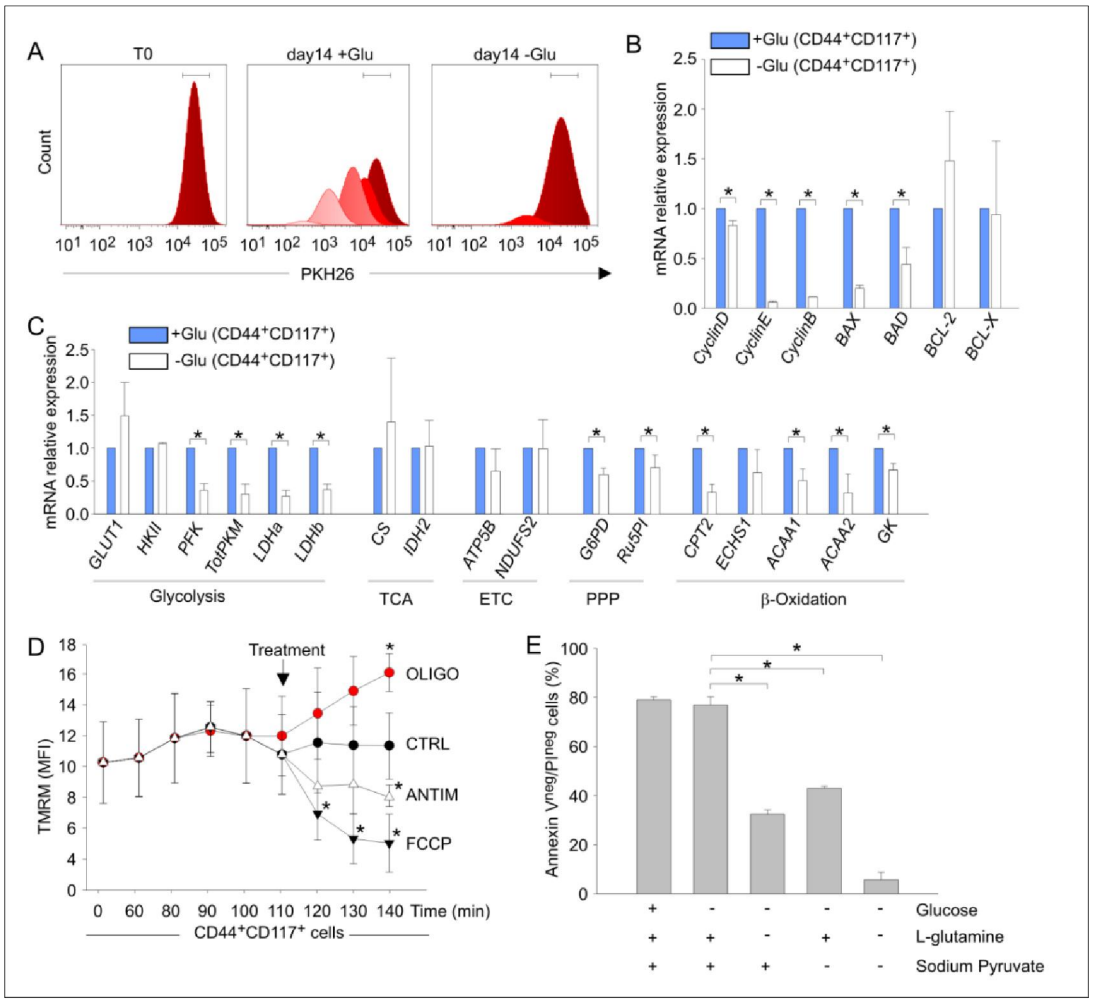

Figure 27: Glucose deprivation modulates the metabolic profile of ovarian cancer CD44$^+$CD117$^+$ cells, while sparing their OXPHOS profile. **A.** Unfractionated EOC effusion cells were labelled with PKH26, and maintained in culture in the presence (+Glu) or absence (-Glu) of glucose. PKH26 staining was evaluated in the two culture conditions 14 days later, and analysed by FlowJo to monitor cell division. One representative experiment out of four is shown. **B.** Unfractionated EOC effusion cells were cultured in the presence (+Glu) or absence (-Glu) of glucose, and the expression of cyclins and apoptosis-associated genes was evaluated by qRT-PCR 14 days later in FACS-sorted CD44$^+$CD117$^+$ cells. The relative expression of each mRNA in glucose-starved CD44$^+$CD117$^+$ cells compared to control CD44$^+$CD117$^+$ cells was calculated as described in the *Supplemental Data*. Mean values ± SD from six samples are shown. *p < 0.05. **C.** The expression of a panel of metabolism-associated genes was evaluated in CD44$^+$CD117$^+$ cells cultured as described in **B**. Relative mRNA expression values were calculated as described above. Shown are mean values ± SD from six samples. *p < 0.05. **D.** Mitochondrial membrane potential ($\Delta\psi_m$) was measured by flow cytometry as detailed in Figure **4D-E** in CD44$^+$CD117$^+$ cells previously cultured for 14 days in the absence of glucose. Antimycin and oligomycin were added to test the $\Delta\psi_m$-generating mode of F_1F_O-ATP synthase. Glucose-starved CD44$^+$CD117$^+$ cells showed a profile fully comparable to that of non-starved CSC (see Figure **4D**), with a significant hyperpolarization in response to oligomycin, demonstrating that glucose deprivation did not change the $\Delta\psi_m$-dissipating "OXPHOS" mode of the F_1F_O-ATP synthase. Shown are mean TMRM MFI values ± SD from three experiments. *p < 0.05 compared to control. **E.** Unfractionated EOC effusion cells were cultured for 14 days in the absence of glucose, and then transferred to media with/without glucose, L-glutamine and sodium pyruvate, as specified on the abscissa. Cell viability was analysed by Annexin V/PI staining 72 h later. Shown are mean percentages of live cells (Annexin V^{neg}/PI^{neg}) ± SD from three experiments. *p < 0.05.

3.7 Metformin and CPI-613, innovative drug targeting metabolism

In conclusion in this study we show that a subpopulation of $CD44^+CD117^+$ EOC cells fulfilling the canonical properties of CSC does not preferentially exploit a glycolytic metabolism, privileging instead the mitochondrial respiratory pathway. These observation may be a possible target of novel treatment strategies against CSC population.
Regarding these premises, the most innovative drugs used to target mitochondria functions are: Metformin and CPI-613.

Metformin, which also inhibits mitochondrial Complex 1 (like rotenone) and is now in the spotlight as a promising anticancer drug, had a dramatic effect on the survival of $CD44^+CD117^+$ cells, with a >50% decrease in viability after 48 hr treatment (Figure 28), whereas $CD44^+CD117^-$ cells did not show any change in viability when cultured for 72 hours in the presence of each inhibitor.

Moreover, in accordance with an anti-Complex I effect, the mitochondrial membrane potential of $CD44^+CD117^+$ cells was dramatically reduced following 90 min incubation with metformin (Figure 29), and, as expected, the addition of oligomycin did not increase $\Delta\psi_m$, a response that was instead evident in the control population.

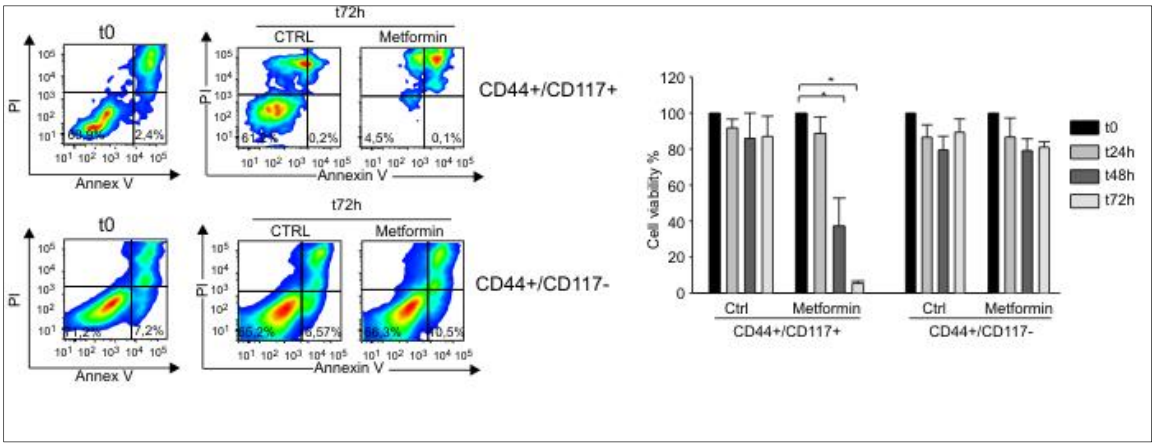

Figure 28: Effect of metformin in $CD44^+CD117^+$ cell viability. Unfractionated EOC effusion cells were incubated in the absence or presence of metformin (1 mM) and cell viability evaluated in $CD44^+CD117^+$ and $CD44^+CD117^-$ cells at various time intervals. Cell viability ratios were calculated at different time points (24, 48, 72h), by AnnexinV/ PI staining, with results expressed as mean values ± SD from three consecutive experiments. *$p < 0.05$.

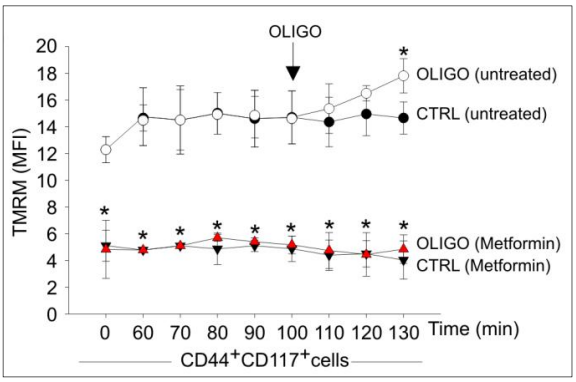

Figure 29: Effect of metformin on ETC inhibition. To validate the effect of metformin on ETC, mitochondrial membrane potential ($\Delta\psi_m$) was measured by flow cytometry with the TMRM probe in $CD44^+CD117^+$ cells from EOC effusions, either untreated (ctrl) or after 90 min of treatment with 1 mM metformin. Oligomycin was added to test the $\Delta\psi_m$-generating mode of F_1F_O-ATP synthase. Shown are mean MFI values ± SD from five experimental repeats. *$p < 0.05$.

Very interesting preliminary results were also obtained with treatment with CPI-613 (Figure 30), specific inhibitor of two key enzymes of TCA cycle: PDH and α-KGH. As a matter of fact, treatment, for 24 hours with different concentration of CPI-613 (1ug -200ug), showed a >80% decrease of CD44/CD117 expression in cell lines IGROV-1 and OC316, in example of primary samples and xenograft. This is a demonstration of the effectiveness of this drug in the target treatment of CD44 + CD117+ cell population.

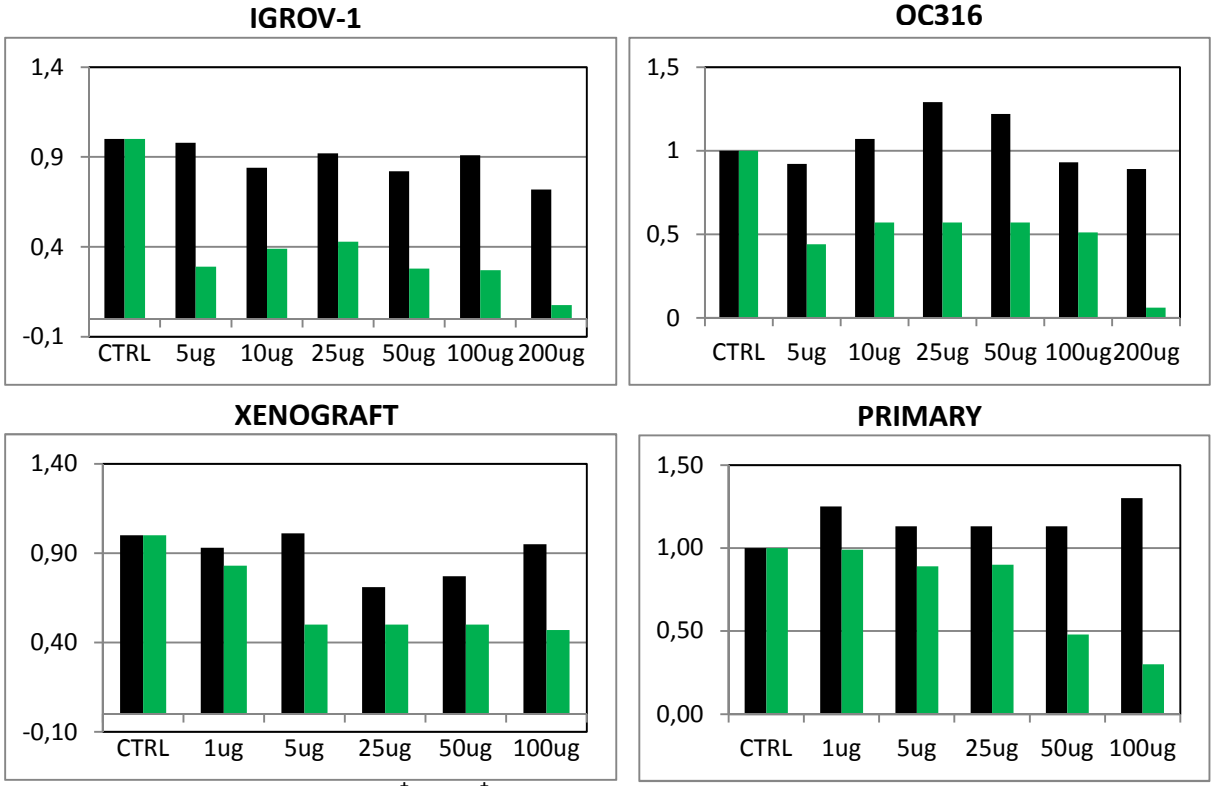

Figure 30: Effect of CPI-613 in $CD44^+CD117^+$ cell viability. Unfractionated EOC effusion cells were incubated in the absence or presence of CPI-613 (different concentrations) and cell viability evaluated in $CD44^+CD117^+$ and $CD44^+CD117^-$ cells at various time intervals. Cell viability ratios were calculated by AnnexinV/ PI staining. (black: DMSO , green: CPI-613).

4. DISCUSSION AND CONCLUSIONS

In this study we investigated the metabolic profile of CSC obtained *ex vivo* from ascitic effusions of EOC-bearing patients. In particular, we addressed our interest to ovarian cancer in view of several considerations:

- ovarian cancer is a very malignant neoplasm, due to late diagnosis and its chemo resistance;
- ovarian cancer cells can be obtained in a relatively easy manner, by taking advantage of their preferential growth as ascitic effusions;
- unlike other types of cancer, where the debate on the markers characterizing CSC is largely open, a body of evidence indicates that ovarian CSC co-express CD44 and CD117, which may help in following the relative enrichment in these cells during the experimental procedures.

The research field of the CSC has been very successful in recent years, considering their property of being "the guilty cells" for maintaining tumor growth and thus for their possible involvement in the improvement of the therapies. Unfortunately, many aspects of their biology are still misunderstood and then the chances of finding therapies targeting these cells are as yet elusive. In particular CSC biology is intricate [14], and the CSC phenotype may encompass a gradient, where tumor progenitors at different stemness levels are comprised under the umbrella of "stem" marker expression [78]. One of the most important difficulty is the lack of a universal marker; each tumor is characterized by its own marker, able to recognize the CSC population in different percentages. Moreover, CSC are able, like normal stem cells, to produce a progenitor cell populations, which later form the differentiated cells. Hence, it is difficult to identify the "true" stem (" the mother of all other cells"); indeed the complexity of the tumor is also characterized by the heterogeneity of the cancer stem cells.

Nonetheless, our data point to the ovarian $CD44^+CD117^+$ subset as a *bona fide* CSC population, which clearly differs molecularly and functionally from the bulk of differentiated tumor cells.

In fact the $CD44^+CD117^+$ cells:

- ✓ Are isolated through the expression of two known stem markers: CD44 and CD117;
- ✓ Are characterized by an over-expression of genes associated to stem-cell pathway (Nanog, Sox2, Oct4), of genes encoding pumps and detoxifying enzymes, involved in drug-resistance, and genes encoding enzymes involved in the process of epithelial-mesenchimal transition;
- ✓ Are able to form spheroids under particular cell culture conditions and present high tumorigenicity *in vivo* in immunodeficient mice.

Based on these premises, the innovative area of interest of our project is the metabolic characterization of these cells, isolated by primary samples. We have demonstrated that:

- ✓ ovarian $CD44^+CD117^+$ cells overexpress key genes associated with glucose uptake, ETC/TCA, PPP, and fatty acid β-oxidation;
- ✓ $CD44^+CD117^+$ cells have lower levels of PDHK1 and phospho-PDH than $CD44^+CD117^-$ cells, indicating their propensity to direct pyruvate utilization towards the Krebs cycle;
- ✓ $CD44^+CD117^+$ cells produce higher levels of mitochondrial ROS, and die when the mitochondrial respiratory chain is blocked. Moreover, a clear-cut qualitative difference in response to inhibition of the F_1F_0-ATP synthase by oligomycin demonstrates that in $CD44^+CD117^+$ cells this enzyme is used to dissipate $\Delta\psi_m$ in order to produce ATP, whereas in $CD44^+CD117^-$ cells it functions in a "reverse mode" to maintain $\Delta\psi_m$ at the expenses of ATP hydrolysis.

Although we could not directly prove higher oxygen consumption and lower lactate production in CSC, as FACS sorting-associated stress precludes determining these functional parameters, the finding that $CD44^+CD117^+$ and $CD44^+CD117^-$ cells express different amounts of PDHK1/phospho-PDH is a crucial clue indicating that ovarian CSC preferentially exploit the mitochondrial respiratory pathway compared to the non-CSC counterpart.

Furthermore, it has been reported that the balance between the *PKM1* and *PKM2* isoforms of *PKM* may be critical in directing pyruvate to either lactate production or mitochondrial utilization [75, 76]. Indeed, in models of enforced expression or silencing of these enzymes in malignant cell lines, PKM2 expression is associated with the Warburg effect [62, 77]. Although we observed a significant elevation in total *PKM* expression in the CSC subset, we did not observe any difference in the relative proportion of *PKM1* and *PKM2* expression between $CD44^+CD117^+$ and $CD44^+CD117^-$ cells. However, molecular and biochemical data on PKM2 may be misleading and may not reflect its actual enzymatic activity, as PKM2 function depends on the formation of dimers/tetramers [77], whose detection is possible under controlled conditions in established cell lines, but unfeasible in our setting.

Our data clearly indicate that EOC $CD44^+CD117^+$ cells are much less dependent on glucose than the $CD44^+CD117^-$ population. This finding is in line with recent observations on *in vitro* resistance of glioblastoma CSC to glucose deprivation [78]. Intriguingly, although the metabolic profile of their $CD133^+$ population was not characterized, these investigators observed pronounced expression of the glucose transporter GLUT3. Our finding of strong surface expression of GLUT1 in ovarian CSC leads us to ask why these relatively quiescent OXPHOS-driven cells should manifest high glucose avidity compared to the bulk tumor cells, and how limiting the Warburg effect might be advantageous to ovarian CSC. We found that ovarian CSC are characterized by high PPP activity, a finding consistent with their high glucose uptake and HKII expression. One key function of the PPP is to maintain high levels of NADPH, which in turn is essential for recharging ROS-scavenging enzymes. Thus, the finding of higher PPP activity, along with high OXPHOS and mitochondrial ROS production, might point to differences in ROS homeostasis between CSC and the bulk tumor cell population, in

order to preserve the integrity of the former, and avoid further DNA damage or irreversible opening of mitochondrial pores. In addition, the higher expression of fatty acid β-oxidation enzymes by $CD44^+CD117^+$ cells could indicate that these metabolites also play an important role within the CSC energy economy, probably to produce intermediates for the Krebs cycle. In this regard, intriguing results obtained in a different setting have shown that inhibition of fatty acid β-oxidation by Etomoxir/Orlistat is associated with selective pro-apoptotic effects in human acute myeloid leukemia progenitors [79].

The metabolic profile and glucose deprivation resistance of ovarian CSC could also help in explaining the refractoriness of EOC to therapies restricting oxygen and nutrient supply. Studies of experimental tumors [80] and human cancer [81, 82,] showed that anti-angiogenic therapies are associated with an increase in the percentage of CSC in the residual tumor mass; indeed, our data on the effect of *in vivo* 2-DG treatment on tumor generation further reinforce this idea. We observed that CSC undergo complete quiescence in the absence of glucose, and down-regulate most metabolic activities, while maintaining an OXPHOS profile; this phenomenon could be instrumental in helping CSC to escape damage in hypo-oxygenated tumor areas, but the mechanisms determining this phenotype are unclear. In this regard, the observed activity of metformin on $CD44^+CD117^+$ cells, which confirms and extends previously reported effects on pancreatic CSC, deserves further investigation, and suggests that approaches combining anti-angiogenic drugs and metformin could be effective for eradicating CSC.

The $CD44^+CD117^+$ cells are characterized by a different metabolism compared to the non-stem counterpart. The possible reason of this metabolic shift could be the possibilities of the CSC to produce more energy in ATP than the tumor cells (36 ATP molecules in mitochondrial metabolism instead of 4 ATP molecules in Warburg-exploiting cells) through a single metabolic cycle. Moreover, many other metabolic pathways are involved in the synthesis of metabolites useful to the Krebs cycle; they guarantee the synthesis of proteins, nucleotides and fatty acids and allow the survival of the CSC. In fact we have demonstrated that the $CD44^+CD117^+$ cells resist the glucose deprivation through the glutamine pathway, as glucose and glutamine starvation induce the death of these cells. Moreover, treatment with CP-613, which also targets the key enzyme α-KGH, showed similar results.

In this regard, we have introduced an innovative drug in our project, actually in clinical trials, the CPI-613, which targets two specific enzymes of the mitochondrial TCA cycle. The finding that treatment with this drug induce a selective death of the CSC has further confirmed our findings of a different metabolism between CSC and non-CSC. Currently, we have only preliminary results of *an in vitro* treatment but it is possible start of a new field of research, studying a possible combination with classical chemotherapy and the drug toxicity *in vivo*. Unfortunately, we have no feedback from clinical trials, as they will end their assessment in 2018.

The finding of a different metabolism in CSC and the good results of the CPI-613 treatments could be a possible therapeutic application, able to eradicate completely the CSC and to stop the phenomenon of aggressive recurrence, typical of ovarian cancer after the first cycle of therapy.

5. FUTURE PERSPECTIVES

This project opens new avenues of investigation, as in literature, little is known about the metabolism of CSC.

First of all, it is interesting to confirm the results obtained with the CPI-613 treatment and organize experimental tests *in vivo* in a mouse model. Really interesting could be the combination of CPI-613 with classical chemotherapy (Doxorubicin, Paclitaxel, Carboplatinum) or with drugs that target cancer metabolism (2DG, Etomoxir, DHEA, Metformine).

Nevertheless, it is necessary to understand the strategies of the CSC to survive in specific stress conditions. Regarding the nutrient deprivation, it is in program to continue the analysis of metabolic strategies, that permit to the CSC to survive and to stay in a quiescent state, as we have demonstrated in our experiments of glucose deprivation. The possibilities could be the glutamine metabolism; Lobo and colleagues have demonstrated that glutaminolysis is another main pillar for energy production. High extracellular glutamine concentrations stimulate tumor growth and are essential for cell transformation [88] and for this reason CPI-613, which targets the enzyme α-KGH, could be a suitable option for cancer cells and for CSC. On the other hand, gluconeogenesis in cancer stem cells could be a field of interest. It is a metabolic pathway that results in the generation of glucose from non-carbohydrate carbon substrates such as pyruvate, lactate, glycerol, and glucogenic amino acids. It is one of the two main mechanisms used by humans and many other mammals to maintain blood glucose levels, avoiding low blood glucose level (hypoglycemia), necessary during a period of nutrient starvation. The other means of maintaining blood glucose levels is through the degradation of glycogen (glycogenolysis) (Figure 31).

At the end, it will be mandatory to investigate the phenomenon of autophagy in CSC. The modulation of autophagy is now recognized as one of the hallmarks of cancer cells. Depending on the context and the type of cancer, autophagy may suppress tumor growth or may allow cancer cells to overcome metabolic stress and the cytotoxicity of chemotherapy. Recent studies have shed light on the role of autophagy in normal stem cells and in cancer stem cells (CSC) [83, 84].

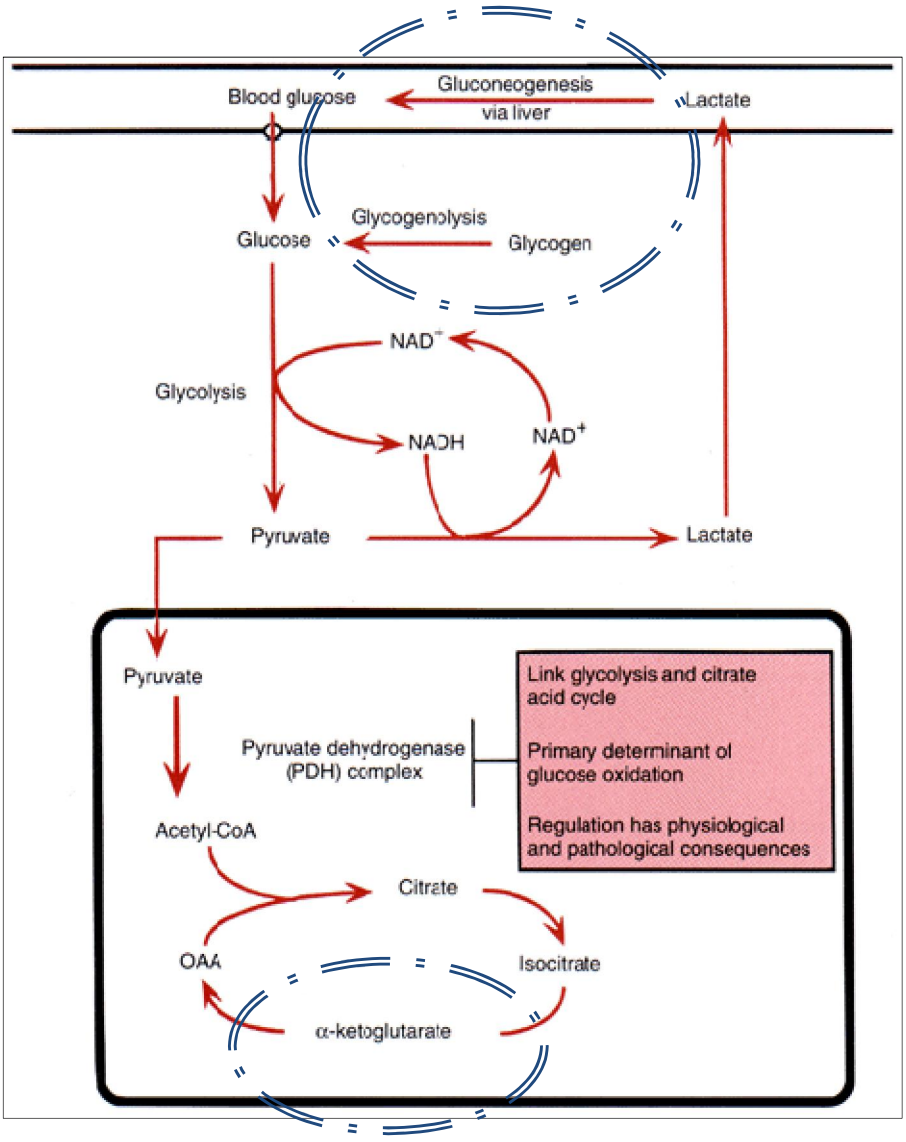

Figure 31: Metabolic strategies for the survival of cancer cells in nutrient starvation. *Critcal care medicine.* Section 5, chapter 74 "Nutritional aspects"

Moreover, current cancer therapies including chemotherapy and ionizing radiation are known to induce autophagy within tumor cells. However, autophagy plays a dual role of either pro-cell survival or pro-cell death in response to these cancer treatments, depending on the cellular context and the nature of the treatment. It could be of interest to correlate between autophagy and metabolism, as the metabolic demand of cancer cells is higher than that of normal cells, and autophagy may help overcome cellular energy deficits (Figure 32) [85]. Furthermore, in a subset of these cancer cells, downregulation of critical autophagy proteins abolishes their tumorigenicity and reduces glucose metabolism indicating the high dependence on autophagy for their survival [86]. Concerning these considerations, autophagy could be a suitable target, as it permits the survival of CSC in stress conditions. However, it remains to be determined how autophagy contributes to the metabolic shift of CSC.

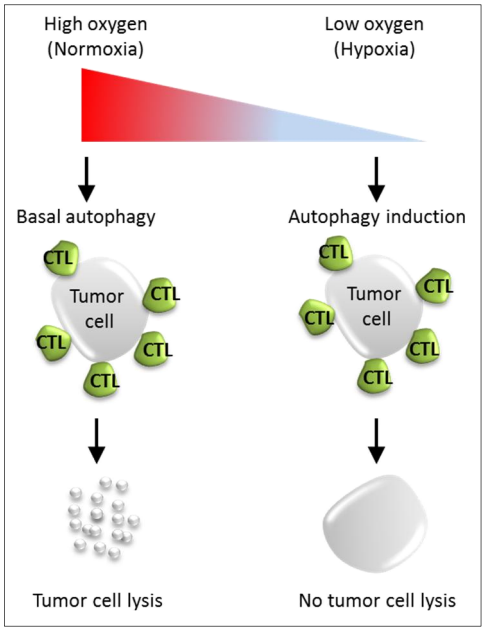

Figure 32: Autophagy induction in specific metabolic stress, like oxygen starvation. Bassam Janji, Elodie Viry, Joanna Baginska, Kris Van Moer and Guy Berchem. *Role of Autophagy in Cancer and Tumor Progression.*

Thus, understanding of pathway biochemistry in cancer cells will help to determine the best targets for possible intervention. Nevertheless, the finding that there is a difference between the metabolism of cancer cells and CSC, and the ability of CSC to survive in specific stress conditions, open an interesting research field, to find particular therapeutic targets, shown in the following pictures as strategic points to hit (Figure 33, pink circle).
Ultimately, these efforts will determine whether a sufficient therapeutic window exists to spare normal tissues from unwanted toxicity and whether further investigation of the anticancer potential of agents that target these enzymes is warranted.

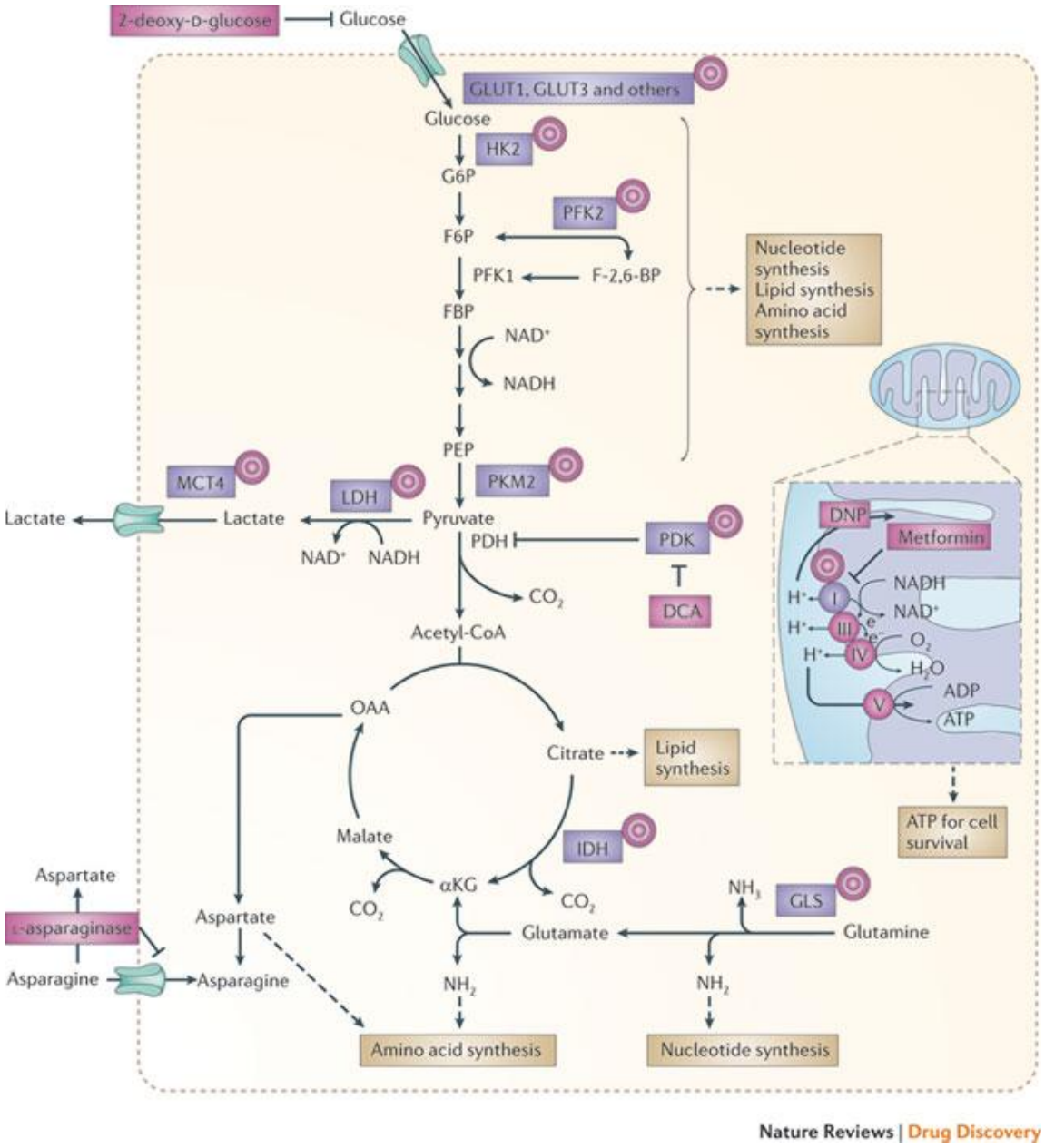

<u>Figure 33:</u> Targeting metabolic enzymes like new hallmarks of cancer. Matthew G. Vander Heiden. Targeting cancer metabolism: a therapeutic window opens. Nature Reviews. 2011; 10:671-684.

6. REFERENCES

[1] Siegel R., Ma J., Zou Z., Jemal A. *Cancer Statistics 2014.* Cancer J Clinic 2014; 64:9-29.

[2] Pastò A., Bellio C., Pilotto G., Ciminale V., Benussi M. S., Guzzo G., Rasola A., Frasson C., Nardo G., Zulato E., Nicoletto M.O., Manicone M., Indraccolo S. e Amadori A. *Cancer stem cells from epithelial ovarian cancer patients privilige oxidative posphorylation, and resist glucose deprivation.* Oncotarget 2014; Vol. 5: 12.

[3] Hanahan D. and Weinberg R. A. *Hallmarks of Cancer: The Next Generation. Cell 2011; 144.*

[4] Goff, B.a. et al. *Ovarian carcinoma diagnosis.* Cancer 2000; 89: 2068.

[5] Bast R. C., Hennessy B and Mills G.B. *The biology of ovarian cancer: new opportunities for translation.* Nature Reviews 2009; 9415-428.

[6] Prat J. *New insight into ovarian cancer pathology.* Ann Oncol 2012; 23: 111-117.

[7] Kurman R.J., Shih I. *The origin of pathogenesis of epithelial ovarian cancer – a proposed unifying theory.* Am J Surg Pathol. 2010; 34(3):433-443.

[8] Prat J. for the FIGO Committee on Gynecologic Oncology. *Staging classification for cancer of the ovary, fallopian tube, and peritoneum.* International Journal of Gynecology and Obestetrics 2013.

[9] Puiffe M.L., Le page C., Filali-Mouhim A., Zietarska M., Ouellet V., Tonin P.N., Chevrette M., Provencher D.M., Mes-Masson A.M. *Characterization of ovarian cancer ascites on cell invasion, proliferation, spheroids formation, and gene expression in an in vitro model of epithelial ovarian cancer.* Neoplasia 2007; 9(10):820-829.

[10] Kim a., Ueda Y., Naka T. and Enomoto T. *Therapeutic strategies in epithelial ovarian cancer.* Journal of Experimental & Clinical Cancer Research *2012; 31:14.*

[11] Abdullah L.N. and Chow E.K. *Mechanisms of chemoresistance in cancer stem cells.* Clin Transl Med. 2013; 2:3.

[12] Ramachandran R.P. and Yelledahalli L.U. *Exploring the recent advances in stem cell research.* J Stem Cell Res Ther 2011; 1:3.

[13] Reya T., Morrison S.J., Clarke M.F., Weissman I.L. *Stem cells, cancer and cancer stem cells.* Nature 2001; 414:105-111.

[14] Clevers H. *The cancer stem cell: premises, promises and challenges.* Nature medicine 2011; 17:3.

[15] Liu H.G., Chen C., Yang H., Pan Y. and Zhang X. *Cancer stem cell subsets and their relationship.* Journal of Translational Medicine 2011; 9:50.

[16] Bonnet D. and Cick J.E. *Human acute myeloid leukemia is organized as a hierarchy that originates from a primitive hematopoietic cell.* Nature Medicine 1997; 3:7.

[17] Al-Hajj et al. *Prospective identification of tumorigenic breast cancer cells*. Proc Natl Acad Sci U S A. 2003;

[18] Singh et al. *Identification of human brain tumor initiating cells.* Nature 2004;

[19] Collins et al. *Stem cell function, self-renewal, and behavioral heterogeneity of cells from the adult muscle satellite cell niche.* Cell 2005.

[20] Bapat SA, Mali AM, Koppikar CB, Kurrey NK. *Stem and progenitor-like cells contribute to the aggressive behavior of human epithelial ovarian cancer.* Cancer Res. 200

[21] Reya T., Morrison S.j., Clarke M.F. and Weissman I.L. *Stem cells, cancer, and cancer stem cells.* Nature 2001; 414:105-111.

[22] Chandler J.M. and Lagasse E. *Cancerous stem cells: deviant stem cells with cancer-causing misbehavior.* Stem Cell Res Ther. 2010; 1(2): 13.

[23] Bjerkvig R., Tysnes B.B., Aboody K.S., Najbauer J. and Terzis A. J. A. *The origin of the cancer stem cell: current controversies and new insights.* Nature Reviews 2005; 5: 899-904.

[24] Tabarestani S. and Ghafouri-Fard S. *Cancer stem cells and response to therapy.* Asian Pacific J Cancer Prev 2012; 13(12): 5947-5954.

[25] Kleffel S. and Schatton T. *Tumor dormancy and cancer stem cells: two sides of the same coin?* Adv Exp Med Biol 2013; 734: 145-79.

[26] Diehn M. and Majeti R. *Metastatic cancer stem cells: an opportunity for improving cancer treatment*. Cell Stem Cell 2010; 6: 502-503.

[27] Mani SA, Guo W, Liao MJ, Eaton EN, Ayyanan A, Zhou AY, Brooks M, Reinhard F, Zhang CC, Shipitsin M, Campbell LL, Polyak K, Brisken C, Yang J and Weinberg RA. *The epithelial-mesenchymal transition generates cells with properties of stem cells.* Cell 2008; 133: 704-715.

[28] Lia W., Ye Y.P., Deng Y.j., Bian X. and Ding Y. *Metastatic cancer stem cells: from the concept to therapeutics.* Am J Stem Cells 2014: 3(2): 46-62.

[29] Tilly J.L. and Rueda B.R. Minireview: stem cell contribution to ovarian development, function, and disease. Endocrinology 2008; 149: 4307-4311.

[30] Bapat S.A., Mali A.M., Koppikar C.B. and Kurrey N.K. Stem and progenitor-like cells contribute to the aggressive behavior of human epithelial ovarian cancer. Cancer Research 2005; 65: 3025-3029.

[31] Zhang S., Balch C., Chan M.W., Lai H.C., Matei D., Schilder J.M., Yan P.S., Huang T. and Nephew K.P. Identification and characterization of ovarian cancer initiating cells from primary human tumors. Cancer Research 2008; 68(11): 4311-4320.

[32] Ojeda D.B., Rueda B.R and Buckanovich R.J. Ovarian cancer stem cell markers: prognostic and therapeutic implications. Cancer Letters 2012.

[33] Baba T.,Convery P.A., Matsumura N., Whitaker R.S., Kondoh E., Perry T., Huang Z., Bentley R.C., Mori S., Fujii S., Marks J.R., Berchuck A., Murphy S.K. *Epigenetic regulation of CD133 and tumorigenicity of CD133+ ovarian cancer cells.* Oncogene 2009; 28: 209-218.

[34] Curley M.D., Therrien V.A., Cummings C.L., Sergent P.A., Koulouris C.R., Friel A.M., Roberts D.J., Seiden M.V., Scadden D.T., Rueda B.R., Foster R. *CD133 expression defines a tumor initiating cell population in primary human ovarian cancer.* Stem Cells 2009; 27:2875-2883.

[35] Silva I.A., Bai S., McLean K., Griffith K., Thomas D., Ginestier C., Johnston C., Kueck A., Reynolds R.K., Wicha M.S., Buckanovich R.J. *Aldehyde dehydrogenase in*

combination with CD133 defines angiogenic ovarian cancer stem cells that portend poor patient survival. Cancer Res 2011; 71:3991-4001.

[36] Landen C.N., Goodman B., Katre A.A., Steg A.D., Nick A.M., Stone R.L., Miller L.D., Mejia P.V., Jennings N.B., Gershenson D.M., Bast R.C., Coleman R.L., Berestein G., Sood A.K. Targeting aldehyde dehydrogenase cancer stem cells in ovarian cancer. Mol Cancer Ther 2010; 9:3186-3199.

[37] Hu L., McArthur C., Jaffe R.B. *Ovarian cancer stem-like side population cells are tumorigenic and chemoresistant.* Br. J. Cancer 2010; 102:1276-1283.

[38] Kobayashi Y., Seino K., Hosonuma S., Ohara T., Itamochi H., Isonishi S., Kita T., Wada H., Kojo S., Kiguchi K. *Side population is increased in paclitaxel-resistant ovarian cancer cell lines regardless of resistance to cisplatin.* Gyn. Oncol. 2011; 121:390-394.

[39] Hosonuma S., Kobayashi Y., Kojo S., Wada H., Seino K., Kiguchi K., Ishizuka B. *Clinical significance of side population in oarian cancer cells.* Hum. Cell 2011; 24: 9-12.

[40] Cao L., Shao M., Schilder J., Guise T., Mohammad K.S., Matei D. *Tissue transglutaminase links to TGF-beta, epithelial to mesenchymal transition and a stem cell phenotype in ovarian cancer.* Oncogene 2012; 31: 2521-2534.

[41] Motohara T., Masuko S., Ishimoto T., Yae T., Onishi N., Muraguchi T., Hirao A., Matsuzaki Y., Tashiro H., Katabuchi H et al. *Transient depletion of p53 followed by transduction of c-Myc and K-Ras converts ovarian stem-like cells into tumor-initiating cells.* Carcinogenesis 2011; 32:1597-1606.

[42] Luo L., Zeng J., Liang B., Zhao Z., Sun L., Cao D., Yang J., Shen K. *Ovarian cancer cells with the CD117 phenotype are highly tumorigenic and are related to chemotherapy outcome.* Exp. Mol. Pathol. 2011; 91:596-602.

[43] Kwon M.J. and Shin Y.K. *Regulation of ovarian cancer stem cells or tumor-initiating cells.* Int. J. Mol. Sci. 2013; 14:6624-6648.

[44] Tomao F., Papa A., Rossi L., Strudel M., Vici P., Lo Russo G. and Tomao S. *Emerging role of cancer stem cells in the biology and treatment of ovarian cancer: basic knowledge and therapeutic possibilities for an innovative approach.* Journal of Experimental and Clinical Cancer research 2013: 32: 48.

[45] Schilder RJ, Sill MW, Lee RB, Shaw TJ, Senterman MK, Klein-Szanto AJ, Miner Z, Vanderhyden BC. *Phase II evaluation of imatinib mesylate in the treatment of recurrent or persistent epithelial ovarian or primary peritoneal carcinoma: a gynecologic oncology group study.* J Clin Oncol 2008, 26 (20):3418 - 3425.

[46] Chen K., Huang Y. and Chen J. *Understanding and targeting cancer stem cells: therapeutic implications and challenges.* Acta Pharmacologica Sinica 2013; 34: 732-740.

[47] Whitworth JM, Londoño-Joshi AI, Sellers JC, Oliver PJ, Muccio DD, AtigaddaVR, Straughn JM Jr, Buchsbaum DJ: The impact of novel retinoids in combination with platinum chemotherapy on ovarian cancer stem cells. Gynecol Oncol 2012,125(1):226–230.

[48] McAuliffe S.M., Morgan S.L., Wyant G.A., Tran L.T., Muto K.w., Chen Y.S., Chin K.T., Partridge J.C., Poole B.B., Cheng K.H., Dagget J., Cullen K., Kantoff E., Hasselbatt K., Berkowitz J., Muto M.G., Berkowitz R.S., Aster J.C., Matulonis U.A. and Dinulescu D.M. *Targeting Notch, a key pathway for ovarian cancer stem cells, sensitizes tumors to platinum therapy.* PNAS 2012; 109:43.

[49] Borovski T., Melo F., Vermeulen L. and Medema J.P. Cancer stem cell niche: the place to be. Cancer Res 2011; 71:634.

[50] Hanahan D. and Weinberg R.A. Hallmarks of cancer: the next generation. Cell 2011; 144: 646-674.

[51] Warburg O., Wind F. and Negelein E. *The metabolism of tumors in the body.* 1926

[52] Warburg O. *On respiratory impairment in cancer cells.* Science 1956; 124:269-270

[53] Fowler JS and Ido T. *Initial and subsequent approach for the synthesis of 18FDG.* Semin Nucl Med, 2002; 32(1): 6-12.

[54] Bardella C, Pollard PJ and Tomlinson I. *SDH mutations in cancer.* Biochim Biophys Acta 2011; 1807: 1432-1443.

[55] Dang L, White DW, Gross S, Bennett BD, Bittinger MA, Driggers EM and Fantin VR et al. *Cancer-associated IDH1 mutations produce 2-hydroxyglutarate.* Nature 2009; 462: 739-744.

[56] Christofk HR, Vander Heiden MG, Harris MH, Ramanathan A, Gerszten RE, Wei R and Fleming MD et al. *The M2 splice isoform of pyruvate kinase is important for cancer metabolism and tumor growth.* Nature 2008; 452: 230-233.

[57] Semenza GL, Roth PH, Fang HM and Wang GL. *Transcriptional regulation of genes encoding glycolytic enzymes by hypoxia-inducible factor 1.* J Biol Chem 1994; 269: 23757-23763.

[58] Semenza GL. *Hypoxia-inducible factors in physiology and medicine.* Cell 2012; 148: 399-408.

[59] Upadhyay M., Smal J., Kandpal M., Singh OV. And Vivekanandan P. *The Warburg effect: insights from the past decade.* Pharmacology and Therapeutics 2013; 137: 318-330.

[60] Barnes K., Mcintosh E., Whetton A.D., Daley G.Q., Bentley J. and Baldwin SA. *Chronic Myeloid leukemia: an investigation into the role of BCR-Abl-induced abnormalities in glucose transport regulation.* Oncogene 2005; 24: 3257-3267.

[61] Zhang X. D., Deslandes E., Villedieu M., Poulain L., Duval M., Gaudochon P., Schwartz L. and Icard P. *Effect of 2-deoxy-o-glucose on various malignant cell lines in vitro*. Anticancer Res 2006; 26: 3561-3566.

[62] *Szokoloczi O., Schwab R., Petak I., Orfi L., Pap A., Eberle A. N., Szuts T. and Keril G. TT232 a novel signal transduction inhibitory compound in the therapy of cancer and inflammatory disease.* J Recept Signal Transduct Res 2005; 25: 217-235.

[63] Madhok B. M., Yeluri S., Perry S. L., Hughers T. A., Jayne D. G. *Targeting glucose metabolism: an emerging concept for anticancer therapy.* Am J Clin Oncol 2011; 34: 628-635.

[64] Herter F. P., Weissman S. G., Thompson H. G., Hyman G. and Martin D. S. *Clinical experience with 6-aminonicotinamide.* Cancer res 1961; 21:31-37.

[65] Rapisarda A., Uranchimeg B., Scudiero D. A., Selby M., Sausville E. A., Shoemaker R. H. and Melillo G. *Identification of small molecule inhibitors of hypoxia-inducible factor 1 transcriptional activation pathway.* Cancer Res 2002; 62: 4316-4324.

[66] Kim S. H. and Lee G. M. *Down-regulation of lactate dehydrogenase-A by siRNAs thrombopoietin*. Appl Microbiol Biotechnol 2007; 74: 152-159.

[67] Flynn P., Wongdagger M., Zavar M., Dean N.M. and Stokoe D. *Inhibition of PDK-1 activity causes a reduction in cell proliferation and survival.* Curr Biol 2000; 10: 1439-1442.

[68] Shijun W., Daqian Z. and Peng Huang. *Targeting cancer cell mitochondria as a therapeutic approach.* Future Med Chem 2013; 5(1): 53-67.

[69] Heather A. Hirsch, Dimitrios Iliopoulos, Philip N. Tsichlis, and Kevin Struhl. *Metformin selectively targets cancer stem cells, and acts together with chemotherapy to block tumor growth and prolong remission.* Cancer Res. 2009; 69(19): 7507–7511.

[70] TaeHun Kim, Dong Hoon Suh, Mi-Kyung Kim, and Yong Sang Son. *Metformin against Cancer Stem Cells through the Modulation of Energy Metabolism: Special Considerations on Ovarian Cancer.* BioMed Research International 2014.

[71] Stuart S., Schauble A., Gupta S., Kennedy A., Keppler B., Bingham P. and Zachar Z. A strategically designed small molecule attacks alpha-ketoglutarate dehydrogenase in tumor cells through a redox process. Cancer and Met. 2014; 2(4).

[72] Zeuner A. and De Maria R. *Not so lonely at the top for cancer stem cells. Cell Stem Cells.* 2011; 9(4):289-290.

[73] Flavahan WA, Wu Q, Hitomi M, Rahim N, Kim Y, Sloan AE, Weil RJ, Nakano I, Sarkaria JN, Stringer BW, Day BW, Li M, Lathia JD, Rich JN and Hjelmeland AB. *Brain tumor initiating cells adapt to restricted nutrition through preferential glucose uptak*e. Nat Neurosci. 2013; 16(10):1373-1382.

[74] Samudio I, Harmancey R, Fiegl M, Kantarjian H, Konopleva M, Korchin B, Kaluarachchi K, Bornmann W, Duvvuri S, Taegtmeyer H and Andreeff M. Pharmacologic inhibition of fatty acid oxidation sensitizes human leukemia cells to apoptosis induction. J Clin Invest. 2010; 120(1):142-156.

[75] Wong N., De Melo J. and Tang D. *PKM2. A central point of regulation in cancer metabolism.* Int J Cell Biol 2013; 2013:242513

[76] Christofk HR, Vander Heiden MG, Wu N, Asara JM and Cantley LC. *Pyruvate kinase M2 is a phosphotyrosine-binding protein.* Nature. 2008; 452(7184):181-186.

[77] Luo W and Semenza GL. *Emerging roles of PKM2 in cell metabolism and cancer progression.* Trends Endocrinol Metab. 2012; 23(11):560-566.

[78] Zulato E, Curtarello M, Nardo G and Indraccolo S. Metabolic effects of anti-angiogenic therapy in tumors. Biochimie. 2012; 94(4):925-931.

[79]Heddleston JM, Li Z, McLendon RE, Hjelmeland AB and Rich JN. The hypoxic microenvironment maintains glioblastoma stem cells and promotes reprogramming towards a cancer stem cell phenotype. Cell Cycle. 2009; 8(20):3274-3284.

[80] Conley SJ, Gheordunescu E, Kakarala P, Newman B, Korkaya H, Heath AN, Clouthier SG and Wicha MS. Antiangiogenic agents increase breast cancer stem cells via the generation of tumor hypoxia. Proc Natl Acad Sci U S A. 2012; 109(8):2784-2789.

[81] Seidel S, Garvalov BK, Wirta V, von Stechow L, Schänzer A, Meletis K, Wolter M, Sommerlad D, Henze AT, Nistér M, Reifenberger G, Lundeberg J, Frisén J and Acker T. A hypoxic niche regulates glioblastoma stem cells through hypoxia inducible factor 2 alpha. Brain. 2010; 133(Pt 4):983-995.

[82] Lobo, C, Ruiz-Bellido MA, Aledo JC, Marquez J, Nunez De Castro I and Alonso FJ. *Inhibition of glutaminase expression by antisense mRNA decreases growth and tumourigenicity of tumour cells*. Biochem. J.2000; 348 (2): 257–261.

[83] Vessoni AT, Muotri AR, Okamoto OK. Autophagy in stem cell maintenance and differentiation. Stem Cells Dev. 2012; 21:513–520.

[84] Guan JL, Simon AK, Prescott M, Menendez JA, Liu F, Wang F,Wang C, Wolvetang E,Vazquez-Martin A, Zhang J. Autophagy in stem cells. Autophagy. 201;, 9:830–849.

[85] Mathew R, Karantza-Wadsworth V, White E. *Role of autophagy in cancer.* Nat Rev Cancer. 2007; 7:961–967.

[86] Guo JY, Chen HY, Mathew R, Fan J, Strohecker AM, Karsli-Uzunbas G, Kamphorst JJ, Chen G, Lemons JM, Karantza V,et al. *Activated Ras requires autophagy to maintain oxidativemetabolism and tumorigenesis.* Genes Dev. 2011, 25:460–470.

PUBLICATION:

Bellio C., Pastò A., Pilotto G., Ciminale V., Benussi M. S., Guzzo G., Rasola A., Frasson C., Nardo G., Zulato E., Nicoletto M.O., Manicone M., Indraccolo S. e Amadori A. *Cancer stem cells from epithelial ovarian cancer patients privilige oxidative posphorylation, and resist glucose deprivation.* Oncotarget 2014; Vol. 5: 12.

SCIENTIFIC CONFERENCES:

- Gynecological tumors - Padova 2012
- NIBIT: Biotherapy of tumors - Padova 2013
- 25th Pezcoller Symposium "Metabolism and tumorigenesis" - Trento 2013
- 26th Pezcoller Symposium "Cancers driven by hormones" - Trento 2014
- Cancer - Discovery on target - Padova 2014
- Discovery on Target - Boston 2014

AWARDS FOR THIS RESEARCH PROJECT:

- NIBIT Awards 2013 (Cancer Bio-Immuno-therapy in Siena XI NIBIT Meeting)
- PEZCOLLER Awards 2014 (26th Pezcoller Symposium – Cancers driven by hormones)